

2016

Exploration of Bimetallic Nickel and Cobalt Complexes for Catalytic Oxidative Cleavage of Alkenes and Hydroformylation

Ciera Vonn Duronslet

Louisiana State University and Agricultural and Mechanical College, cduronslet@gmail.com

Follow this and additional works at: https://digitalcommons.lsu.edu/gradschool_dissertations



Part of the [Chemistry Commons](#)

Recommended Citation

Duronslet, Ciera Vonn, "Exploration of Bimetallic Nickel and Cobalt Complexes for Catalytic Oxidative Cleavage of Alkenes and Hydroformylation" (2016). *LSU Doctoral Dissertations*. 4283.

https://digitalcommons.lsu.edu/gradschool_dissertations/4283

This Dissertation is brought to you for free and open access by the Graduate School at LSU Digital Commons. It has been accepted for inclusion in LSU Doctoral Dissertations by an authorized graduate school editor of LSU Digital Commons. For more information, please contact gradetd@lsu.edu.

EXPLORATION OF BIMETALLIC NICKEL AND COBALT
COMPLEXES FOR CATALYTIC OXIDATIVE CLEAVAGE OF
ALKENES AND HYDROFORMYLATION

A Dissertation

Submitted to the Graduate Faculty of the
Louisiana State University and
Agricultural and Mechanical College
in partial fulfillment of the
requirement for the degree of
Doctor of Philosophy

in

The Department of Chemistry

by
Ciera Vonn Duronslet
B.S. Nicholls State University, 2010
December 2016

Acknowledgements

Firstly, I would like to thank God for blessing me with this opportunity and for giving me the continued strength I needed to finish this journey. I would like to thank Professor Stanley for his constant support, encouragement, and guidance throughout my years at LSU. His willingness to help and belief in me has given me the knowledge and wisdom I needed to pursue the PhD and a career in science. I thank my mom and grandma for always being my backbones and believing in me when I did not believe in myself.

I would like to thank my husband and friend, Johuan, for his constant support and tough love. He has helped to give me a stronger platform that I can use to push myself to greater heights. I would also like to thank my son and stepdaughter, Aschere and Dillan; because of them, I strive to lead by example. A special thanks is also extended to all of my family and friends who have supported me continuously throughout the years. Because of you, I never gave up on this journey, even when times became rough.

I would like to thank my committee members, Drs. Maverick, Ragains, and Luo for their continued support and patience through this process. I would also like to thank Dr. Connie David in the Mass Spec facility, Dr. Thomas Weldeghiorghis in the NMR facility, and Dr. Frank Fronczek for his X-ray crystallography analyses. I have learned much from each of you, and I thank you for your support with my research. I would also like to specifically thank the Stanley research group, both past and current members, for all of the beneficial discussions, suggestions, and friendships.

Table of Contents

Acknowledgements	ii
List of Abbreviations	vi
Abstract	vii
Chapter 1: Introduction to Oxidative Cleavage of Alkenes and Unsaturated Fatty Acids	1
1.1 Importance of Industrial Alkene Oxidation	1
1.2 Catalytic Oxidative Cleavage	4
1.3 Autooxidation of Phosphines and Hydrocarbons	5
1.4 Transition Metal-Catalyzed Autooxidations with O ₂	7
1.5 Alkene Oxidative Cleavage	9
1.6 History of Alkene Oxidative Cleavage in Stanley Lab	9
1.7 Mechanistic Possibilities and Beyond	13
1.8 Oxidative Cleavage of Unsaturated Fatty Acids	18
1.9 References	20
Chapter 2: Investigations into Nickel-Phosphine and Cobalt Mediated Oxidative Cleavage of Unsaturated Fatty Acids	24
2.1 Background	24
2.2 Results and Discussion	25
2.2.1 Oxidative Cleavage of Oleic Acid using <i>meso</i> - and <i>rac</i> -Ni ₂ Cl ₄ (<i>et</i> , <i>ph</i> -P ₄)	27
2.2.2 Esterification of Oleic Acid	30
2.2.3 Oxidative Cleavage of Oleic Acid Methyl Ester using <i>meso</i> - and <i>rac</i> - Ni ₂ Cl ₄ (<i>et</i> , <i>ph</i> -P ₄)	30
2.2.4 Isolation of Ricinoleic Acid	31
2.2.5 Oxidative Cleavage of Ricinoleic Acid using <i>meso</i> - and <i>rac</i> - Ni ₂ Cl ₄ (<i>et</i> , <i>ph</i> -P ₄)	32
2.2.6 Oxidative Cleavage of Oleic Acid using <i>meso</i> - and <i>rac</i> - Ni ₂ Cl ₄ (<i>et</i> , <i>ph</i> -P ₄ -Ph)	32
2.2.7 Oxidative Cleavage of Oleic Acid using <i>meso</i> - and <i>rac</i> - <i>et</i> , <i>ph</i> -P ₄ (old ligand)	33
2.2.8 Oxidative Cleavage of Oleic Acid using <i>meso</i> - and <i>rac</i> - <i>et</i> , <i>ph</i> -P ₄ (new ligand)	34
2.2.9 Oxidative Cleavage of Oleic Acid using Other Phosphine Ligands	35
2.2.10 Reactivity of the Dinickel Complexes with H ₂ O	36
2.2.11 ³¹ P NMR Studies of <i>rac</i> -Ni ₂ Cl ₄ (<i>et</i> , <i>ph</i> -P ₄) Reactivity with H ₂ O	37
2.2.12 ³¹ P NMR Studies of <i>meso</i> -Ni ₂ Cl ₄ (<i>et</i> , <i>ph</i> -P ₄ -Ph) Reactivity with H ₂ O	42
2.2.13 ³¹ P NMR Studies of <i>rac</i> -Ni ₂ Cl ₄ (<i>et</i> , <i>ph</i> -P ₄ -Ph) Reactivity with H ₂ O	46
2.2.14 Oxidative Cleavage of Oleic Acid using <i>meso</i> - and <i>rac</i> - Co ₂ Cl ₄ (<i>et</i> , <i>ph</i> -P ₄)/(<i>et</i> , <i>ph</i> -P ₄ -Ph)	46
2.2.15 Oxidative Cleavage of Oleic Acid using [Co(H ₂ O) ₆][BF ₄] ₂	47
2.2.16 Oxidative Cleavage of Alkenes using Drago's Catalyst (CoSMDPT)	47

2.3 Conclusion	49
2.4 References	51
Chapter 3: Synthetic Strides Towards a Bimetallic Cobalt Catalyst for Hydroformylation and Aldehyde-Water Shift Catalysis	
3.1 Introduction	53
3.1.1 Discovery of Cobalt-Catalyzed Hydroformylation	54
3.1.2 Modified vs Unmodified Cobalt Hydroformylation	56
3.1.3 Commercial Hydroformylation and the Low Pressure Oxo Processes	58
3.1.4 Hydroformylation Research Goals	60
3.2 Results and Discussion	66
3.2.1 Background Research	66
3.2.2 Attempted Reduction of <i>meso</i> - and <i>rac</i> -Co ₂ Cl ₄ (<i>et</i> , <i>ph</i> -P4) and (<i>et</i> , <i>ph</i> -P4-Ph)	67
3.2.3 Synthesis of <i>meso</i> - and <i>rac</i> -Co ₂ Cl ₄ (<i>et</i> , <i>ph</i> -P4) and (<i>et</i> , <i>ph</i> -P4-Ph)	68
3.2.4 H ₂ /CO Reduction of <i>meso</i> - and <i>rac</i> -Co ₂ Cl ₄ (<i>et</i> , <i>ph</i> -P4) and (<i>et</i> , <i>ph</i> -P4-Ph)	72
3.2.5 NaBH ₄ Reduction of <i>meso</i> - and <i>rac</i> -Co ₂ Cl ₄ (<i>et</i> , <i>ph</i> -P4) and (<i>et</i> , <i>ph</i> -P4-Ph)	82
3.2.6 Lithium Aluminum Hydride (LAH) Reduction of <i>meso</i> -Co ₂ Cl ₄ (<i>et</i> , <i>ph</i> -P4-Ph)	84
3.2.7 Super Hydride Reduction of <i>meso</i> - and <i>rac</i> -Co ₂ Cl ₄ (<i>et</i> , <i>ph</i> -P4-Ph)	85
3.2.8 Mg and Zn Reduction of <i>meso</i> - and <i>rac</i> -Co ₂ Cl ₄ (<i>et</i> , <i>ph</i> -P4) and (<i>et</i> , <i>ph</i> -P4-Ph)	86
3.2.9 Attempted Chloride Abstractions of <i>meso</i> -Co ₂ Cl ₄ (<i>et</i> , <i>ph</i> -P4-Ph) with AgBF ₄ or AgPF ₆	92
3.2.10 Reactions with Co ₂ (CO) ₈	93
3.2.11 Ligand Substitution Reactions of Co ₂ (CO) ₆ (<i>nbd</i>) ₂ with <i>meso</i> - and <i>rac</i> - <i>et</i> , <i>ph</i> -P4	93
3.2.12 Direct Reaction of <i>meso</i> - <i>et</i> , <i>ph</i> -P4 with Co ₂ (CO) ₈	98
3.2.13 Exploration of Non-Halide Containing Starting Materials	101
3.2.14 Reaction of [Co(H ₂ O) ₆][BF ₄] ₂ with <i>rac</i> - <i>et</i> , <i>ph</i> -P4 and <i>et</i> , <i>ph</i> -P4-Ph	102
3.2.15 H ₂ /CO and Zn Reduction Attempts of <i>rac</i> -[Co ₂ (H ₂ O/OH) _x (<i>et</i> , <i>ph</i> -P4)/(<i>et</i> , <i>ph</i> -P4-Ph)] ⁴⁺	102
3.2.16 Hydroformylation of 1-Hexene Attempts with Dicobalt Complexes	104
3.3 Conclusion	106
3.4 References	108
Chapter 4: Experimentals	
4.1 General Comments	113
4.2 Oxidative Cleavage Reactions	114
4.2.1 Type I	114
4.2.2 Type II	114
4.2.3 Reaction Tables	115
4.3 ¹ H NMR Oxidative Cleavage Quantification Experiments	118
4.4 Esterification of Oleic Acid	119

4.5 Attempted Isolation of Ricinoleic Acid	119
4.6 ³¹ P NMR Studies of the Dinickel Complexes' Reactivity with H ₂ O	120
4.7 Synthesis of Drago's Catalyst, CoSMDPT	121
4.8 Oxidative Cleavage of Isoeugenol using Drago's Catalyst	121
4.9 Synthesis of <i>meso</i> -/ <i>rac</i> -Co ₂ Cl ₄ (<i>et</i> , <i>ph</i> -P4) and <i>meso</i> -/ <i>rac</i> -Co ₂ Cl ₄ (<i>et</i> , <i>ph</i> -P4-Ph)	121
4.10 Reduction of <i>meso</i> -/ <i>rac</i> -Co ₂ Cl ₄ (<i>et</i> , <i>ph</i> -P4) and <i>meso</i> -/ <i>rac</i> -Co ₂ Cl ₄ (<i>et</i> , <i>ph</i> -P4-Ph)	122
4.10.1 H ₂ /CO Reduction Experiments	122
4.10.2 NaBH ₄ Reduction Experiments	123
4.10.3 Attempted LAH Reduction Experiment	123
4.10.4 Super Hydride Reduction Experiments	124
4.10.5 Attempted Mg Reduction Experiments	124
4.10.6 Zn Reduction Experiments	125
4.10.7 Attempted Chloride Abstractions using AgBF ₄ /AgPF ₆	125
4.11 Reactions with Co ₂ (CO) ₈	126
4.11.1 Synthesis of Co ₂ (CO) ₄ (<i>nbd</i>) ₂	126
4.11.2 Reactions of Co ₂ (CO) ₄ (<i>nbd</i>) ₂ with <i>et</i> , <i>ph</i> -P4	126
4.11.3 Reactions of Co ₂ (CO) ₈ with <i>meso</i> - <i>et</i> , <i>ph</i> -P4	127
4.12 Synthesis of [Co(H ₂ O) ₆][BF ₄] ₂	127
4.13 Synthesis of <i>rac</i> -[Co ₂ (H ₂ O) _x (<i>et</i> , <i>ph</i> -P4)][BF ₄] ₄ and <i>rac</i> -[Co ₂ (H ₂ O) _x (<i>et</i> , <i>ph</i> -P4-Ph)][BF ₄] ₄	127
4.14 Attempted H ₂ /CO Reduction of <i>rac</i> -[Co ₂ (H ₂ O) _x (<i>et</i> , <i>ph</i> -P4-Ph)][BF ₄] ₄	128
4.15 Attempted Zn Reduction of <i>rac</i> -[Co ₂ (H ₂ O) _x (<i>et</i> , <i>ph</i> -P4)][BF ₄] ₄	128
4.16 Hydroformylation of 1-Hexene Attempts with Dicobalt Complexes	128
4.17 References	129
 Chapter 5: Final Conclusion/Future Studies	 130
5.1 Oxidative Cleavage of Alkenes	130
5.2 ³¹ P NMR Studies of Dinickel Complexes' Reactivity with H ₂ O	131
5.3 Synthetic Strides Towards a Bimetallic Cobalt-Carbonyl Catalyst.....	133
5.4 References	136
 Appendix: Additional ¹ H and ³¹ P NMR Data	 137
 Vita	 145

List of Abbreviations

CoSMDPT	Cobalt (II) <i>bis</i> -[3-(salicyclideneamino) propyl] methylamine
COSY	correlation spectroscopy
DCM	dichloromethane
DFT	density functional theory
DMF	N,N-dimethylformamide
DMSO	dimethylsulfoxide
Dppe	1,2-bis(diphenylphosphino)ethane
dppm	1,2-bis(diphenylphosphino)methane
equiv.	Equivalents
GC/MS	gas chromatography/mass spectrometry
¹ H NMR	proton NMR
Hz	Hertz
LC-MS (ESI)	liquid chromatography-mass spectrometry (electrospray ionization)
<i>Meso</i>	<i>mesomeric</i>
mL	milliliters
mM	millimolar (mmol/L)
NMR	nuclear magnetic resonance
ORTEP	Oak Ridge thermal ellipsoid plot program
PBu ₃	tributylphosphine
PEt ₃	triethylphosphine
³¹ P NMR	phosphorus NMR
ppm	parts per million
Psig	pounds per square inch, gauge
<i>Rac</i>	<i>racemic</i>
THF	tetrahydrofuran
TOF	turnover frequencies
Triphos	bis(diphenylphosphinoethyl)phenylphosphine

Abstract

The “old” bimetallic nickel complexes, *meso*- and *rac*-Ni₂Cl₄(*et,ph*-P₄) were investigated as possible “catalysts” for the oxidative cleavage of alkenes using an unsaturated fatty acid, oleic acid, as the substrate. The “new” bimetallic nickel complexes with a stronger chelating tetraphosphine ligand, *meso*- and *rac*-Ni₂Cl₄(*et,ph*-P₄-Ph), were also synthesized and tested for the oxidative cleavage of oleic acid. All four dinickel complexes were found to be active for the oxidative cleavage of oleic acid, producing extremely small amounts of aldehyde product. The Stanley research group also discovered the oxidative cleavage of alkenes using only the “old” *et,ph*-P₄ tetraphosphine ligands with no metal centers.

As a result of this discovery, the oxidative cleavage of oleic acid was attempted with both “old” and “new” tetraphosphine ligands (without metal centers) and found to be active, producing extremely small amounts of aldehyde as well. In attempt to make the system catalytic, some simple phosphine ligands (PPh₃, P(C₆H₁₁)₃, and dppm) and some mono- and bimetallic cobalt complexes were tested for the oxidative cleavage of oleic acid. The phosphine ligands and monometallic cobalt complex, [Co(H₂O)₆][BF₄]₄, found to be active, but still only producing an extremely small amount of aldehyde.

The reactivity of the bimetallic nickel complexes with H₂O was investigated through ³¹P NMR studies and the bridged-hydroxide complexes, *rac*-[Ni₂(μ-OH)Cl₂(*et,ph*-P₄)]⁺ and *meso*- and *rac*-[Ni₂(μ-OH)Cl₂(*et,ph*-P₄-Ph)]⁺ was proposed to be the most stable intermediate during the reaction. Further studies, such as COSY-NMR, are needed to prove this proposal, however.

Numerous synthetic methods were explored to synthesize a bimetallic cobalt carbonyl complex for hydroformylation and aldehyde-water shift catalysis. The first method was the reduction of the dicobalt tetrachloride complexes, *meso*- and *rac*-Co₂Cl₄(*et,ph*-P₄)/(*et,ph*-P₄-Ph),

in the presence of CO using 1:1 H₂/CO, NaBH₄, LAH, LiEt₃BH, Mg, and Zn. Of these reducing agents, Zn resulted in the cleanest reduction by FT-IR analyses, yielding a proposed mixture of the dicationic penta- and hexacarbonyl dicobalt complexes, *meso*- and *rac*-[Co₂(CO)₅₋₆(*et,ph-P4*)/(*et,ph-P4-Ph*)]²⁺. The H₂/CO reduction results indicated that perhaps, a 1:6 H₂/CO, not the 1:1 mixture originally used, would be a more suitable autoclave gas mixture. Future experiments will be performed to test this hypothesis. Experiments using Co₂(CO)₈ resulted in a mixture of cobalt carbonyl complexes, including the formation of [Co(CO)₄]⁻. Preliminary experiments to reduce the non-halide containing dicobalt complexes, [Co₂(H₂O)_x(*et,ph-P4*)/(*et,ph-P4-Ph*)] [BF₄]₂, using 1:1 H₂/CO and Zn resulted in incomplete reductions. Future experiments using a stronger one-electron reducing agent in the presence of CO with an easily isolable by product should be a better synthetic route for the formation of a bimetallic cobalt carbonyl complex.

Chapter 1: Introduction to Oxidative Cleavage of Alkenes and Unsaturated Fatty Acids

1.1 Importance of Industrial Alkene Oxidation

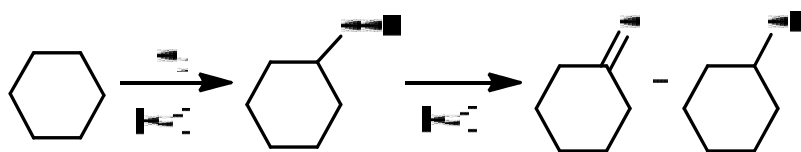
The conversion of aldehydes, ketones, alcohols, and carboxylic acids is important for organic syntheses and industrial applications. In organic syntheses, carbonyl compounds are important precursors for many larger compounds such as proteins and antibodies. In addition, aldehydes, ketones, alcohols, and carboxylic acids are profitable precursors for many industrial applications such as Nylon and plasticizers.^{1,2,3} These important chemicals are usually produced through the oxidation of a starting material, most often an olefin. In fact, the direct oxidation of olefins is an attractive pathway to obtain oxygen-containing intermediates.¹ Upgrades to this industrial process can lead to enhanced production and profitability.⁴

The Stanley group, through the financial support of Sasol, has put much effort and research in pursuit of such transformations, particularly alkene hydration. Alkene hydration is the addition of water to a carbon-carbon double bond to form a primary alcohol and is typically catalyzed by acids, metal oxides, zeolites, and clays.⁴ Following Markovnikov's rule, however, the proton bonds to the less substituted carbon in these processes which makes it very difficult to obtain primary alcohols. Primary alcohols are more industrially profitable given their usefulness in bulk chemical and pharmaceutical manufacturing. Currently indirect protocols to yield the anti-Markovnikov product lead to stoichiometric amounts of unrecyclable boron waste and safety concerns with the use of peroxides for large-scale production.^{4,5} Due to increased environmental and public awareness, "greener" alternatives for traditional chemical manufacturing have become a focus of much catalytic research.²

One such transformation is the production of adipic acid. Adipic acid is produced commercially for the manufacture of Nylon-6. It is also used heavily in the chemical,

pharmaceutical, food, and perfume industries. The traditional method for producing adipic acid is through a two-step oxidation of cyclohexane using nitric acid. In the first step, cyclohexane is catalytically oxidized to a mixture of cyclohexanone and cyclohexanol. This is followed by an oxidation of the mixture using nitric acid to yield the final product, adipic acid. Figure 1.1 shows a diagram depicting this transformation.⁶

Step 1-Cyclohexane Oxidation:



Step 2-Cyclohexanol/Cyclohexanone Oxidation:

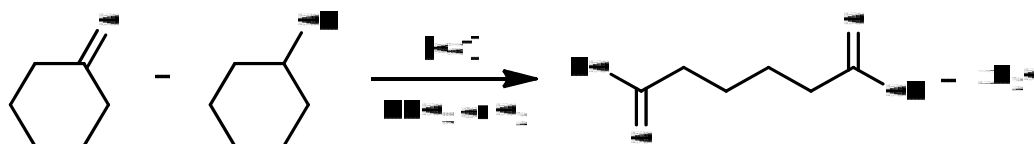


Figure 1.1 Commercial production of adipic acid

Another important commercial transformation is the production of azelaic and pelargonic acids. These acids have many industrial applications such as in plasticizers, Nylons, lubricants, painting materials, and corrosion inhibitors. Azelaic acid has also found application in biological systems as a possible anti-inflammatory and anti-tumoural agent.^{3,7} These acids are commercially produced through the ozonolysis of oleic acid. Oleic acid is a renewable raw material that is widely used in chemical industry.³ In fact, the cleavage of oleic acid to form pelargonic and azelaic acid is the most important industrial application of ozonolysis.⁸ The ozonolysis of oleic acid is a two-step oxidation that proceeds through an unstable ozonide intermediate. This transformation is shown in Figure 1.2.⁶

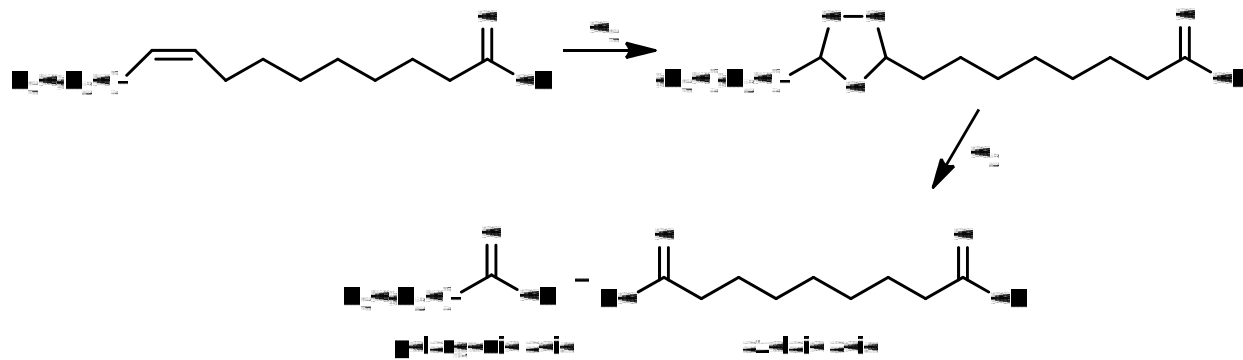


Figure 1.2 Commercial production of azelaic and pelargonic acids

The double bond in unsaturated fatty acids, like oleic acid, provides a very useful point of oxidative attack or cleavage. Ozonolysis provides the advantage of a large scale production of these acids which can easily be reduced to other products and sold as alcohols, aldehydes or amines.⁹

However, the wider use of both commercial processes is hindered by many technical and economical problems.¹⁰ In the production of adipic acid, the use of nitric acid (HNO_3) produces nitrous oxide (N_2O) as a byproduct. N_2O is a pollutant and very effective greenhouse gas contributing to ozone depletion and global warming.¹¹ Commercial ozonolysis of oleic acid involves complex engineering, side reactions, and the serious risk of explosion.¹² Research attempts to replace these processes have limitations and have not succeeded in replacing the commercial production methods. For example, Deng et al.² proposed a direct catalytic oxidation of cyclohexene to adipic acid using hydrogen peroxide (H_2O_2) and a peroxy-tungstate catalyst. This reaction was able to produce more than 90% adipic acid in 24 hours and complete conversion of cyclohexene. However, almost 90% of the total volume of the reaction mixture was 30% H_2O_2 . With such a large volume of H_2O_2 used and slow reaction rates, this system is impractical for commercial use. The authors clearly state, “We are currently investigating...using oxygen or air to replace some of the H_2O_2 .”²

To replace the commercial ozonolysis of oleic acid, a series of ruthenium tetraoxide catalysts using sodium periodate (NaIO_4) as the oxidant and a mixture of solvents have been proposed and tested.^{3,13} These systems have resulted in up to 100% oleic acid conversion in 1 hour using certain co-solvents³ and about 73% yield of azelaic acid in 2 hours.¹³ Despite good results, these techniques utilized multiple solvents, including carbon tetrachloride, which is known to be toxic; and expensive instrumentation such as ultrasound irradiation, which cannot be scaled to commercial production.

1.2 Catalytic Oxidative Cleavage

There have been a few examples of transition metal catalyzed oxidative cleavage with molecular oxygen reported in the literature. Wang *et al.* reported the oxidative cleavage of some terminal and internal alkenes using a $\text{Pd}(\text{OAc})_2$ complex in the presence of a strong acid with yields up to 88%. However, the system operates at high temperature (100°C) and high pressure of O_2 (117 psi).¹⁴

Tokunaga *et al.* reported the oxidative cleavage of aromatic enol ethers using $\text{Cu}(\text{II})$, $\text{Pd}(\text{II})$, and $\text{Ru}(\text{II})$ catalysts. Of the three catalysts, they found the CuCl_2 system to be the most effective yielding up to 86% conversion to ketone under mild conditions. However, this system only works for aromatic enol ethers and has not been demonstrated to be effective for other alkenes.¹⁵ Kaneda *et al.* reported that a RuO_2 catalyst with excess acetaldehyde oxidatively cleaved $\text{C}=\text{C}$ double bonds of terminal alkenes to yield aldehydes. However, the aldehydes would then be further oxidized to the corresponding carboxylic acids.¹⁶

Drago *et al.* reported the most active catalyst for oxidative cleavage of isoeugenol to vanillin and acetaldehyde using a CoSMDPT system (Figure 1.3).

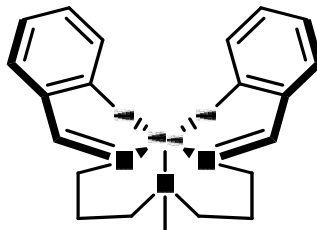


Figure 1.3 Cobalt(II) *bis*-[3-(salicylideneamino)propyl]methylamine, CoSMDPT

The reactions were run at relatively mild conditions, 25°C and 75 psi O₂ utilizing toluene as the solvent. However, the scope of this work has been limited to using isoeugenol as the substrate and has not been reproduced.¹⁷ The Stanley research group is currently pursuing this system for the oxidative cleavage of less activated and simpler alkenes, such as 1-octene.

1.3 Autooxidation of Phosphines and Hydrocarbons

The autooxidation of both phosphines and hydrocarbons has also been well established in the literature. Autooxidation is defined as oxidation that occurs by oxygen gas at normal temperatures without “visible flame or electric spark.”¹⁸ Coordinated and uncoordinated phosphines have been shown to be oxidized at room temperature in the presence of a polar organic solvent under an oxygen atmosphere.^{19,20} Generally the autooxidation of uncoordinated phosphines has been shown to proceed through a radical mechanism yielding mixed phosphine oxide/ester products. However, in the presence of a metal center, the phosphine oxidation gives oxygen adducts that can be replaced with more stable ligands.^{19,20}

Hydrocarbon autooxidation occurs through the activation of molecular oxygen, which is generally accomplished by using light, heat, metallic ions, or some other molecules that decompose to give free radicals under reaction conditions. The reaction proceeds through a radical oxidative attack mechanism beginning with an initiation step (Figure 1.4).

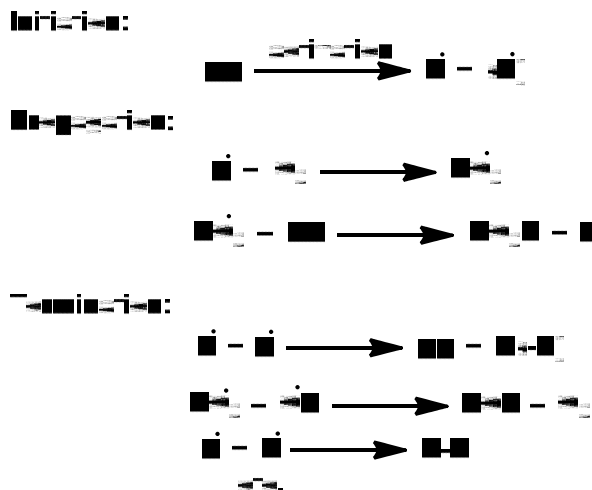


Figure 1.4 General free radical chain mechanism¹⁸

The best known catalysts for liquid-phase autooxidations are soluble transition metal complexes, such as naphthenates and stearates of cobalt, manganese, copper, nickel and iron. These catalysts have been shown to initiate the activation of oxygen and play a role in hydroperoxide decomposition.¹⁸

The autooxidation of fatty acids, including oleic acid, has also been documented in the literature. Saturated and unsaturated fatty acids have been shown to react with molecular oxygen in a mechanism similar to that with hydrocarbons. The reactions are usually run at higher temperatures (above 50°C) and pressures and give various oxidation products, including aldehydes, ketones, carboxylic acids, and esters.²¹ Transition metal catalysts are typically employed for these reactions as well. In fact, cobalt, manganese, lead, and iron can be used for the autooxidation of elaidic acid, the *trans* isomer of oleic acid. Of these catalysts, cobalt was found to be appreciably more active than the other metals. As expected, the C=C double bond of unsaturated fatty acids is the most susceptible to oxidative attack and cleavage.^{22,23}

1.4 Transition Metal-Catalyzed Autooxidations with O₂

A large amount of research has been dedicated to controlling the autooxidation of hydrocarbons using transition metal complexes. Under typical conditions, most organic compounds are kinetically unreactive toward O₂. Oxygen's triplet ground state forbids its direct combination with singlet organic compounds. However, transition metals have multiple spin and oxidation states that are not necessarily subject to this type of restriction. Once molecular oxygen is complexed to a metal center, its properties change and its reactivity toward organic compounds is increased. This leads to direct activation of molecular oxygen which can then be used for catalytic and controlled autooxidation of hydrocarbons and phosphines.²⁴

Homogeneous catalytic oxidations can be separated into four broad categories: free radical autooxidations, attack by oxygen-containing nucleophiles on metal coordinated substrates, oxygen atom transfers, and epoxidation of olefins. One of the major goals in transition metal-controlled autooxidation is the demonstration of oxidation functionalities by the metal-bound O₂. These metal-O₂ adducts have been well studied and are usually reversible.^{25a} However, there are only a limited number of transition metals known that can reversibly interact with molecular oxygen, with iron(II), copper(I), and cobalt(II) being the most studied examples. Cobalt(II) has been noted as the most outstanding of the three to act as an oxygen carrier.²⁶

There are many examples of cobalt-O₂ adducts and their modes of binding in the literature.^{27,28,29,30,31} There are also several examples of oxidation involving these cobalt-O₂ adducts, a few which have been previously discussed. One well-studied transformation is the oxidation of substituted phenols. Phenol oxidation using cobalt complexes and O₂ has been the subject of numerous studies to determine what factors influence this oxidation and what role a cobalt-dioxygen adduct plays in the mechanism.^{25b,c,d,e,f} The reaction can give a wide range of

products depending upon the cobalt complex used in the oxidation. EPR and kinetics studies have provided evidence for a cobalt(II)-O₂ adduct in the mechanism. An example of the mechanism can be seen in Figure 1.5. Step 2 involves the complexation of the Co-O₂ adduct to the phenoxy radical and has been shown to be the rate-determining step.³¹

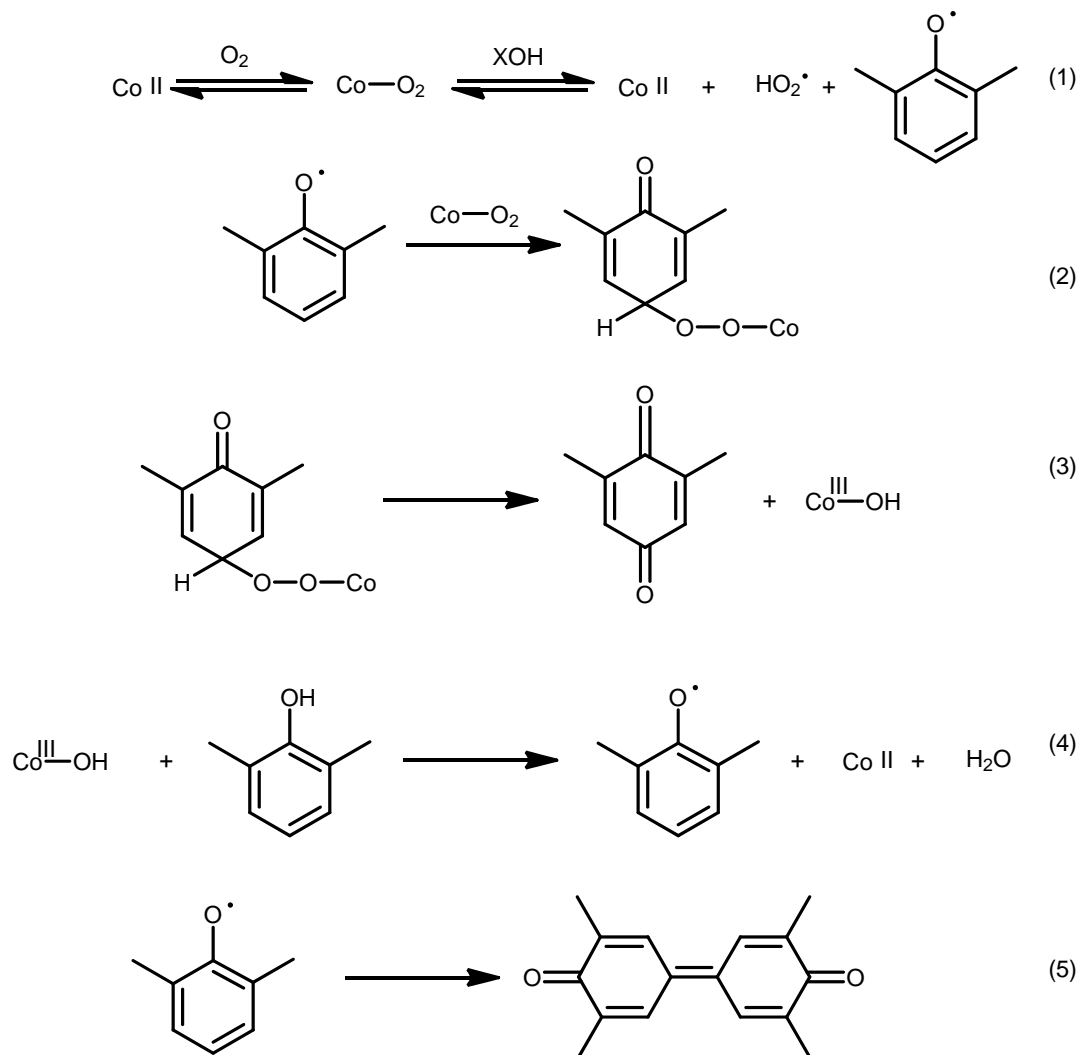


Figure 1.5 Mechanism of a cobalt-dioxygen oxidation of a substituted phenol³¹

Generally, it has been shown that first row transition metals give rise to autooxidation reactions while second and third row metals lead to selective oxidation of olefins. However, a study in which the CoSMDPT (Figure 1.5) catalyst was utilized, along with a primary alcohol solvent and molecular oxygen, found selective oxidation of terminal olefins. 2 products were

observed, the corresponding 2-ketone and 2-alcohol. The lack of peroxide decomposition products provided evidence for a more selective oxidation as opposed to an autooxidation.³¹

1.5 Alkene Oxidative Cleavage

While attempting alkene hydration of 1-hexene, the Stanley group discovered, and has been able to demonstrate, the oxidative cleavage of alkenes using O₂ and dinickel tetrachloride-tetraphosphine complexes: *rac*- or *meso*-Ni₂Cl₄(*et*,*ph*-P₄), which are shown in Figure 1.6.

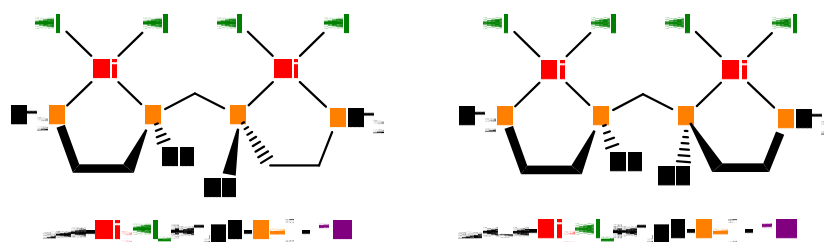


Figure 1.6 *meso*- and *racemic*-Ni₂Cl₄(*et*,*ph*-P₄)

This reaction has shown a tolerance for a variety of different substrates, some with terminal and some with internal alkene functional groups. In addition, this reaction is performed under

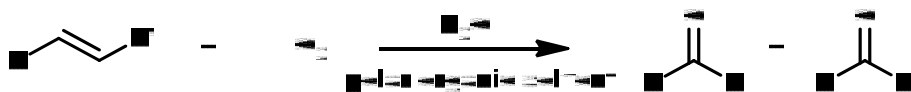


Figure 1.7 Oxidative Cleavage of Alkenes

“green” or mild reaction conditions using only an H₂O/polar organic solvent mixture and balloon pressure (1-2 psig) O₂ as the oxidant. A typical reaction scheme for the oxidative cleavage of alkenes using this method is shown in Figure 1.7. This reaction, however, is not catalytic and produces only a small amount of aldehyde.

1.6 History of Alkene Oxidative Cleavage in the Stanley Lab

Since the discovery of alkene oxidative cleavage in the Stanley group, much effort has been put into making the system more effective and, possibly, catalytic. Dr. William Schreiter, a

previous member of the Stanley group, established the importance of water to the reaction through a series of NMR experiments.³² At least 5% water is required for the formation of the aldehyde. Without water present, no aldehyde would be formed. Several different alkene substrates were tested for oxidative cleavage using these bimetallic nickel complexes, and their corresponding aldehydes were detected via ¹H NMR and GC/MS (Figure 1.8).

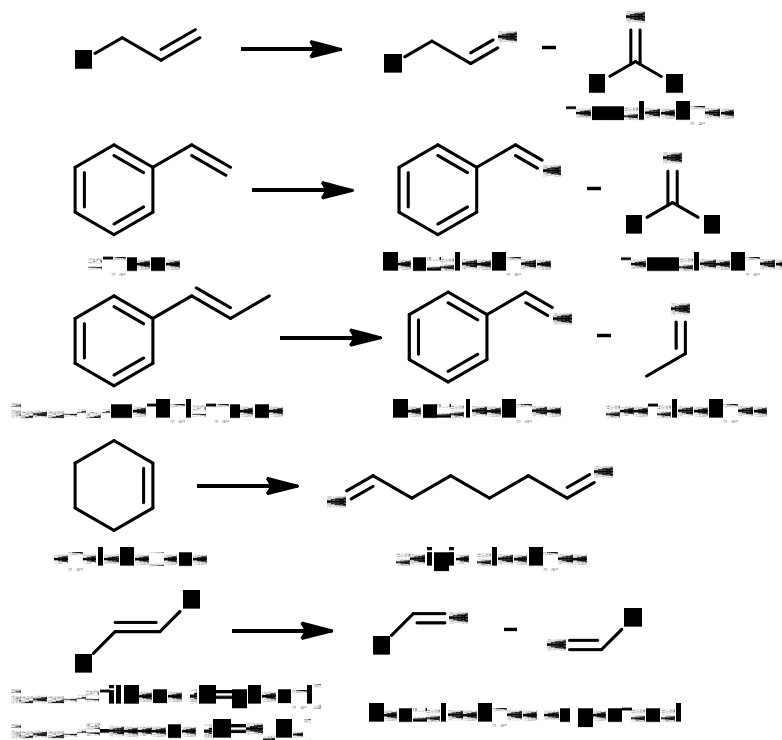


Figure 1.8 Some substrates tested for oxidative cleavage and their products³²

Since the reaction is not catalytic, several reaction conditions were also adjusted in attempt to make the reaction catalytic. First, the reactions were run under higher O₂ pressures (50-100 psi) and the organic solvent systems were varied. Under higher pressures, the aldehyde would be produced in 1-2 hours, much quicker than under air or O₂ balloon pressure. However, the amount of aldehyde would not increase over time. Acetone, acetonitrile (CH₃CN), DMSO, methanol (MeOH), ethanol (EtOH), THF and DMF were all tested as possible solvents for the reaction. The amounts of aldehyde produced in most of the solvents were the same. THF and DMF showed no

production of aldehyde. DMSO showed production of aldehyde with and without water. Presumably, the DMSO was not properly dried and contained at least 5% water.³²

Several additives were also used to narrow down the type of oxidation occurring in these reactions. Radical inhibitors were one of the first additives tested. Free radicals are present during the course of the reactions, such as autooxidation. Radical inhibitors can slow down or completely suppress the oxidation in many of these reactions. In the case of our oxidative cleavage reactions, smaller amounts of inhibitor slowed down the reaction while larger amounts (more than 10 moles, relative to the complex) completely suppressed the reactivity. This result was the first hint that the reaction mechanism had some radical character.³²

NaCl and some other metal salts containing chloride ligands were also added to determine if the reactivity between the starting complex and water involved some chloride ligand dissociation. Since water reacted with the complex to form new species that could only be present through chloride ligand dissociation, which corresponds with the production of the aldehyde, the addition of NaCl should slow down the reaction and lead to more aldehyde production. However, this was not the case. While the reactivity did either slow down or was completely suppressed in some cases, the amount of aldehyde did not increase.³²

Several other additives, such as acids, bases, reducing agents, phosphine ligands, and metal salts were also tested in attempt to make the reaction catalytic. Acetic, ascorbic, and malonic acids were some of the acids tested, as these weak acids (ascorbic and malonic) can act as reducing agents as well. 10 moles of acetic acid and malonic acid had no effect on the reaction, and 10 moles of ascorbic acid completely suppressed the reaction. Cesium hydroxide (CsOH) and potassium carbonate (K₂CO₃) were some of the bases tested as additives. With the addition of these bases, the reaction did not occur at all.³²

Alcohols (ethanol, 2-propanol, and 1-butanol), aldehydes (propanal and isobutyraldehyde), ascorbic acid, malonic acid, and potassium oxalate ($K_2C_2O_4$) were all tested as reducing agents for the reaction. The broad resonances present on the ^{31}P NMR were initially believed to be caused by paramagnetic Ni complexes formed during the oxidative cleavage reaction. It was theorized that these agents could reduce the oxidized complex back to the active species. However, this was not the case. The alcohols and aldehydes caused no change in the reaction. The addition of $K_2C_2O_4$ led to decomposition of the starting complex.³²

The addition of other phosphine ligands (PPh_3 and dppe) were tested to see if any increase in the amount of aldehyde production would occur. With the addition of up to 10 moles of the phosphine ligand, there was no increased amount of aldehyde produced. In some cases the reaction did not occur at all. The other metal salts tested for the reaction had no effect ($Fe(BF_4)_2$), slowed down, or completely hindered the reaction ($CuCl$ and $CoCl_2$).³²

Chelating nitrogen ligands were tested with Ni salts to determine if they would be active for oxidative cleavage (Figure 1.9). Using balloon pressure O_2 , none of the complexes showed any activity for oxidative cleavage via GC/MS or NMR analysis.

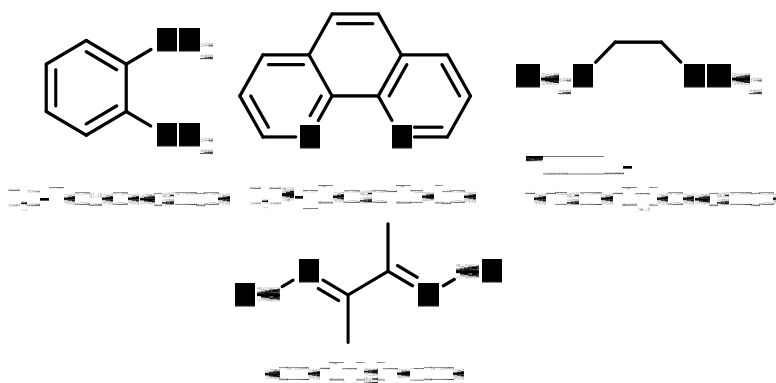


Figure 1.9 Chelating nitrogen ligands tested for oxidative cleavage³²

A few other transition metal/phosphine complexes were tested for oxidative cleavage as well. Specifically, *trans*- $PdCl_2(PPh_3)_2$, *cis*- $PtCl_2(PPh_3)_2$, $RhCl(PPh_3)_3$, and metal salt/dppe

combinations of CoCl_2 , $\text{Fe}(\text{BF}_4)_2$, CuSO_4 , and RhCl_3 were tested. As with the Ni salts, none of these complexes/combinations produced any aldehyde products.³²

A series of monometallic nickel complexes were tested for use as a possible oxidative cleavage catalyst. The complexes tested were $\text{NiCl}_2(\text{dppe})$, $\text{NiCl}_2(\text{dppp})$, $\text{NiCl}_2(\text{PPh}_3)$, and $\text{NiCl}_2(\text{dcpe})$. When these reactions were tested at either balloon pressure or high pressure O_2 , the only complex that did not produce some aldehyde was $\text{NiCl}_2(\text{PPh}_3)$. Very little aldehyde, less than what we produce with our bimetallic nickel complexes, was formed with these monometallic complexes. In some cases the amounts produced were so small, that Dr. Schreiter was not able to definitively identify whether any product was formed via GC/MS or ^1H NMR.³²

1.7 Mechanistic Possibilities and Beyond

As a result of this previous work, Dr. Stanley proposed two possible mechanisms for the oxidative cleavage of alkenes using bimetallic nickel complexes. The first proposed mechanism (Figure 1.10) involves the direct coordination of the alkene to one of the nickel metal centers through dissociation of one of the chloride ligands. This is followed by a migratory insertion of the bridging peroxide ligand to the alkene. A subsequent series of electron transfers and rearrangements leads to the two aldehyde products.

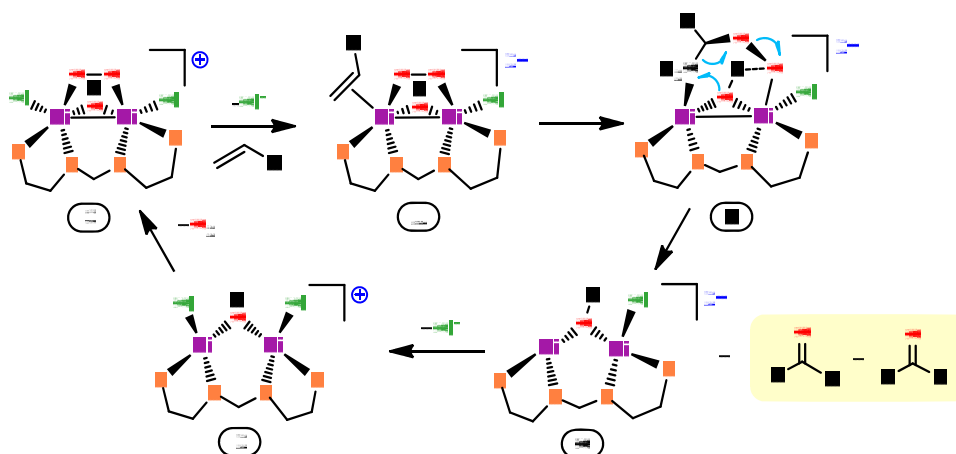


Figure 1.10 First proposed mechanism

The second proposed mechanism (Figure 1.11) involves an alkene directly interacting with the bridging peroxide ligand. This interaction leads to a dioxetane ring via a cycloaddition. Rearrangement of the ring subsequently leads to the two aldehyde products.

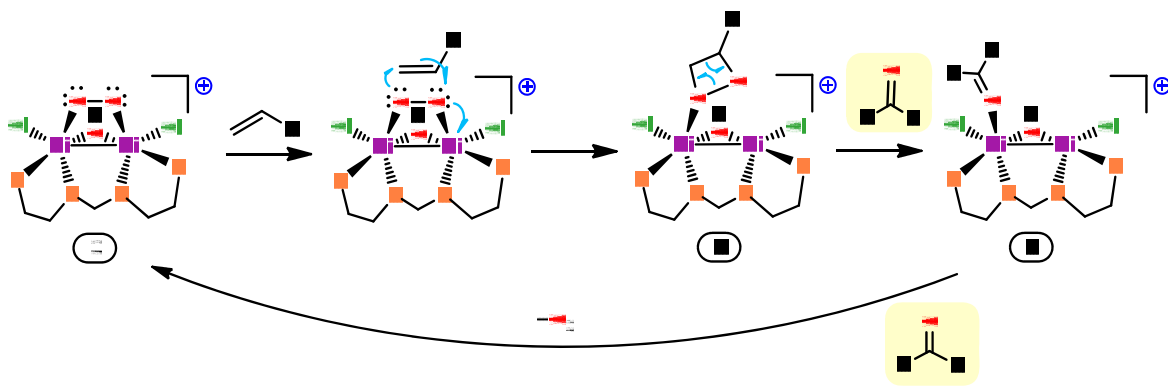


Figure 1.11 Second proposed mechanism

Neither of these mechanisms are supported by any spectroscopic evidence. DFT calculations using Gaussian were performed on the peroxo- and hydroxo-bridged dinickel complex (Structure 3 in Figure 1.12), which optimized nicely and led to Dr. Stanley's proposal of the mechanisms. Structure 3 is the result of the predicted reaction between *meso*-Ni₂Cl₄(*et,ph*-P4) with water and O₂ (Figure 1.12). Schreiter believed there is some NMR evidence for this structure³²; however, this evidence is based on the previously characterized hydroxide bridged complex, [Ni₂Cl₂(μ-OH)(*meso-et,ph*-P4-Ph)]⁺ shown in Figure 1.13.

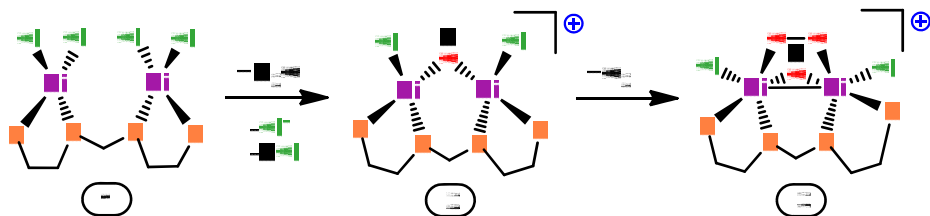


Figure 1.12 Proposed reaction between *meso*-Ni₂Cl₄(*et,ph*-P4) with H₂O and O₂

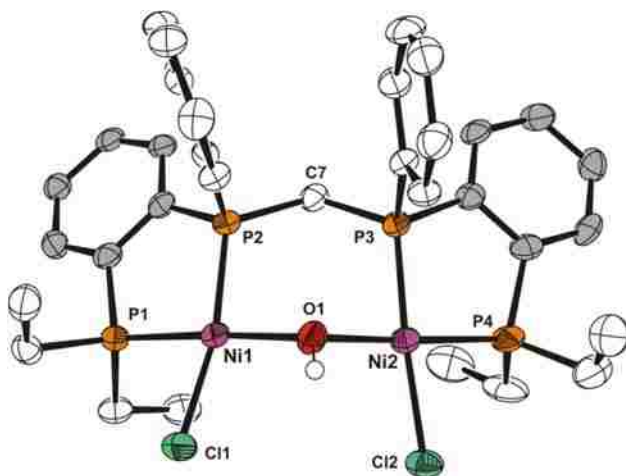


Figure 1.13 ORTEP plot of $[\text{Ni}_2\text{Cl}_2(\mu\text{-OH})(\textit{meso}\text{-et,ph-P4-Ph})]^+$

One of the biggest differences between the two mechanisms is that the first involves the direct coordination of the alkene to the Ni metal center and the second involves only an interaction between the alkene and bridging peroxide ligand. Since several different alkenes, including the 18-carbon chain oleic acid, were used for this reaction, steric factors would influence their direct binding to the Ni metal center. This led to the conclusion that the second mechanism was more plausible choice of the two proposed schemes.

During the oxidative cleavage of alkenes using the bimetallic nickel complexes, ^{31}P NMR analysis revealed the presence of two broad resonances (Figure 1.14). The resonances only appeared in the presence of both water and O_2 and corresponded with the production of the aldehyde, indicating that they were linked with the oxidative cleavage reaction.

Through a series of ^{31}P NMR experiments, Schreiter proved that the broad resonances were caused by an interaction between the tetrakisphosphine oxide and NiCl_2 , shown in Figure 1.15. During the course of the reaction, the phosphine ligand becomes completely oxidized and forms an inactive species. The inactive species was identified by the presence of a green solid that would form through the course of the reaction. Through further NMR analysis, this inactive species was shown to be $\textit{meso}\text{-}[\text{Ni}_2(\mu\text{-Cl})(\textit{et,ph-P4})_2]^{3+}$ (Figure 1.16).³²

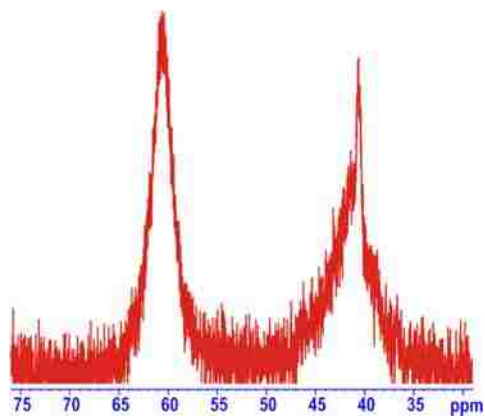


Figure 1.14 ^{31}P NMR spectrum of *meso*- $\text{Ni}_2\text{Cl}_4(\text{et,ph-P4})$ after the oxidative cleavage reaction³²

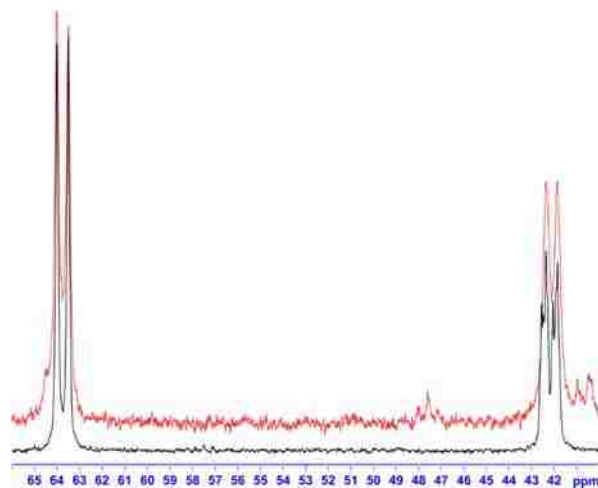


Figure 1.15 Comparison between the tetraphosphine oxide/ NiCl_2 (black spectrum) dissolved in D_2O and the green solid dissolved in D_2O (red spectrum)³²

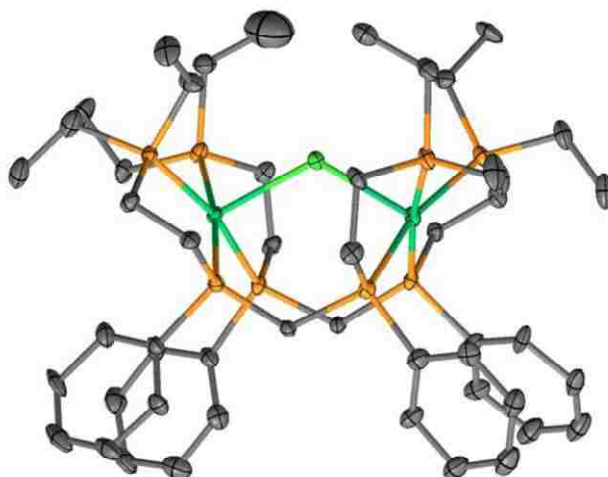


Figure 1.16 ORTEP plot of *meso*- $[\text{Ni}_2(\mu\text{-Cl})(\text{et,ph-P4})_2]^{3+}$

Complete oxidation of the phosphine ligand shuts down the production of the aldehyde, which keeps the system from becoming catalytic. The ethylene linkage connecting the two phosphorus groups of the ligand is not as strongly chelating as initially thought and has posed problems for hydroformylation in our group in the past as well. With these issues in mind, a “new”, stronger chelating ligand was synthesized by Dr. Alex Monteil, a previous member of the Stanley group.³³ This ligand replaces the ethylene linkage with a phenylene linkage, thus providing stronger coordination to the metal centers (Figure 1.17). It is similar to the old one in that it is also diastereomeric, with *rac* and *meso* forms. Optimization of the synthesis and separation of the diastereomers through column chromatography was performed by Dr. Katerina Kalachnikova and the Stanley group.

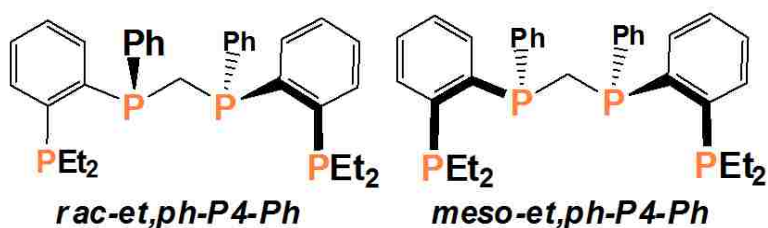


Figure 1.17 *meso*- and *racemic*-et,ph-P4-Ph

Dinickel complexes using this “new” ligand were synthesized and used for the oxidative cleavage of alkenes. Dr. Stanley proposed that the stronger chelation provided by the new ligand would prevent the complete oxidation of the ligand and perhaps make the system catalytic. However, these new dinickel complexes were not found to produce any aldehyde products. This indicated the significance of the oxidation of the phosphine to the reactivity of this system.

Initially, studies indicated the reaction would not occur without the Ni metal centers present. However, NMR analysis performed by Kalachnikova revealed that no free phosphine oxide was formed during the reaction. The only signals present were the two broad resonances, shown above in Figure 1.14, which corresponded to the interaction between the phosphine oxide

and Ni metal centers (Figure 1.15). As a result, she studied the reaction of our tetraphosphine ligand, et,ph-P4, with O₂ through a series of NMR experiments. Her experiments showed that upon exposure to air for up to 8 days, around 68% by integration of the ³¹P signals were due to unreacted et,ph-P4. This indicated the ligand was not as air sensitive as previously assumed.³⁴

The stability of the ligand in air and the lack of free phosphine oxide formed during the oxidative cleavage reactions with the dinickel complexes led to studies with only free et,ph-P4 ligand and no Ni centers. Surprisingly, these reactions produced a small amount of aldehyde products with H₂O and O₂. Without O₂ present, no aldehyde was formed.³⁴ Reactions with the “new” tetraphosphine ligand et,ph-P4-Ph only were also performed and will be discussed in Chapter 2. The presence of aldehyde without the metal centers was another piece of evidence pointing towards an autooxidation type of mechanism.

1.8 Oxidative Cleavage of Unsaturated Fatty Acids

The focus of this research was geared toward finding a suitable catalyst or catalytic conditions in the Stanley group to oxidatively cleave unsaturated fatty acids. The industrial use of fatty oils as opposed to petroleum-based resources is important for economical and ecological reasons as stated previously.^{12,35} Oleic acid, oleic acid methyl ester, and ricinoleic acid were used since they are among the simplest of the fatty acids, bearing 18 carbons with one double bond at the carbon 9 position. The products of the oxidative cleavage of oleic acid, nonanal and 9-oxononanoic acid bear a strong resemblance to the carboxylic acids formed from the commercial ozonolysis of oleic acid. Pelargonic acid is the carboxylic acid derivative of nonanal, and azelaic acid is the dicarboxylic acid derivative of 9-oxononanoic acid. The oxidative cleavage of oleic acid and its methyl ester are shown in Figure 1.18, and the oxidative cleavage of ricinoleic acid can be found in Figure 1.19.

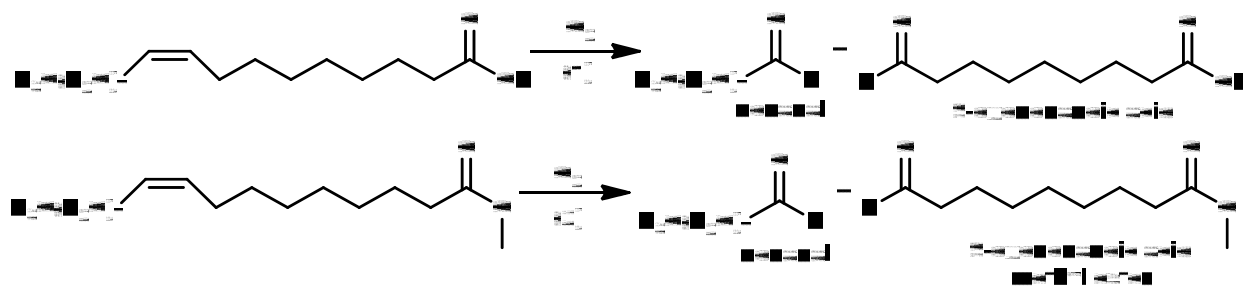


Figure 1.18 Oxidative cleavage of oleic acid (1) and oleic acid methyl ester (2)

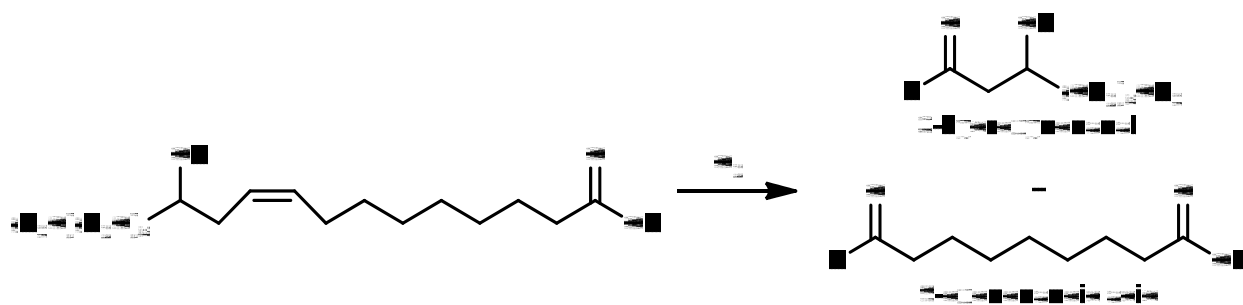


Figure 1.19 Oxidative cleavage of ricinoleic acid

Oleic acid methyl ester was synthesized separately using a commercially available acid catalyst, Amberlyst-15, through an esterification reaction. The purpose of using the methyl ester was to counteract the effects associated with the weak acidity of the carboxylic acid and possible coordination of the carboxyl group to one of the nickel metal centers. Amberlyst-15 is an inexpensive heterogeneous catalyst that is easy to handle, can be reused at least 3 times, gives enhanced reaction rates and good selectivity, and requires simple work-up conditions.¹⁰ The reaction scheme is depicted in Figure 1.20.

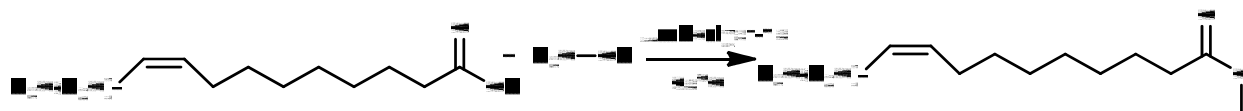


Figure 1.20 Esterification of oleic acid

Ricinoleic acid differs from oleic acid in that it contains an alcohol functional group at the carbon-12 position. Interest in whether the hydroxyl group would inhibit the reactivity of the

double bond at the carbon-9 position led to oxidative cleavage studies. Ricinoleic acid has found applications as pigments, dye dispersers in ink, textile finishing, and dry-cleaning soaps. Its main use is as an intermediate to produce other oleochemicals.³⁶ Ricinoleic acid is produced through the saponification of castor oil. Castor oil is composed of many fatty acid triglycerides with ricinoleic acid at about 90% of its composition. Castor oil is one of the few naturally occurring triglycerides that is close to being a pure compound and is the only major vegetable oil that is composed mainly of the triglyceride of a hydroxy acid. Ricinoleic acid gives castor oil its unique properties and versatility.³⁷ Castor oil is also inexpensive, environmentally-friendly, and has health benefits as a laxative and labor- inducer.^{38,39}

The isolation of ricinoleic acid from castor oil is done through an adapted saponification and acidification procedure.⁴⁰ Once the ricinoleic acid was isolated and purified, it was reacted with O₂ and the dinickel complexes. All three of these fatty acids were tested for oxidative cleavage using the bimetallic nickel complexes. However, they were only shown to produce a small amount of aldehyde as well.

1.9 References

1. Cho, Y.; Lee, D.; Lee, H.; Kim, K.; Park, Y. Catalytic Activities of Pt(II), Pd(II) and Ni(II)-diphosphine Complexes for Styrene Oxidation. *Bull. Korean Chem. Soc.* **1997**, *18*, 334-336.
2. Deng, Y.; Ma, Z.; Wang, K.; Chen, J. Clean Synthesis of Adipic Acid by Direct Oxidation of Cyclohexene with H₂O₂ over Peroxytungstate-Organic Complex Catalysts. *The Royal Society of Chemistry.* **1999**, 275-276.
3. Rup, S.; Zimmerman, F.; Meux, E.; Schneider, M.; Sindt, M.; Oget, N. The Ultrasound-Assisted Oxidative Scission of Monoenic Fatty Acids by Ruthenium Tetraoxide Catalysis: Influence of the Mixture of Solvents. *Ultrason. Sonochem.* **2009**, *16*, 266-272.
4. Kolodziej, R.; Dutt, S. Improve Direct Hydration Processes: Technology Enhancements Increase Yields and Decrease Capital Costs of Making Alcohols. *Hydrocarbon Processing*. [Online] **2001**, 103-110.
5. Dong, G.; Teo, P.; Wickens, Z. K.; Grubbs, R. H. Primary Alcohols from Terminal Olefins: Formal Anti-Markovnikov Hydration via Triple Relay Catalysis. *Science.* **2011**, *333*, 1609-1612.

6. Weissermel, K.; Arpe, H. J. *Industrial Organic Chemistry*, 2nd ed.; VCH Publishers, Inc.: New York, 1993; pp 204-239.
7. Breathnach, A. S. Azelaic acid: potential as a general antitumoural agent. *Medical Hypotheses*. **1999**, *53*, 221-226.
8. Biermann, U.; Griedt, W.; Lang, S.; Luhs, W.; Machmuller, G.; Metzger, J. O.; Klaas, M. R.; Schafer, H. J.; Schneider, M. P. New Syntheses with Oils and Fats as Renewable Raw Materials for the Chemical Industry. *Angew. Chem. Int. Edit.* **2000**, *39*, 2206-2224.
9. Baumann, H.; Buhler, M.; Fochem, H.; Hirsinger, F.; Zobelein, H.; Falbe, J. Natural Fats and Oils—Renewable Raw Materials for the Chemical Industry. *Angew. Chem. Int. Edit.* **1988**, *27*, 41-62.
10. Chari, M. A. Amberlyst-15: an efficient and reusable catalyst for multi-component synthesis of 3,4-dihydroquinoxalin-2-amine derivatives at room temperature. *Tetrahedron Lett.* **2011**, *52*, 6108-6112.
11. Sato, K.; Masao, A. A "Green" route to adipic acid: direct oxidation of cyclohexenes with 30 percent hydrogen peroxide. *Science*. **1998**, *281*, 1646-1652.
12. Dapurkar, S. E.; Kawanami, H.; Yokoyama, T.; Ikushima, Y. Catalytic Oxidation of Oleic Acid in Supercritical Carbon Dioxide Media with Molecular Oxygen. *Top. Catal.* **2009**, *52*, 707-713.
13. Zimmerman, F.; Meux, E.; Mieloszynski, J.; Lecuire, J.; Oget, N. Ruthenium Catalysed Oxidation without CCl₄ of Oleic Acid, Other Monoenic Fatty Acids and Alkenes. *Tetrahedron Lett.* **2005**, *46*, 3201-3203.
14. Wang, A.; Jiang, H. Palladium-Catalyzed Direct Oxidation of Alkenes with Molecular Oxygen: General and Practical Methods for the Preparation of 1,2-Diols, Aldehydes, and Ketones. *J. Org. Chem.* **2010**, *75*, 2321-2326.
15. Tokunaga, M.; Shirogane, Y.; Aoyama, H.; Obora, Y.; Tsuji, Y. Copper-catalyzed oxidative cleavage of carbon-carbon double bond of enol ethers with molecular oxygen. *J. Organomet. Chem.* **2005**, *690*, 5378-5382.
16. Kaneda, K.; Haruna, S.; Imanaka, T.; Kawamoto, K. Ruthenium-catalysed oxidative cleavage reaction of carbon-carbon double bonds using molecular oxygen. *J. Chem. Soc., Chem. Commun.* **1990**, *21*, 1467-1468.
17. Drago, R. S.; Corden, B. B.; Barnes, C. W. Novel cobalt(II)-catalyzed oxidative cleavage of a carbon-carbon double bond. *J. Am. Chem. Soc.* **1986**, *108*, 2453-2454.
18. Frank, C. E. Hydrocarbon Autoxidation. *Chem. Rev.* **1950**, *46*, 155-169.
19. Yoke, J. T.; Schmidt, D. D. Autoxidation of a coordinated trialkylphosphine. *J. Am. Chem. Soc.* **1971**, *93*, 637-640.
20. Buckler, S. A. Autoxidation of Trialkylphosphines. *J. Am. Chem. Soc.* **1962**, *84*, 3093-3097.
21. Brodnitz, M. H. Autoxidation of Saturated Fatty Acids. A Review. *J. Agr. Food Chem.* **1968**, *16*, 994-999.

22. Ellis, G. W. Autoxidation of the fatty acids: The oxygen uptake of elaidic, oleic and stearic acids. *Biochem. J.* **1932**, *26*, 791-800.
23. Ellis, G. W. Autoxidation of the fatty acids: Oxido-elaidic acid and some cleavage products. *Biochem. J.* **1936**, *30*, 753-761.
24. Hanzlik, R. P.; Williamson, D. Oxygen activation by transition metal complexes. 2. Bis(acetylacetonato)cobalt(II)-catalyzed oxidation of tributylphosphine. *J. Am. Chem. Soc.* **1976**, *98*, 6570-6573.
25. (a) Zombeck, A.; Drago, R. S.; Corden, B. B.; Gaul, J. H. Activation of Molecular Oxygen. Mechanistic Studies of the Oxidation of Hindered Phenols with Cobalt-Dioxygen Complexes. *J. Am. Chem. Soc.* **1981**, *103*, 7580-7585. (b) Vogt, L. H.; Wirth, J. G.; Finkbeiner, H. L. Selective Autooxidation of Some Phenols Using Bis(salicylaldehyde)ethylenediiminecobalt Catalysts. *J. Org. Chem.* **1969**, *34*, 273-277. (c) Tomaja, D. L.; Vogt, L. H.; Wirth, J. G. Autooxidation of Some Phenols Catalyzed by Ring-Substituted Salcomines. *J. Org. Chem.* **1970**, *35*, 2029-2031. (d) Kothari, V. P.; Tazuma, J. J. Selective Autooxidation of Some Phenols Using Salcomines and Metal Phthalocyanines. *J. of Catal.* **1976**, *41*, 180-189. (e) Nishinga, A.; Nishizawa, K.; Tomita, H.; Matsuura, T. *J. Am. Chem. Soc.* **1977**, *99*, 1287-1288. (f) White, L. S.; Que, L. Cobalt-Catalyzed Oxidative Cleavage of Semiquinones. *J. of Mol. Catal.* **1985**, *33*, 139-149.
26. Ralph G, W. Uptake of Oxygen by Cobalt(II) Complexes in Solution. *Bioinorg. Chem.* **1971**, *100*, 111-134.
27. Gavrilova, A. L.; Qin, C. J.; Sommer, R. D.; Rheingold, A. L.; Bosnich, B. Bimetallic Reactivity. One-Site Addition Two-Metal Oxidation Reaction of Dioxygen with a Bimetallic Dicobalt(II) Complex Bearing Five- and Six-Coordinate Sites. *J. Am. Chem. Soc.* **2001**, *124*, 1714-1722.
28. Saum, S. E.; Askham, F. R.; Fronczek, F. R.; Stanley, G. G. Reaction of Oxygen with a Binuclear Cobalt(II) Hexaphosphine Complex. Single-crystal X-ray Structure of an Extended Chain Cobalt (II) Hexaphosphine Oxide System. *Polyhedron.* **1988**, *7*, 1785-1788.
29. Bakac, A.; Espenson, J. H. Formation and Homolysis of a Mononuclear Cobalt-Oxygen Adduct. *J. Am. Chem. Soc.* **1990**, *112*, 2273-2278.
30. Tovrog, B. S.; Kitko, D. J.; Drago, R.S. Nature of the Bound Oxygen in a Series of Cobalt Dioxygen Adducts. *J. Am. Chem. Soc.* **1976**, *98*, 5144-5153.
31. Bailey, C. L.; Drago, R. S. Utilization of O₂ for the Specific Oxidation of Organic Substrates with Cobalt(II) Catalysts. *Coord. Chem. Rev.* **1987**, *79*, 321-332.
32. Schreiter, W. J. *Investigations into Alkene Hydration and Oxidation Catalysis*. Ph.D. Dissertation, Louisiana State University, Baton Rouge, May **2013**.
33. Monteil, A. R. *Investigation into the Dirhodium-Catalyzed Hydroformylation of 1-Alkenes and Preparation of a Novel Tetrphosphine Ligand*. Ph.D. Dissertation, Louisiana State University, Baton Rouge, December **2006**.

34. Kalachnikova, E. *Improved Synthesis, Separation, Transition Metal Coordination and Reaction Chemistry of a New Binucleating Tetrphosphine Ligand*. Ph.D. Dissertation, Louisiana State University, Baton Rouge, May **2015**.
35. Kadhun, A. A. H.; Wasmi, B. A.; Mohamad, A. B.; Al-Amiery, A. A.; Takriff, M. S. Preparation, Characterization, and Theoretical Studies of Azelaic Acid Derived from Oleic Acid by Use of a Novel Ozonolysis Method. *Res. Chem. Intermed.* **2012**, *38*, 659-668.
36. Puthli, M. S.; Rathod, V. K.; Pandit, A. B. Enzymatic Hydrolysis of Castor Oil: Process Intensification Studies. *Biochem. Eng. J.* **2006**, *31*, 31-41.
37. Naughton, F.C. Production, Chemistry, and Commercial Applications of Various Chemicals from Castor Oil. In *Novel Uses of Agricultural Oils*, Presented in Symposium at the AOCS Spring Meeting, New Orleans, LA, April 1973; *J. Am. Oil Chem. Soc.* **1973**, *51*, 65-71.
38. Ogunniyi, D.S. Castor Oil: A Vital Industrial Raw Material. *Bioresour. Technol.* **2006**, *97*, 1086-1091.
39. Williams, S.C.P. Castor Oil's Health Benefits Tied to Ricinoleic Acid Chemistry. *Huff Post Science* [Online] **2012**. http://www.huffingtonpost.com/2012/05/21/castor-oils-health-benefits-ricinoleic-acid_n_1534787.html (accessed July 11, 2012).
40. Vaisman, B.; Shikanov, A.; Domb, A.J. The Isolation of Ricinoleic Acid from Castor Oil by Salt-solubility-based Fractionation for the Biopharmaceutical Applications. *J. Am. Oil Chem. Soc.* **2008**, *85*, 169-184.

Chapter 2: Investigations into Nickel-Phosphine and Cobalt Mediated Oxidative Cleavage of Unsaturated Fatty Acids

2.1 Background

While studying alkene hydration of 1-hexene using *meso*-Ni₂Cl₄(*et,ph*-P₄), the Stanley group discovered the oxidative cleavage of a C=C double bond to yield two aldehyde products. The reactions were not catalytic and only produced a small amount of aldehyde. As previously described, it was believed the reaction would only occur with these complexes and in the presence of water. Schreiter demonstrated that water and O₂ react with *meso*-Ni₂Cl₄(*et,ph*-P₄) to form the double ligand species, *meso*-[Ni₂(μ-Cl)(*et,ph*-P₄)₂]³⁺ (Figure 1.16) which was not active for the oxidative cleavage of alkenes. As a result of the weaker chelation of the old ligand, *et,ph*-P₄, a “new” stronger chelating tetrphosphine ligand, *et,ph*-P₄-Ph (Figure 1.17) was synthesized and its diastereomers were separated via column chromatography. Dinickel complexes with this ligand were synthesized and tested for oxidative cleavage of alkenes. Initially, these complexes were not shown to be active for oxidative cleavage under the same conditions.

NMR studies by Kalachnikova performed on the old ligand, *et,ph*-P₄, revealed that it was more air stable than initially believed. Furthermore, she proposed that just the old P₄ ligand was involved in the O₂ activation and oxidative cleavage. As a result, oxidative cleavage reactions were run with only the ligand (no metals) to determine if any reactivity would occur. To our surprise, a small amount of aldehyde was produced with only the ligand in the presence of O₂ or air and water. As with the dinickel complexes, the use of pure O₂ enhanced the reactivity time of the oxidative cleavage reactions but not the amount of aldehyde production; the reactions were still not catalytic.

The oxidative cleavage of oleic acid and similar unsaturated fatty acids was performed to test the viability and industrial usefulness of the reaction. The reactions were initially done with the bimetallic nickel complexes, *meso*- and *rac*-Ni₂Cl₄(*et,ph*-P₄). Once the new ligand was

available, the oxidative cleavage of oleic acid was attempted using these bimetallic nickel complexes. The reactions were also performed using only the tetrakisphosphine ligands (both the new and old) with no metals present. A series of monometallic and bimetallic cobalt complexes and some simpler, commercially available phosphine ligands were tested to determine if the reaction could be made catalytic or produce a more appreciable amount of aldehyde.

2.2 Results and Discussion

The oxidative cleavage of some simple alkenes was performed using 10 mM *meso*- or *rac*-Ni₂Cl₄(*et*,*ph*-P₄), 10 or 15% H₂O/polar organic solvent system, 30 or 40 equiv. of alkene, and O₂ balloon pressure for approximately 24 hours. Each reaction was then analyzed by GC/MS for the presence of aldehyde products. A list of the alkenes and their corresponding aldehyde products can be found in Figures 2.1 and 2.2. These alkenes contain a mixture of some terminal and some internal C=C bonds. The results revealed that the dinickel complexes were able to oxidatively cleave both terminal and internal C=C bonds under very mild pressures (~15 psi O₂) and at room temperature (~25°C). 1-hexene, cyclohexene, α -methylstyrene and styrene all showed the presence of small amounts of aldehyde products via GC/MS using 15% H₂O/acetone solvent mixture. 1-octene, *trans*-5-decene, and *trans*-4-nonene also showed the presence of small amounts of aldehyde products via GC/MS using 10 or 15% H₂O and acetone or acetonitrile (CH₃CN). The oxidative cleavage of 1-dodecene was inconclusive. Long chain hydrocarbons, like 1-dodecene, have poor solubility in polar organic solvents like acetone and CH₃CN. The amount of dinickel complex used in these reactions remained consistent (10 mM), while the amount of aldehyde produced was found, using 1-hexene as the substrate, to be only about 3 mM.¹ The results are reproducible for most of the alkenes, except cyclopentene and 1-dodecene as previously discussed. Water and O₂ must be present for the reaction to occur.

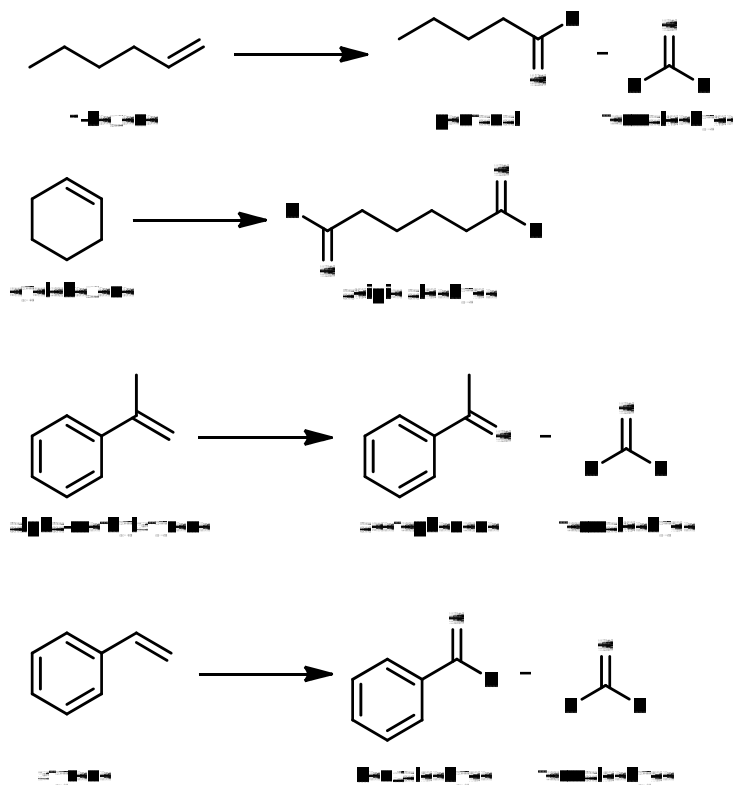


Figure 2.1 Oxidative cleavage reactions of 1-hexene, cyclohexene, styrene, and α -methylstyrene

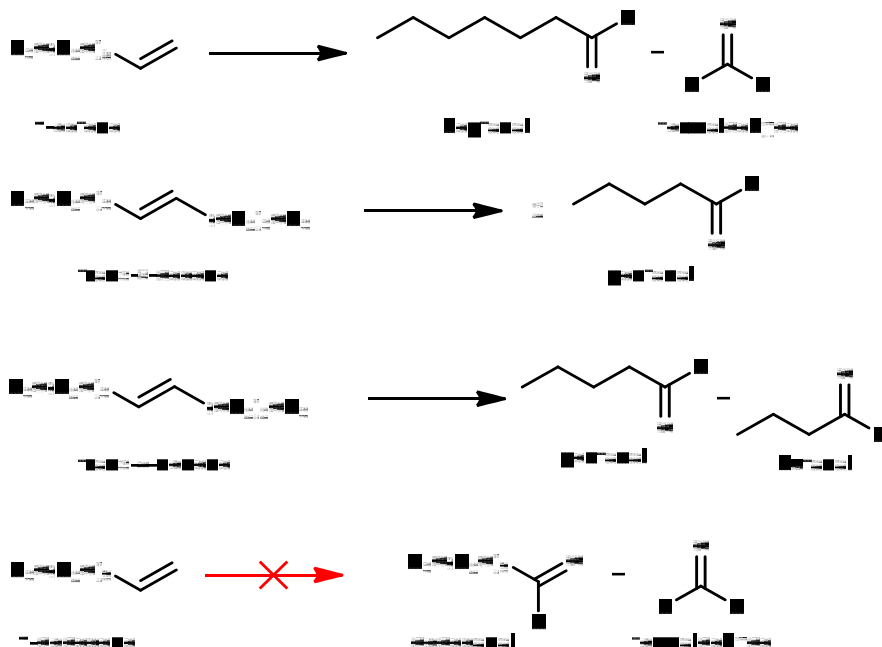


Figure 2.2 Oxidative cleavage reactions of 1-octene, *trans*-5-decene, *trans*-4-nonene, and 1-dodecene

2.2.1 Oxidative Cleavage of Oleic Acid using *meso*- and *rac*-Ni₂Cl₄(et,ph-P4)

The oxidative cleavage of oleic acid (Figure 1.17) was attempted using 10 mM *meso*- and *rac*-Ni₂Cl₄(et,ph-P4), 30 equiv. of oleic acid, an H₂O/polar organic solvent mixture, and O₂ balloon pressure. As expected, both diastereomeric forms of the complex showed the presence of small amounts of aldehyde products in the same polar organic solvent systems. The amount of water was lowered from 15% to 10% because oleic acid is not miscible with water. The solvents tested for oxidative cleavage of oleic acid were acetone, CH₃CN, THF, methanol (MeOH), DCM, DMSO, and CH₃CN/acetic acid (AcOEt). The acetone/H₂O and CH₃CN/H₂O solvent systems were the only ones to show the presence of aldehyde products via GC/MS and ¹H NMR after 24 hours of reaction time. Figure 2.3 shows the partial ¹H NMR of an oxidative cleavage of oleic acid reaction after approximately 24 hours. The broad signals around 7.5 ppm are the phenyl region of the tetraphosphine ligand, and the small signal around 9.7 ppm is the aldehyde peak.

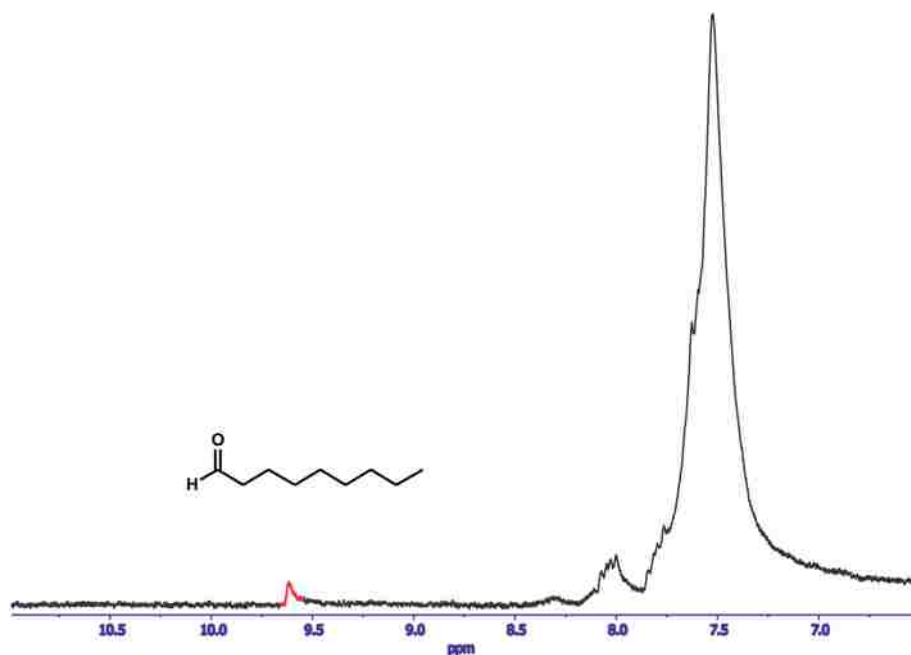


Figure 2.3 Partial ¹H NMR spectrum of oxidative cleavage of oleic acid with 10 mM *rac*-Ni₂Cl₄(et,ph-P4) in 10% D₂O/CD₃CN (spectrum expanded to focus on phenyl and aldehyde region)

Using ^1H NMR quantification studies with 1,1,2,2-tetrachloroethane as the internal standard, the reaction produces about .32 mM (5 mL total volume) nonanal. This amount is extremely small compared to the amount of oleic acid used in the reaction. The ^1H NMR signals are also much broader than expected, which could be from the presence of any paramagnetic Ni species or poor shimming of the instrument. Schreiter demonstrated that the old P4 ligand in the dinickel complexes oxidizes during the course of the reaction to form the phosphine oxide. This can be noted by its color change from deep orange to yellow/green. This oxidation leads to weaker coordination of the tetraphosphine ligand and decomposition of the complex. The formation of some monometallic nickel species has been demonstrated to occur during reactions with the *meso* dinickel complexes.² If any of these species is paramagnetic, such as the tetrahedral species $[\text{NiCl}_4]^{2-}$, that would lead to broadening of the signals on the NMR.

THF displayed strange reactivity during these reactions with traces of solvent oxidation via GC/MS. Using MeOH, traces of oleic acid methyl ester were detected via GC/MS. This was not surprising since MeOH is one of the reactants used to convert oleic acid to the methyl ester. However, the amount of methyl ester was not significant enough to consider the dinickel complexes as suitable catalysts for the esterification reaction. DCM and DMSO (with and without water) displayed no reactivity. In fact, the oleic acid is poorly miscible with DCM and DMSO, which ruled much of the data inconclusive.

A few reactions were attempted with an $\text{H}_2\text{O}/\text{CH}_3\text{CN}/\text{AcOEt}$ solvent system (4/3/3 ratio) to mimic the results obtained in the literature. The authors used this solvent system for the oxidative cleavage of oleic acid using ultrasonic irradiation and a ruthenium tetroxide catalyst.³

These results provided the idea for a new solvent system that utilized H₂O with two polar organic solvents in combination with the bimetallic nickel complexes. However, no aldehydes were detected via GC/MS using this system.

During the oxidative cleavage of oleic acid, the only product detected using our GC/MS was nonanal. Due to the higher polarity and boiling point of the other product, 9-oxononanoic acid, our GC/MS could not be utilized for detection. Liquid chromatography-mass spectrometry (LC/MS) using electrospray ionization (ESI) was conducted in attempt to detect this product. These studies determined that small amounts of the sodium salt of 9-oxononanoic acid was present in the reaction with a mass-to-charge ratio (*m/z*) of 195.0998 (Figure 2.4). The electrospray ionization spectrum shows this fragment as the largest peak in this region of the spectrum.

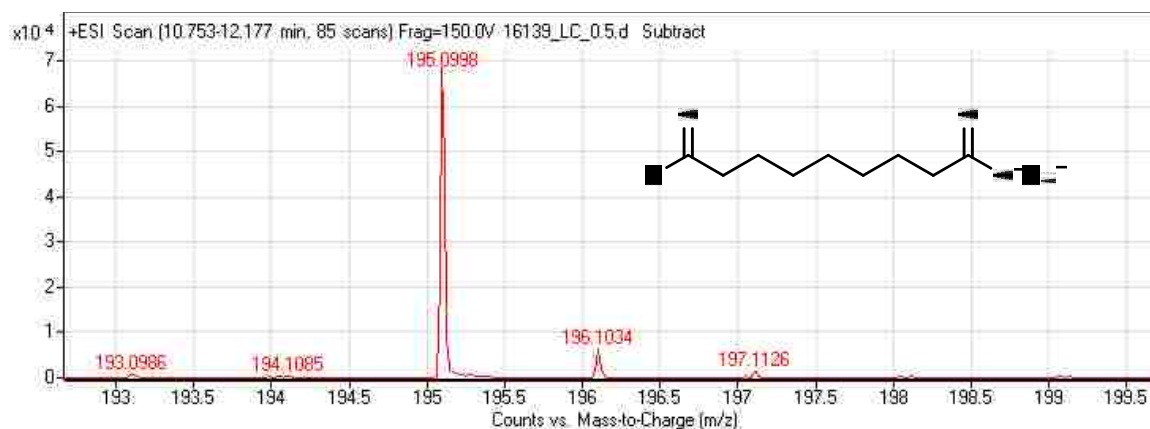


Figure 2.4 LC-MS (ESI) detection of the sodium adduct of 9-oxononanoic acid

Reactions run with the old dinickel complexes, *rac*- and *meso*-Ni₂Cl₄(*et*,*ph*-P₄), without water using only acetone or CH₃CN did not reveal any presence of aldehyde products via GC/MS. As previously stated, the reaction quickly changed color from deep orange to yellow/green upon the complete oxidation of the ligand in the presence of H₂O and O₂. When we first attempted the oxidative cleavage of oleic acid under these conditions we hypothesized that the carboxylic acid might acidify the reaction and/or coordinate to one of the nickel metal centers, which could

potentially poison the catalyst. In an attempt to counteract this effect, we attempted the oxidative cleavage of oleic acid methyl ester.

2.2.2 Esterification of Oleic Acid

The esterification of oleic acid was performed using a solid heterogeneous catalyst in an adapted procedure.⁴ The catalyst is an inexpensive sulfonic acid-based catalyst called Amberlyst-15, shown below in Figure 2.5.

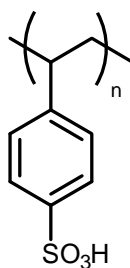


Figure 2.5 Structure of Amberlyst-15

This reaction was very efficient and gave yields of methyl ester at around 90%. The oleic acid methyl ester was isolated through extraction and removal of the solvent in vacuo.

2.2.3 Oxidative Cleavage of Oleic Acid Methyl Ester using *meso*- and *rac*-Ni₂Cl₄(*et*,*ph*-P4)

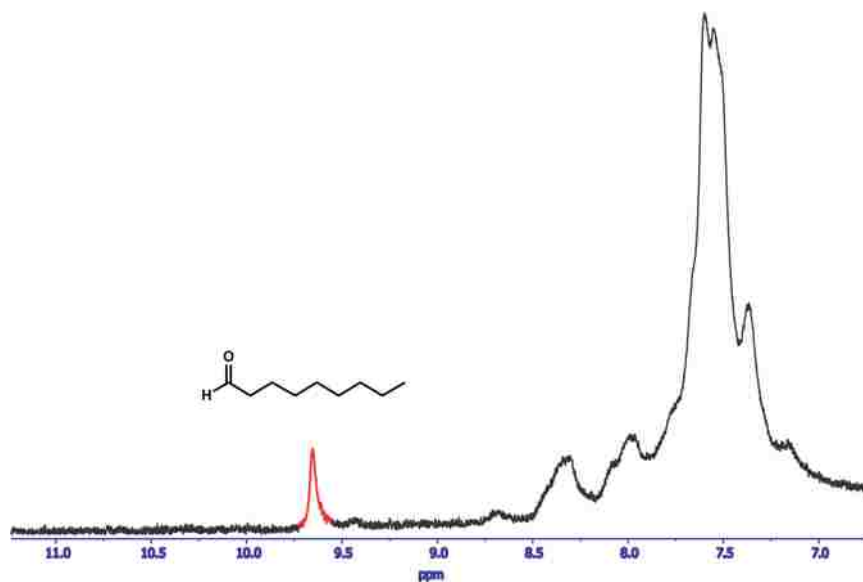


Figure 2.6 Partial ¹H NMR spectrum of oxidative cleavage of oleic acid methyl ester with 10 mM *meso*-Ni₂Cl₄(*et*,*ph*-P4) in 10% D₂O/d₆-acetone (spectrum expanded to focus on phenyl and aldehyde region)

The only solvents tested for the oxidative cleavage of oleic acid methyl ester (Figure 1.18) were acetone, CH₃CN, and MeOH. Of these systems, only the acetone and CH₃CN systems revealed the presence of a small amount of nonanal via GC/MS and the small aldehyde peak at 9.7 ppm via ¹H NMR. The partial NMR spectrum can be found above in Figure 2.6. These results were exactly the same as for the oxidative cleavage of oleic acid. In this spectrum, as opposed to Figure 2.3, the phenyl region of the tetraphosphine ligand is much better defined and contains sharper signals.

2.2.4 Isolation of Ricinoleic Acid

Ricinoleic acid is structurally similar to oleic acid except that it contains a hydroxyl group at carbon-12 of the chain (Figure 2.7). Interest in whether this hydroxyl group would inhibit the reactivity of the double bond led to additional oxidative cleavage studies. Ricinoleic acid is prepared by isolation from castor oil. Castor oil is composed of many fatty acid triglycerides with ricinoleic acid representing about 90% of its composition. Ricinoleic acid gives castor oil its unique properties and versatility.⁵ Castor oil is also inexpensive, environmentally-friendly, and has health benefits as a laxative and labor-inducer.^{6,7}

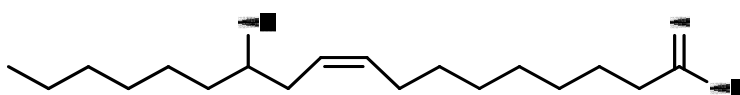


Figure 2.7 Structure of ricinoleic acid

The saponification of castor oil was performed through a mixed saponification/acidification technique.⁸ The procedure involved refluxing the castor oil with a potassium hydroxide (KOH)/EtOH solution, dissolving the potassium ricinoleate salt in water, acidifying with concentrated HCl, and extraction with ethyl acetate. This procedure was attempted about 4 times, varying the amounts of KOH from 1 M to about 2 M. The 2 M KOH solution in

EtOH gave the best results with the temperature lowered from 180°C to 100°C. Two of the impurities present at the end of the reaction were oleic and linoleic acids, though in small concentrations.

2.2.5 Oxidative Cleavage of Ricinoleic Acid using *meso*- and *rac*-Ni₂Cl₄(*et,ph*-P4)

The oxidative cleavage of ricinoleic acid (Figure 1.19) was performed in the same manner as oleic acid and its methyl ester, using 10 mM *meso* or *rac*-Ni₂Cl₄(*et,ph*-P4), 30 equiv. of acid, a 10% H₂O/polar organic solvent system, at room temperature, and for 24 hours. Acetone and CH₃CN were the only solvents tested for this reaction. The results were ruled inconclusive for both systems. Due to the higher polarity and boiling point of ricinoleic acid, GC/MS detection of the substrate proved difficult. Additionally, the isolation of ricinoleic acid left traces of solvent present, which made the reaction mixtures more dilute. Only with a longer (and higher temperature-up to 325°C) GC/MS method were we able to detect ricinoleic acid in some reactions. We were not able to detect the oxidative cleavage products, 3-hydroxynonanal and 9-oxononanoic acid, in any of the reactions.

2.2.6 Oxidative Cleavage of Oleic Acid using *meso*- and *rac*-Ni₂Cl₄(*et,ph*-P4-Ph)

Initial reactions run using 10% H₂O/acetone or CH₃CN and the new dinickel complexes did not reveal any presence of aldehyde products via GC-MS. We believed that since the new ligand did not oxidize as quickly as the old one, the oxidative cleavage would not occur. Previously, Dr. Schreiter discovered that the oxidation of the old ligand was directly linked to the oxidative cleavage of alkenes.² However, after the discovery of the oxidative cleavage of alkenes by use of only the old tetraphosphine ligand¹, reactions with the new dinickel complexes based on the *et,ph*-P4-Ph ligands were repeated and more extensively studied. In these studies, the oxidative cleavage of oleic acid occurred using *meso*-Ni₂Cl₄(*et,ph*-P4-Ph) with 10% H₂O/acetone solvent

system, 30 equiv. of acid, and at room temperature. Nonanal was detected via GC/MS and ^1H NMR (Figure 2.8) after 24 hours of reaction time. Based on ^1H NMR quantification experiments, approximately .12 mM (5 mL total volume) nonanal is produced in these reactions. This amount is less than what was produced with the old dinickel complexes, which suggests that the oxidation of the tetraphosphine ligands plays a role in the oxidative cleavage of the alkenes.

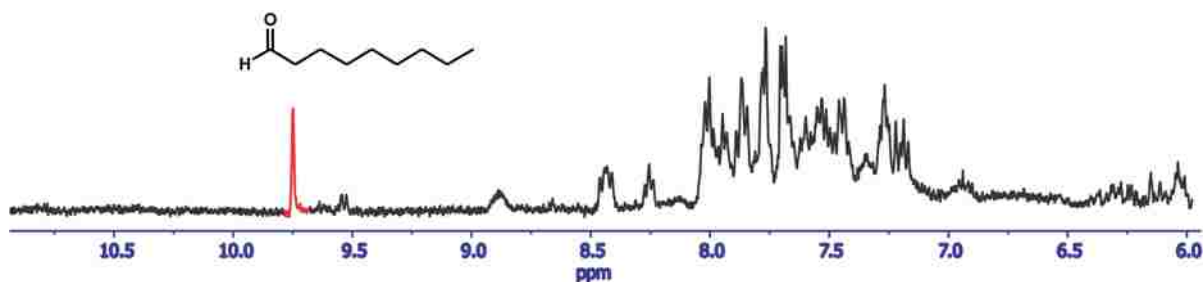


Figure 2.8 Partial ^1H NMR spectrum of oxidative cleavage of oleic acid with 10 mM *meso*- $\text{Ni}_2\text{Cl}_4(\text{et},\text{ph-P4-Ph})$ in 10% $\text{D}_2\text{O}/d_6$ -acetone (spectrum expanded to show phenyl and aldehyde region)

2.2.7 Oxidative Cleavage of Oleic Acid using *meso*- and *rac*-*et*,*ph*-P4 (old ligand)

After the discovery of the oxidative cleavage of alkenes using the old tetraphosphine ligands only (no metal centers), additional reactions were attempted to oxidatively cleave oleic acid under typical conditions. Most of these reactions were run with about 10 mM *et*,*ph*-P4, 30 equiv. of oleic acid, 10% $\text{H}_2\text{O}/\text{acetone}$ or CH_3CN , at room temperature, and without an O_2 balloon (exposed to air only). Using an O_2 balloon or higher pressures of O_2 had no effect upon the amount of aldehyde produced using the old dinickel complexes. The reactions produced roughly the same amount of aldehyde with air exposure.^{1,2} With this in mind, we began oxidative cleavage studies under the presence of air only.

After 24 hours, nonanal was detected via GC/MS and ^1H NMR (Figure 2.9) using both the CH_3CN and acetone solvent systems. A few reactions were run at elevated temperatures (around

60°C) and these reactions were also active for oxidative cleavage. However, neither the amount of product nor reactions times were increased by a significant amount. According to ^1H NMR quantification experiments, approximately .3 mM (5 mL total volume) nonanal is produced in these reactions. This is about the same amount as produced with the old dinickel complexes. As expected, the reactions gave the same results for both the *meso* and *rac* diastereomeric forms of the ligand.

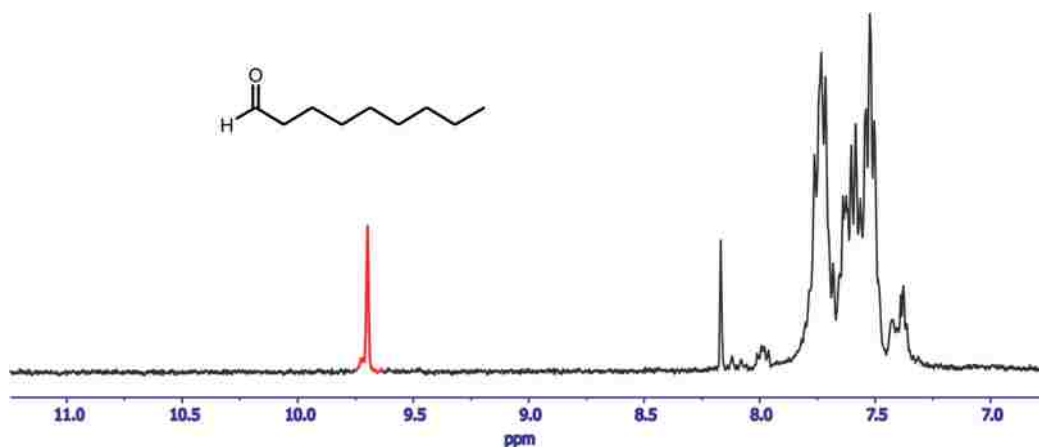


Figure 2.9 Partial ^1H NMR spectrum of oxidative cleavage of oleic acid with 10 mM *meso*-et,ph-P4 in 10% $\text{D}_2\text{O}/\text{d}_6$ -acetone (spectrum expanded to show phenyl and aldehyde region)

2.2.8 Oxidative Cleavage of Oleic Acid with *meso*- and *rac*-et,ph-P4-Ph (new ligand)

Once the oxidative cleavage of oleic acid using the old ligand was discovered, we became interested in whether the new ligand would have the same results. Using about 35 mM *meso*-et,ph-P4-Ph, 30 equiv. of oleic acid, and 10% $\text{H}_2\text{O}/\text{acetone}$ system, oxidative cleavage reactions were run under the same conditions as the old ligand reactions. After 24 hours, nonanal was detected via GC/MS and ^1H NMR (Figure 2.10). The amount of nonanal produced in these reactions was about .8 mM (5 mL total volume). This is more than what is produced with both sets of dinickel complexes and the old tetraphosphine ligand, but not significant from an overall conversion percentage.

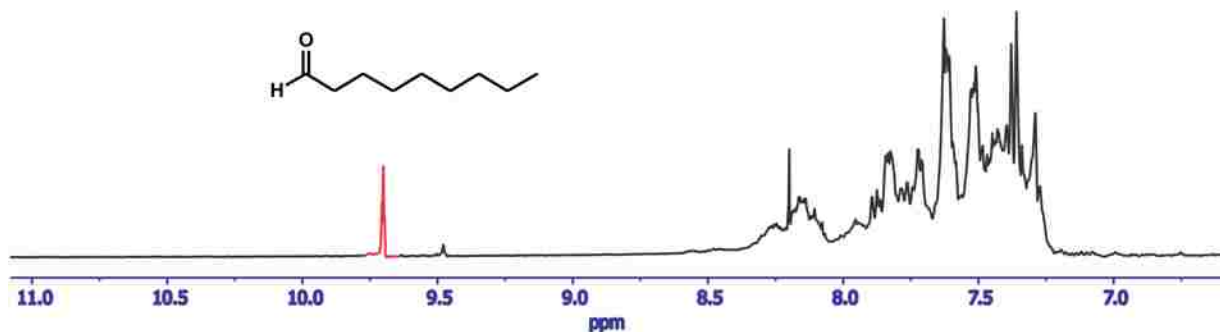


Figure 2.10 Partial ^1H NMR spectrum of oxidative cleavage of oleic acid with *meso*-et,ph-P4-Ph in 10% $\text{D}_2\text{O}/\text{d}_6$ -acetone (spectrum expanded to show phenyl and aldehyde region)

One interesting result discovered with these reactions was that water does not need to be present for the reaction to occur. With both tetraphosphine ligands, the reaction will occur with or without H_2O in the presence of air. This is quite the contrary for the *meso* and *racemic* P4 and P4-Ph dinickel complexes. Both water and O_2 (or air) are necessary for the oxidative cleavage reaction to occur with the dinickel systems. One hypothesis for the necessity of water is that it aids in displacing the phosphine ligands from the nickel metal centers. Dr. Schreiter demonstrated the reactivity of H_2O with the old P4 *meso* dinickel complex to form the double ligand species, *meso*- $[\text{Ni}(\mu\text{-Cl})(\text{et,ph-P4})_2]^{3+}$. This species can only be formed through the displacement of both the chloride ligands and the phosphine from one of the nickel metal centers.² The oxidative cleavage of alkenes with the tetraphosphine ligands and no H_2O provide more evidence for a phosphine oxide-initiated radical type of reactivity. With such little product being formed, however, it is not time effective to track down exactly what type of mechanism occurs in these reactions.

2.2.9 Oxidative Cleavage of Oleic Acid using other Phosphine Ligands

The oxidative cleavage of oleic acid was attempted using a few other phosphine ligands, dpmm, tricyclohexylphosphine ($(\text{C}_{18}\text{H}_{33})\text{P}$), and triphenylphosphine (PPh_3), shown in Figure 2.11. The conditions were the same as previous experiments: 10 mM phosphine ligand, 30 equiv. of oleic acid, 10% H_2O /organic solvent mixture, and at room temperature. Phosphine ligands had

previously been tested for oxidative cleavage of alkenes in the Stanley group. However, they either produced an insignificant amount of aldehyde or no aldehyde at all.² All three phosphine ligands tested for the oxidative cleavage of oleic acid using 10% H₂O/acetone as the solvent system showed the presence of nonanal via GC/MS after 24 hours. The amount of aldehyde produced was about the same as with the old P4 dinickel complexes.

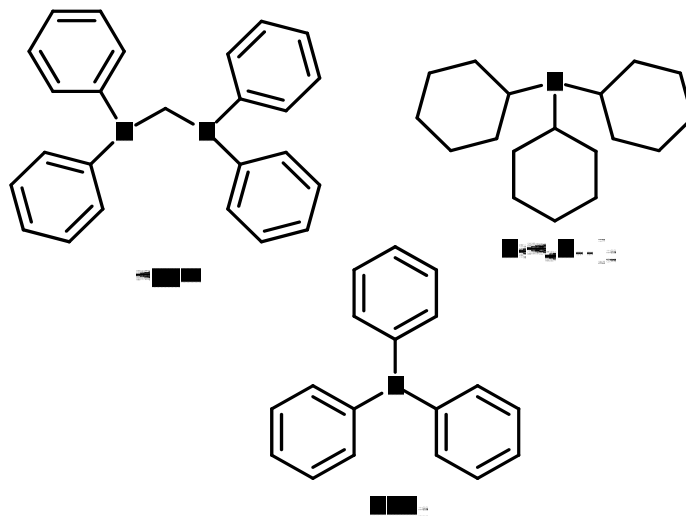


Figure 2.11 Other phosphine ligands tested for oxidative cleavage of oleic acid

2.2.10 Reactivity of the Dinickel Complexes with H₂O

As previously mentioned, Schreiter studied in a fair bit of detail the oxidation of the old tetraphosphine ligand during the course of the oxidative cleavage reactions with the dinickel complexes. He also studied the reactivity of H₂O with *meso*- and *rac*-Ni₂Cl₄(*et*,*ph*-P₄). His studies of *meso*-Ni₂Cl₄(*et*,*ph*-P₄) with H₂O under inert atmosphere indicated that upon the addition of 5-30% D₂O in d₆-acetone, the complex falls apart to form multiple new species. He was able to identify a few of these species by ³¹P NMR and crystallized the double ligand species, as discussed in Chapter 1. The *rac* complex was shown to react similarly with much less H₂O present (5%), but that system was not characterized as well as the *meso* system.²

The new P4-Ph dinickel complexes, however, have not been studied carefully. We proposed that the stronger chelation of the new ligand would make the nickel complexes more stable to H₂O and O₂. This could have, perhaps, made the oxidative cleavage reaction catalytic or able to produce a more appreciable amount of aldehyde. However, these complexes do not produce a more appreciable amount of aldehyde. Though they do not oxidize as quickly as the old complexes (no color change occurs from orange to yellow/green as with the old complexes), they also appear to be reactive with H₂O.

2.2.11 ³¹P NMR Studies of *rac*-Ni₂Cl₄(et,ph-P4) Reactivity with H₂O

The reactivity of *rac*-Ni₂Cl₄(et,ph-P4) with H₂O was investigated using ³¹P NMR over the course of 7 days. The most suitable common solvent discovered for use with both the old *rac*- and new P4-Ph dinickel complexes was d₇-DMF. The complexes are insoluble in acetone and only partially soluble in CH₃CN. Each reaction used 10 mM dinickel complex, 10% D₂O/d₇-DMF, at room temperature, and under N₂ atmosphere (not exposed to air). The complexes were initially dissolved in the appropriate amount of d₇-DMF (2mL total), from which a sample was taken. Next, 10% D₂O was added and samples were drawn from this mixture. Both samples, with and without D₂O, were analyzed by ³¹P NMR, and the sample containing the D₂O was covered in parafilm and allowed to stand at room temperature for at least 7 days.

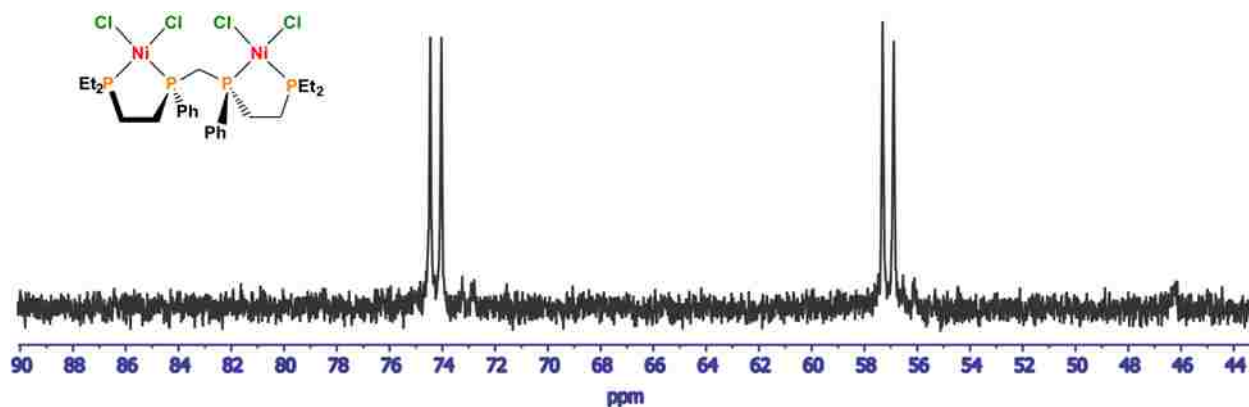


Figure 2.12 ³¹P NMR spectrum of *rac*-Ni₂Cl₄(et,ph-P4) dissolved in d₇-DMF

The initial ^{31}P NMR spectrum of *rac*- $\text{Ni}_2\text{Cl}_4(\text{et,ph-P4})$ is shown above in Figure 2.12. It contains the standard doublets representing the external phosphorus atoms of our tetraphosphine ligand at 74 ppm and the internal phosphorous atoms at 56.7 ppm. Schreiter investigated the coupling constants for these signals in great detail, and noted that the large splitting between the external and internal phosphorous groups would vary depending on the solvent by 2-3 Hz. He studied the coupling constants for the signals in CD_3CN , d_6 -acetone, and d_2 -DCM and found them to be 69.6, 73.1, and 75.1, respectively.²

Upon the addition of H_2O , the spectrum completely changes and the formation of a new species begins (Figure 2.13). The dominant signals are two triplets, at 28 and 46 ppm. A closer look at these signals can be found in Figure 2.14. We believe these signals are associated with the same symmetrical species. Schreiter observed these same pseudo-triplets in his reaction of the old P4 *rac*-dinickel complex with 15% $\text{D}_2\text{O}/\text{DMSO}$. He also noticed the signals did not change after several days. He proposed the signals to be associated with a *rac* double ligand species, similar to the *meso* double ligand species, $[\text{Ni}(\mu\text{-Cl})(\text{et,ph-P4})_2]^{3+}$.²

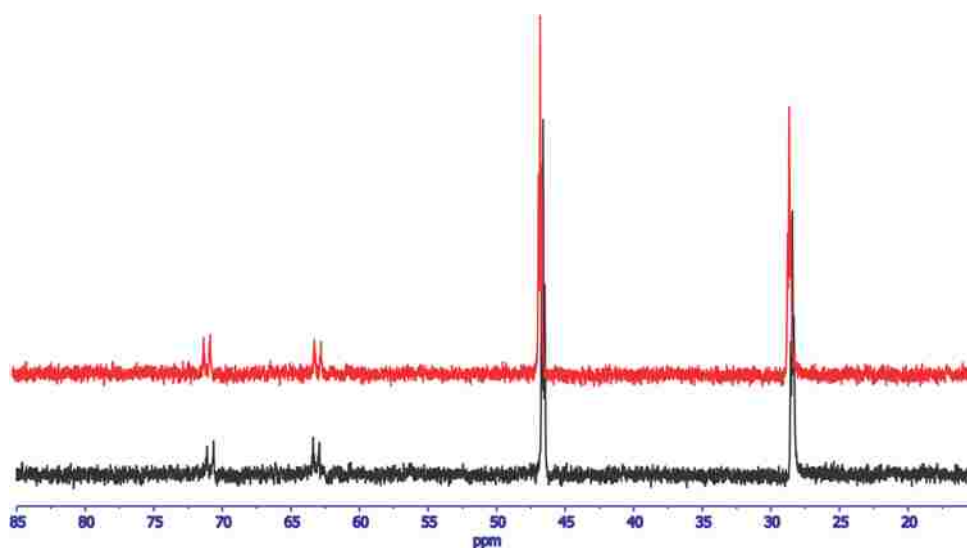


Figure 2.13 ^{31}P NMR spectra of the reaction of *rac*- $\text{Ni}_2\text{Cl}_4(\text{et,ph-P4})$ with D_2O immediately after addition (black spectrum) and 3 hours later (red spectrum)

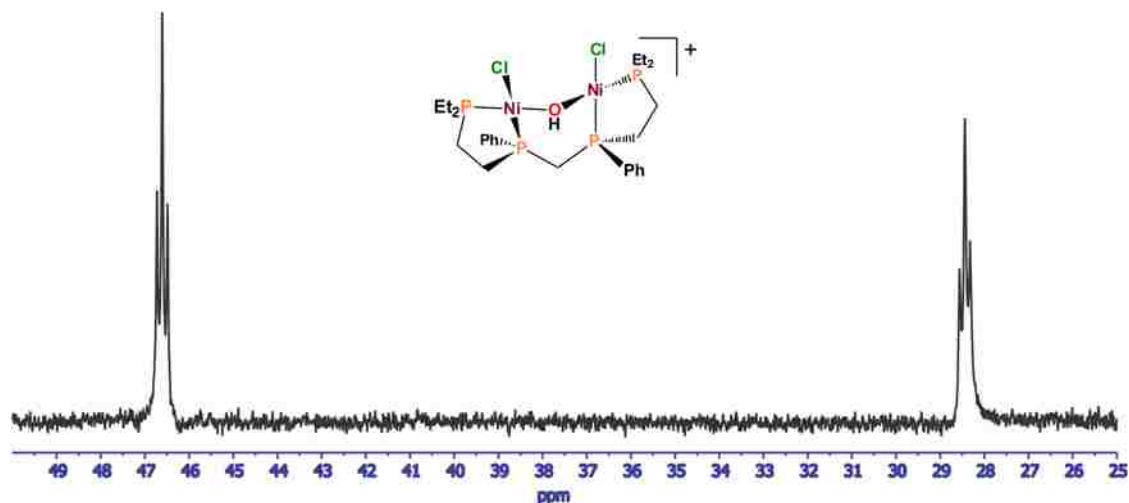


Figure 2.14 Partial ^{31}P NMR Spectrum of the reaction of *rac*- $\text{Ni}_2\text{Cl}_4(\text{et,ph-P4})$ with D_2O immediately after addition (spectrum zoomed in to show pseudo-triplets)

However, we no longer agree with his assumption. We propose instead, based on Dr. Stanley's DFT calculations, that these ^{31}P NMR signals are associated with the OH-bridged complex, *rac*- $[\text{Ni}_2(\mu\text{-OH})\text{Cl}_2(\text{et,ph-P4})]^{1+}$ (Figure 2.15), similar to Monteil's new *meso* P4-Ph hydroxide-bridged dinickel complex shown in Figure 1.13. DFT studies have shown that this complex should have a symmetrical pattern similar to the signals at 28 and 46 ppm.

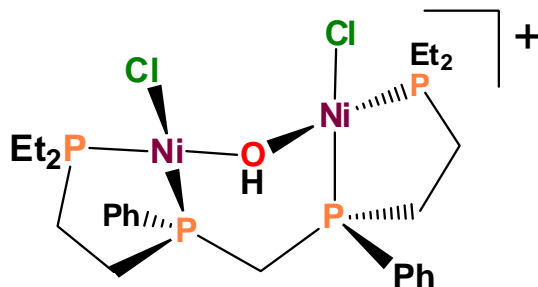


Figure 2.15 Structure of *rac*- $[\text{Ni}_2(\mu\text{-OH})\text{Cl}_2(\text{et,ph-P4})]^{1+}$

The second set of signals at around 63 and 71 ppm are most likely from the initial starting dinickel tetrachloride complex; however, they are shifted further downfield. These changes do not appear to be as drastic as the experiments run by Schreiter in CH_3CN . He observed the formation

of multiple species even with only 5% D₂O/CH₃CN. In this 10% D₂O/d₇-DMF system, however, the formation of the species at 28 and 46 ppm dominates the spectrum.

As shown above in Figure 2.13, the spectrum does not change after about 3 hours, and the species remain constant. However, the signals at 63 and 71 ppm begin to disappear after 48 hours (Figure 2.16), and the spectrum is completely dominated by the two pseudo-triplets. After 7 days, the triplet at around 28 ppm has noticeably split into a doublet of triplets, which is most likely a sign that the bridged hydroxide dinickel complex is beginning to decompose.

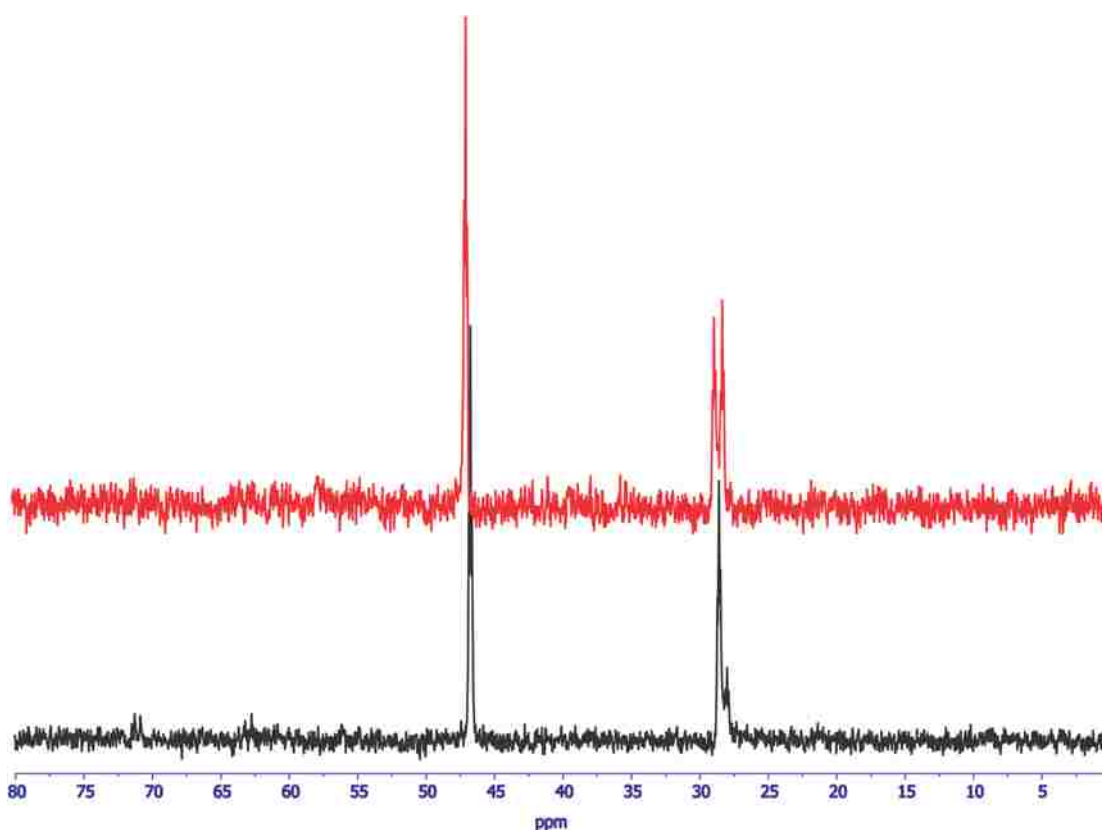


Figure 2.16 ³¹P NMR spectra of the reaction of *rac*-Ni₂Cl₄(et,ph-P₄) with D₂O after 48 hours (black spectrum) and 7 days (red spectrum)

Figure 2.17 shows the ³¹P NMR spectrum after 22 days. The two triplets at 28 and 46 ppm, which we believe correspond to the bridged hydroxide dinickel complex as previously discussed, are still the most dominant species, but many other signals are present due to decomposition and the formation of some new, perhaps, unsymmetrical monometallic nickel complexes.

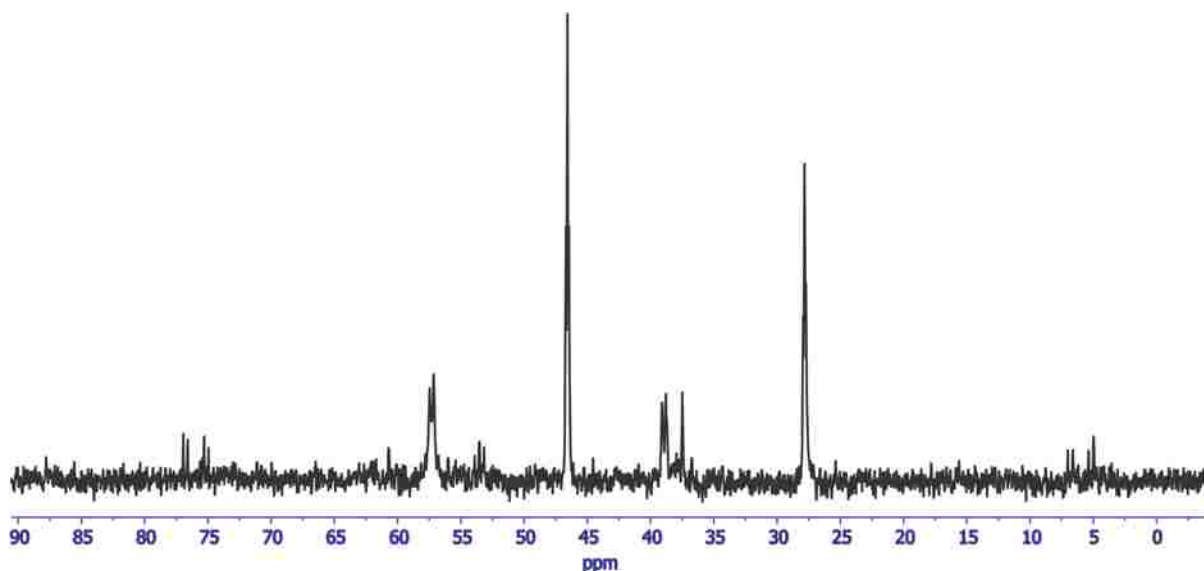


Figure 2.17 ^{31}P NMR spectrum of the reaction of *rac*- $\text{Ni}_2\text{Cl}_4(\text{et,ph-P}_4)$ with D_2O after 22

Schreiter also observed similar sets of resonances with much larger intensities in his preliminary studies with the old P4 *rac*-dinickel complex. He proposed based on COSY NMR experiments and coupling constant assignments that the signals at 76, 54, 37, and 5 ppm are the result of the same unsymmetrical monometallic complex, shown in Figure 2.18.

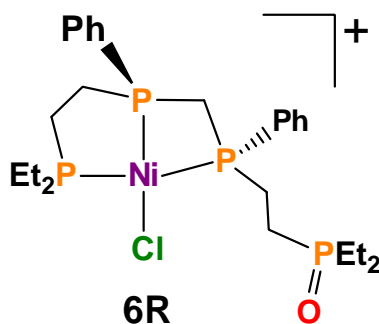


Figure 2.18 Proposed structure of unsymmetrical monometallic nickel complex

Since his experiments were performed with exposure to air, he proposed that the dangling phosphine arm had become oxidized which would give it a higher resonance of 37 ppm. However, he was not able to isolate and characterize any of this complex.² We propose that a similar unsymmetrical species is being formed in our case but in a much lesser quantity because these experiments were performed under inert atmosphere. Over time, since the NMR tubes were left

out, air could have seeped in through the caps. Additionally, we see two doublets at 39 and 57 ppm that we believe correspond to the same species, perhaps the bridging chloride dinickel complex, shown in Figure 2.19.

DFT calculations performed by Dr. Stanley have shown the bridging hydroxide to be more stable than the bridging chloride dinickel complex, but we propose the bridging chloride to be an intermediate to the formation of the bridging hydroxide complex. Dr. Schreiter's studies contained two broad signals at 39 and 57 ppm, which could be from a dynamic exchange between these two complexes.² This explanation is reasonable since chloride dissociation occurs rapidly with these systems in the presence of H₂O giving rise to free chloride ligands in solution.

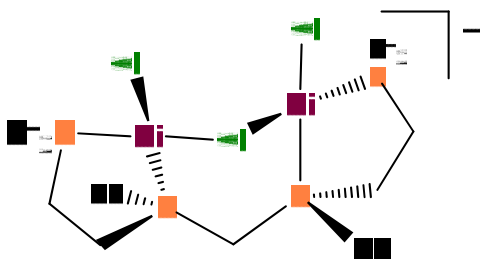


Figure 2.19 Structure of *rac*-[Ni₂(μ -Cl)Cl₂(et,ph-P₄)]¹⁺

2.2.12 ³¹P NMR Studies of *meso*-Ni₂Cl₄(et,ph-P₄-Ph) Reactivity with H₂O

Preliminary ³¹P NMR studies of the new dinickel complexes, *meso*- and *rac*-Ni₂Cl₄(et,ph-P₄-Ph), have revealed a great deal about their reactivity with H₂O. Figure 2.20 shows the ³¹P NMR spectra of the dinickel complexes in d₇-DMF before D₂O is added. Both spectra contain the standard doublets corresponding to the external phosphorus atoms at 67 and 68 ppm and the internal phosphorus atoms at 48 and 49 ppm of our tetraphosphine ligand.

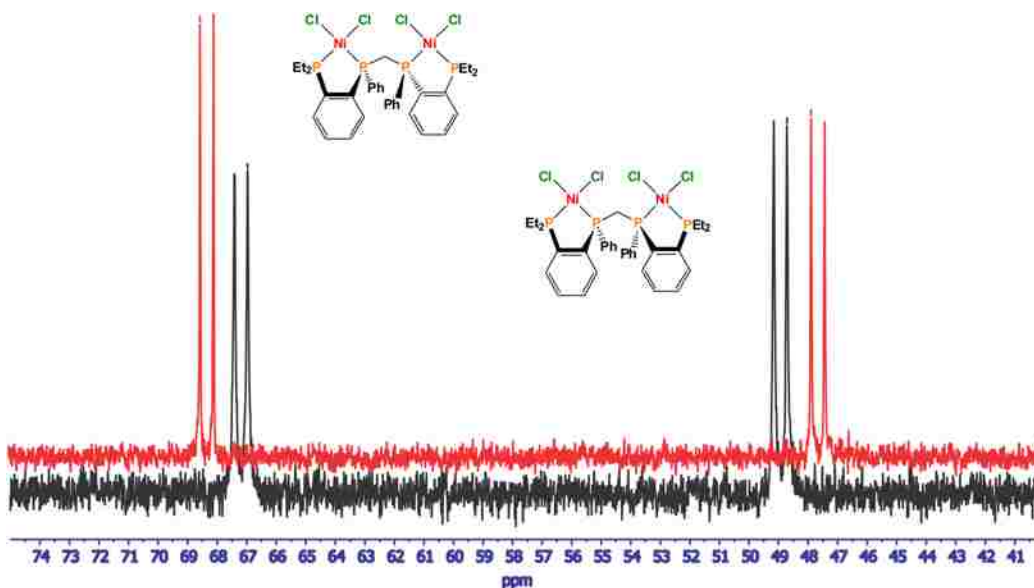


Figure 2.20 ^{31}P NMR spectra of *meso*- (black spectrum) and *rac*- $\text{Ni}_2\text{Cl}_4(\text{et,ph-P4-Ph})$ (red spectrum) dissolved in d^7 -DMF

Upon the addition of 10% H_2O to the new P4-Ph *meso* dinickel species (Figure 2.21), the two doublets completely convert to four distorted triplets instead with the peaks at 68 and 49 ppm broadened out. We believe these broad signals to be associated with an exchange occurring in which the original complex is present along with another species, perhaps the bridged hydroxide species, *meso*- $[\text{Ni}_2\text{Cl}_2(\mu\text{-OH})(\text{et,ph-P4-Ph})]^{1+}$ (Figure 1.13). Within 2 hours of the addition of H_2O , the distorted triplets and broad signals begin to disappear and the two singlets at 64 and 65 ppm get larger in intensity. After 24 hours, the broad signals have completely disappeared, which denotes the end of the exchange and these two singlets dominate the spectrum.

Within 3 days (Figure 2.22), the four distorted triplets have disappeared and two new distorted triplets have risen at -13 ppm. We can most likely attribute these new signals to a mono- or bimetallic nickel complex with a “dangling” phosphine group. Schreiter noticed the formation of “dangling” phosphine groups with the old *meso* P4 system reactivity with H_2O as well. The negative shift of these signals indicates the phosphine is not attached to the metal center.² It appears though that the singlets at 64 ppm still remain the dominant species.

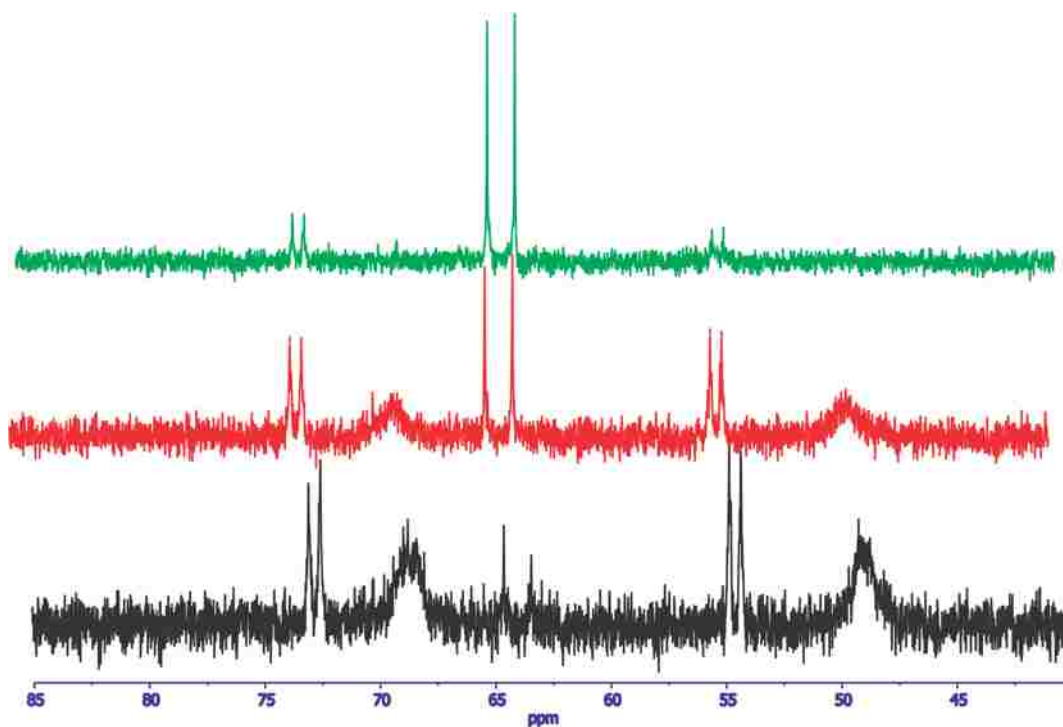


Figure 2.21 ^{31}P NMR spectra of reaction of *meso*- $\text{Ni}_2\text{Cl}_4(\text{et,ph-P4-Ph})$ with D_2O immediately after addition (black spectrum), 2 hours later (red spectrum) and 24 hours later (green spectrum)

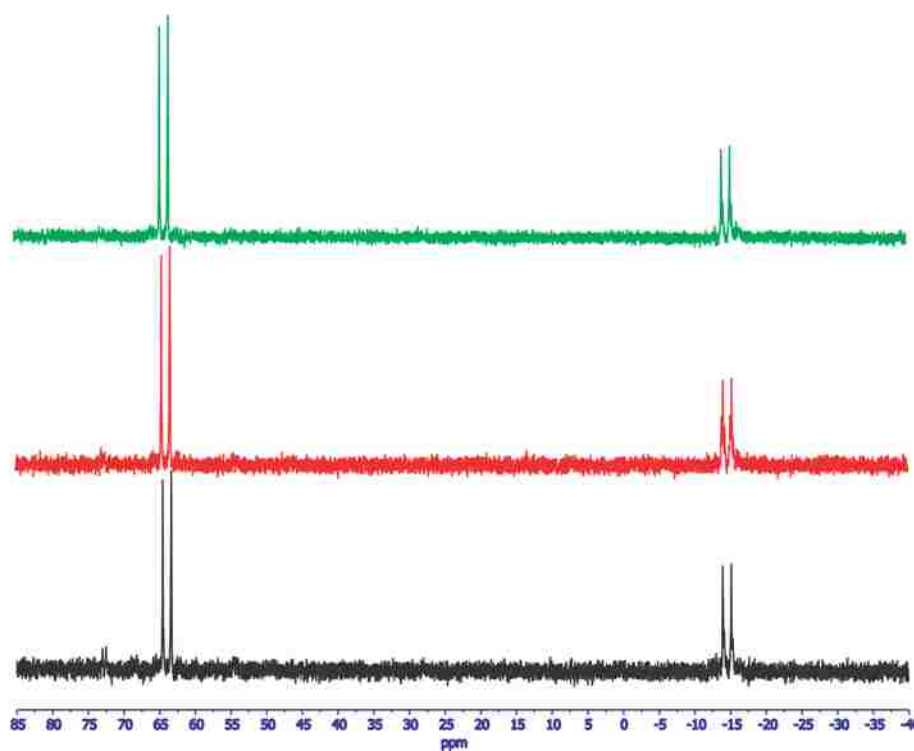


Figure 2.22 ^{31}P NMR spectra of reaction of *meso*- $\text{Ni}_2\text{Cl}_4(\text{et,ph-P4-Ph})$ with D_2O 3 days later (black spectrum), 8 days (red spectrum), and 14 days (green spectrum)

As previously mentioned, the formation of the hydroxide-bridged complex can most likely be associated with these signals. Unlike the old P4 *meso* and *rac* dinickel system, the hydroxide bridged new P4-Ph dinickel complex remains somewhat stable after 14 days and does not decompose into multiple monometallic complexes. The formation of the nickel species with the dangling phosphine group also appears to be relatively stable and does not decompose over time. This explanation is reasonable given the stronger chelation of the new P4-Ph tetraphosphine ligands, which form stronger metal ligand bonds.

Kalachnikova performed LC-MS (ESI) studies on the reaction mixtures after oxidative cleavage reactions using the new P4-Ph *meso* dinickel tetrachloride complex. Her studies detected the proposed hydroxide bridged complex at an m/z ratio of 765.0155 as the largest signal in the mixture (Figure 2.23). This provides some evidence for the formation of the bridged hydroxide complexes in the new P4-Ph dinickel systems. Further studies to isolate and characterize this complex are currently underway.

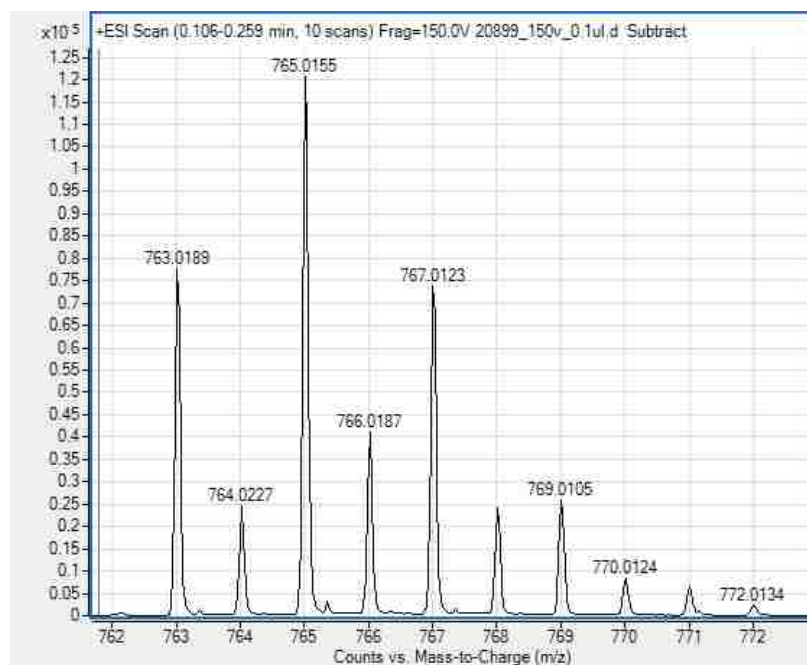


Figure 2.23 Kalachnikova's LC-MS (ESI) spectrum of an oxidative cleavage reaction mixture using *meso*-Ni₂Cl₄(*et*,*ph*-P4-Ph)

2.2.13 ^{31}P NMR Studies of *rac*- $\text{Ni}_2\text{Cl}_4(\text{et,ph-P4-Ph})$ Reactivity with H_2O

The new *rac* dinickel complex appears to follow the same type of reactivity as the *meso* form, but with higher sensitivity to the amount of H_2O . With the addition of approximately 10% H_2O to the complex dissolved in d_7 -DMF, an orange material immediately precipitated out of solution. This material makes ^{31}P NMR analysis very difficult. Experiments are currently underway using less H_2O (at least 5%) to track this complex's reactivity with water.

2.2.14 Oxidative Cleavage of Oleic Acid using *meso*- and *rac*- $\text{Co}_2\text{Cl}_4(\text{et,ph-P4/et,ph-P4-Ph})$

With the unsuccessful attempts to make the reaction catalytic using dinickel complexes or the tetraphosphine ligands, new ideas for a possible catalyst were explored. Given the important industrial applications for this type of reactivity (Chapter 1), an efficient catalyst could have a major impact in this field. While working on a synthesis for a dicobalt catalyst for hydroformylation and aldehyde water shift catalysis (Chapter 3), several cobalt precursors were tested for the oxidative cleavage of oleic acid.

Cobalt's ability to act as an oxygen carrier makes it an attractive metal for oxidation catalysis.^{9,10} With this in mind, the dicobalt complexes, *meso*- and *rac*- $\text{Co}_2\text{Cl}_4(\text{et,ph-P4})$ and the new ligand versions (*meso*- and *rac*- $\text{Co}_2\text{Cl}_4(\text{et,ph-P4-Ph})$) were tested for use as an alkene oxidative cleavage catalyst. These reactions were run using 10 mM dicobalt complex, 30 equiv. of oleic acid, at room temperature, and analyzed by GC/MS after 24 hours. The two solvent systems tested with the old ligand complexes were 10% H_2O /acetone and MeOH. In the H_2O /acetone reaction, the GC/MS results did not reveal any traces of nonanal. In the MeOH reaction, only traces of the methyl ester were detected. With the new ligand complexes, only 10% H_2O /acetone was used as the solvent system. No nonanal was detected during these reactions via GC/MS analysis.

Additionally, these dicobalt complexes contain metal centers that are in the +2 oxidation state, which makes them paramagnetic, so NMR analyses could not be performed to analyze the reaction mixtures. There was no color change during the reactions to suggest phosphine oxidation was occurring as it does with the dinickel complexes. As stated above, we believe the oxidation of the tetraphosphine ligands plays a key role in the oxidative cleavage of alkenes under our conditions.

2.2.15 Oxidative Cleavage of Oleic Acid using $[\text{Co}(\text{H}_2\text{O})_6][\text{BF}_4]_2$

The complex, $[\text{Co}(\text{H}_2\text{O})_6][\text{BF}_4]_2$, was synthesized according to a literature procedure.¹¹ It was initially explored as a possible precursor for a dicobalt catalyst. However, due to the large amount of H_2O present, it was interesting to see how it would react in our oxidative cleavage reactions. All of the reactions were run using acetone as the solvent, with about 10 mM cobalt complex, 30 equiv. of oleic acid, and at room temperature for 24 hours. A few were run with an added 10% H_2O . Interestingly, nonanal was detected via GC-MS in all of the reactions with this complex. However, the amount of nonanal detected was small, roughly the same amount produced using the old P4 dinickel complexes. The addition of 10% H_2O and O_2 balloon pressure did not increase the amount of aldehyde formed nor did the reactivity increase.

The interesting aspect of this reactivity is that no phosphine ligand was present with this complex. Though cobalt has been shown to be an oxygen activator (Chapter 1), our work had not shown any evidence of the oxidative cleavage working without the phosphine ligands present up until this point. This led to the conclusion that this reactivity is more complex than initially thought. We are still unsure of exactly what is occurring and how this simple monometallic cobalt complex could be oxidatively cleaving oleic acid under such mild conditions, but the low yields are not promising and may not merit much additional study.

2.2.16 Oxidative Cleavage of Alkenes using Drago's Catalyst (CoSMDPT)

Drago's catalyst (CoSMDPT), shown in Figure 2.24, was used to catalyze the oxidative cleavage of isoeugenol to produce vanillin and acetaldehyde (Figure 2.25).¹² To our knowledge, no subsequent results have been published for the use of this catalyst with any other alkenes (Chapter 1). As a result, we wanted to study it further. We prepared this monometallic cobalt catalyst according to a literature procedure in high yield (>80%).¹³

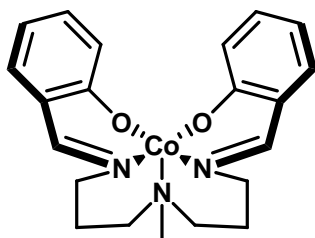


Figure 2.24 Structure of Drago's catalyst, CoSMDPT

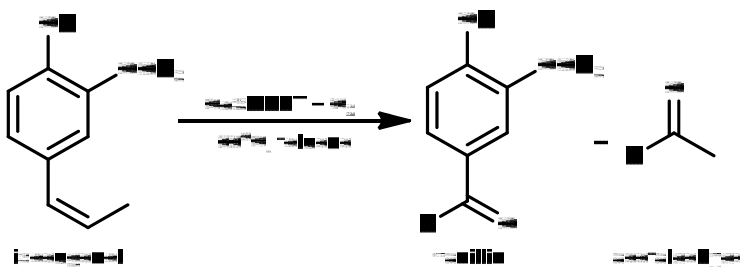


Figure 2.25 Oxidative cleavage of isoeugenol by CoSMDPT¹²

Drago's reaction was repeated using 2.46×10^{-4} mol of CoSMDPT and 2.46×10^{-3} mol of isoeugenol in a toluene solvent system at 60°C with 75 psig O_2 . A preliminary reaction gave the same results as the literature with almost complete conversion of the alkene.¹² ^1H NMR (Figure 2.26) was used for the detection of vanillin and acetaldehyde. The ^1H NMR reveals signals for both acetaldehyde (red) and vanillin (green). The presence of these signals verifies that the reaction was successful in oxidatively cleaving isoeugenol.

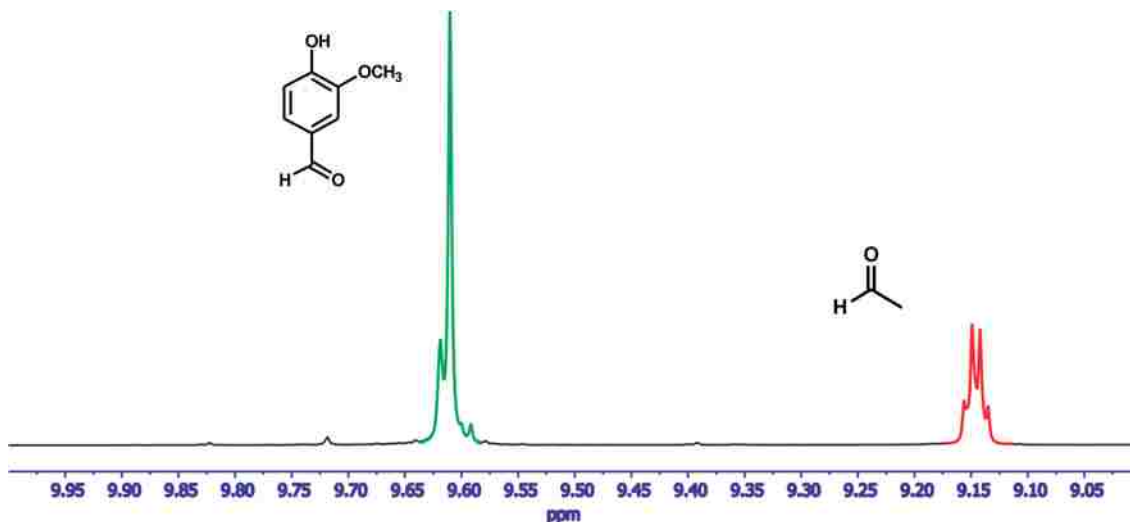


Figure 2.26 Partial ^1H NMR spectrum of the oxidative cleavage of isoeugenol reaction mixture using Drago's catalyst

Studies are currently underway to get turnover number/frequency data for this reaction and test this catalyst for the oxidative cleavage of simpler alkenes, such as 1-octene.

2.3 Conclusion

The dinickel complexes, tetraphosphine ligands, cobalt complex $[\text{Co}(\text{H}_2\text{O})_6][\text{BF}_4]_2$, and a few other phosphine ligands (dppm, PPh_3 and $\text{P}(\text{C}_6\text{H}_{11})_3$) all showed reactivity for the oxidative cleavage of oleic acid. However, attempts to make the reaction catalytic were unsuccessful. We initially believed that this reaction could be made catalytic based on Dr. Stanley's proposed mechanisms for the oxidative cleavage of alkenes with bimetallic nickel complexes, with the second mechanism (Figure 2.27) being the most plausible for this reaction based on the bulky unsaturated fatty acid. This mechanism involves the direct interaction of the alkene with the peroxide bridged ligand rather than alkene coordination to the metal. Since the fatty acids are 18-carbon chains, they would be less likely to coordinate to the metal center directly.

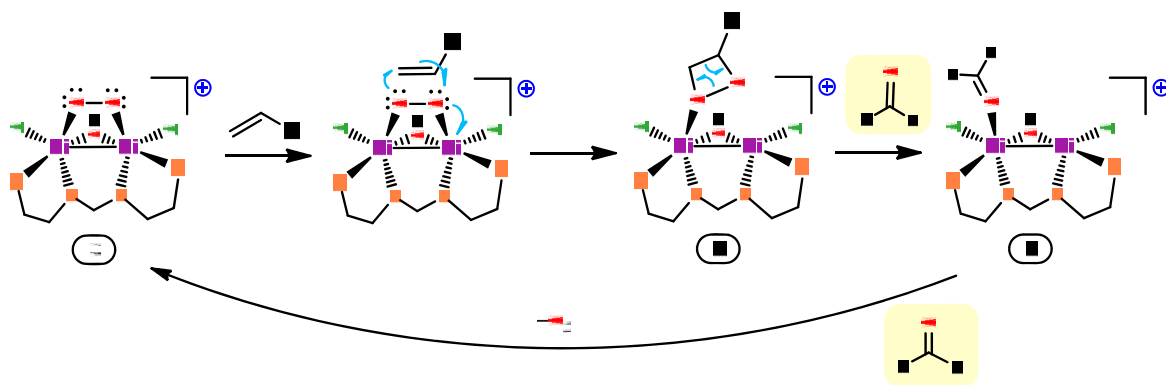


Figure 2.27 Dr. Stanley's second proposed mechanism for the oxidative cleavage of alkenes with bimetallic nickel complexes

We believe, however, this reactivity is more complex than that. It is most likely not a straight radical based reactivity either. Typically radical reactions produce a variety of oxidation products such as aldehydes, ketones, carboxylic acids, esters and ethers (Chapter 1). This reaction, on the other hand, appears to be clean; only aldehydes appear to be produced, albeit in extremely low yields.

Additionally, the proposed Ni-based mechanisms were disproven with the discovery of the oxidative cleavage using only the tetraphosphine ligands. Dr. Kalachnikova demonstrated through ^{31}P NMR studies that the old tetraphosphine ligand was not as sensitive to air as we thought. After 8 days of exposure to air, the ^{31}P signals due to *meso*-et,*ph*-P4 were still around 68% by integration.¹ With these results in mind, she also demonstrated that the oxidative cleavage of alkenes occurs with only the tetraphosphine ligand and H_2O /polar organic solvent mixture in air. No pure O_2 or metal complexes were needed for the aldehydes to be produced in low yields.

Due to the range of species tested and active for oxidative cleavage, it would be very difficult and tedious to track down how this reaction proceeds. With such a small amount of product being produced as well, there is really no benefit in putting more time into studying this reaction. It can be said that due to cobalt's affinity for oxygen, it is not entirely surprising that the

reaction works far better with Drago's monometallic catalyst. Cobalt adducts that oxidize alkenes are well known and well documented in the literature (Chapter 1).

My hypothesis for the oxidative cleavage of oleic acid is that it is proceeding by some oxygen-initiated autooxidation type of mechanism. Oxygen is essential, and it needs an initiator, which in our case can be either a metal (Ni or Co) complex or phosphine ligand. Once the initiation occurs, the conditions are set up so that only the aldehydes are produced through the cleavage of the C=C double bond. Once the aldehydes are produced or the phosphine is oxidized, however, the system shuts down and no further oxidation occurs.

2.4 References

1. Kalachnikova, E. *Improved Synthesis, Separation, Transition Metal Coordination and Reaction Chemistry of a New Binucleating Tetrphosphine Ligand*. Ph.D. Dissertation, Louisiana State University, Baton Rouge, May **2015**.
2. Schreiter, W. J. *Investigations into Alkene Hydration and Oxidation Catalysis*. Ph.D. Dissertation, Louisiana State University, Baton Rouge, May **2013**.
3. Rup, S.; Zimmerman, F.; Meux, E.; Schneider, M.; Sindt, M.; Oget, N. The Ultrasound-Assisted Oxidative Scission of Monoenic Fatty Acids by Ruthenium Tetraoxide Catalysis: Influence of the Mixture of Solvents. *Ultrason. Sonochem.* **2009**, *16*, 266-272.
4. Chari, M. A. Amberlyst-15: an efficient and reusable catalyst for multi-component synthesis of 3,4-dihydroquinoxalin-2-amine derivatives at room temperature. *Tetrahedron Lett.* **2011**, *52*, 6108-6112.
5. Naughton, F.C. Production, Chemistry, and Commercial Applications of Various Chemicals from Castor Oil. In *Novel Uses of Agricultural Oils*, Presented in Symposium at the AOCS Spring Meeting, New Orleans, LA, April 1973; *Journal of the American Oil Chemists' Society.* **1973**, *51*, 65-71.
6. Ogunniyi, D.S. Castor Oil: A Vital Industrial Raw Material. *Bioresource Technology.* **2006**, *97*, 1086-1091.
7. Williams, S.C.P. Castor Oil's Health Benefits Tied to Ricinoleic Acid Chemistry. *Huff Post Science* [Online] **2012**.
8. Vaisman, B.; Shikanov, A.; Domb, A.J. The Isolation of Ricinoleic Acid from Castor Oil by Salt-solubility-based Fractionation for the Biopharmaceutical Applications. *J. Am. Oil. Chem. Soc.* **2008**, *85*, 169-184.
9. Ralph G, W. Uptake of Oxygen by Cobalt (II) Complexes in Solution. *Bioinorg. Chem.* **1971**, *100*, 111-134.

10. Bailey, C. L.; Drago, R. S. Utilization of O₂ for the Specific Oxidation of Organic Substrates with Cobalt(II) Catalysts. *Coord. Chem. Rev.* **1987**, *79*, 321-332.
11. Holt, D.G.L.; Larkworthy, L.F.; Povey, D.C.; Smith, G.W. Facile Synthesis of Complexes of Vanadium(II) and the Crystal and Molecular Structures of Hexaaquavanadium(II) Trifluoromethylsulphonate. *Inorganica Chimica Acta.* **1990**, *169*, 201-205.
12. Drago, R. S.; Corden, B. B.; Barnes, C. W. Novel Cobalt(II)-Catalyzed Oxidative Cleavage of a Carbon-Carbon Double Bond. *J. Am. Chem. Soc.* **1986**, *108*, 2453-2454.
13. Drago, R. S.; Cannady, J. P.; Leslie, K. A. Hydrogen-Bonding Interactions Involving Metal-Bound Dioxygen. *J. Am. Chem. Soc.* **1980**, *102*, 6014-6019.

Chapter 3: Synthetic Strides Towards a Bimetallic Cobalt Catalyst for Hydroformylation and Aldehyde-Water Shift Catalysis

3.1 Introduction

Cobalt is the 33rd most abundant element and has major uses in the petrochemical and plastic industries as both hetero and homogeneous catalysts. The three main uses of cobalt catalysis are in hydro-treating and desulfurization for oil and gas, the production of terephthalic acid (TPA) and dimethyl terephthalate (DMT), and hydroformylation to make alcohols and aldehydes. Hydrodesulfurization is a process in which refineries remove organic sulfur from oil by converting it to hydrogen sulfide. This process is critical for health and safety reasons as crude oils contain 0.1 to 2.5% sulfur. The purpose of removing sulfur is to reduce the sulfur dioxide emissions into the environment. The CoMOX catalysts used for this process are typically 3-5% cobalt oxide (Co_3O_4), 14% molybdenum trioxide (MoO_3), and the balance being alumina (Al_2O_3).^{1,2}

Mixed cobalt acetate/manganese sodium bromide homogeneous catalysts are used for the production of TPA and DMT. These materials are used to manufacture resins for plastics and polyester. A total of about 1700 tons of cobalt is used per year worldwide in this process. The third main use of cobalt is in the hydroformylation of alkenes to produce alcohols and aldehydes (Figure 3.1). These alcohols and aldehydes are both final products and intermediates for bulk chemicals such as esters and amines used heavily in the plastic and detergent industries. Industrially, the cobalt precursor for hydroformylation can be introduced as a metal oxide, hydroxide or an inorganic salt which is then converted into the catalytically active homogeneous species, $\text{HCo}(\text{CO})_4$. Hydroformylation, or the oxo synthesis, involves the addition of H_2 and CO across a carbon-carbon double bond.^{1,2}

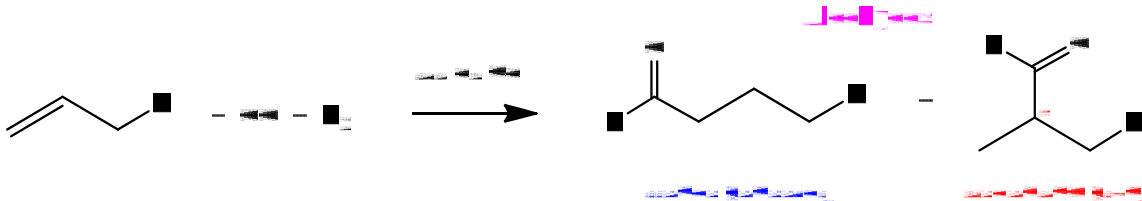


Figure 3.1 Hydroformylation of alkenes

Cobalt's use as a catalyst depends on several of its properties. First, its ability to form 5 different valence states, -1, 0, +1, +2, and +3 gives the metal much versatility in oxidation-reduction reactions. Secondly, the ease with which cobalt accepts atoms from other molecules makes it useful in coordination chemistry. Lastly, solid cobalt compounds have vacancies in their crystal lattices that can be used for catalysis.^{1,2}

3.1.1 Discovery of Cobalt-Catalyzed Hydroformylation

Cobalt-catalyzed hydroformylation was discovered in 1938 by Otto Roelen. Roelen was studying the Fischer-Tropsch reaction which converts H_2/CO into alkenes and alkanes. In trying to improve the yields by recycling ethylene, he noticed the solid-supported cobalt catalyst was producing some propanal. It was rapidly established through studying this unexpected reaction that it was occurring in the organic phase, which is considered the birth of homogeneous catalysis. Since this time, hydroformylation of olefins to yield aldehydes and alcohols has become one of the largest-scale industrial homogeneous catalytic processes.³

In the 1950's the active catalyst of the cobalt hydroformylation cycle was identified as $HCo(CO)_4$ and the catalytic cycle was postulated (Figure 3.2). It involves firstly the replacement of a CO ligand with the alkene. Much research and debate went into whether 3 or 4 CO ligands were present on the active species. Finally, Breslow and Heck put this debate to rest with a brief communication on the spectroscopic evidence that supports only 3 CO ligands are present with the species reacting with the alkene. Though the 2 species, $HCo(CO)_4$ and $HCo(CO)_3$, are in

equilibrium in the catalytic cycle, the latter is a 16 electron species which gives it an open coordination site to bind with the alkene.^{3,4}

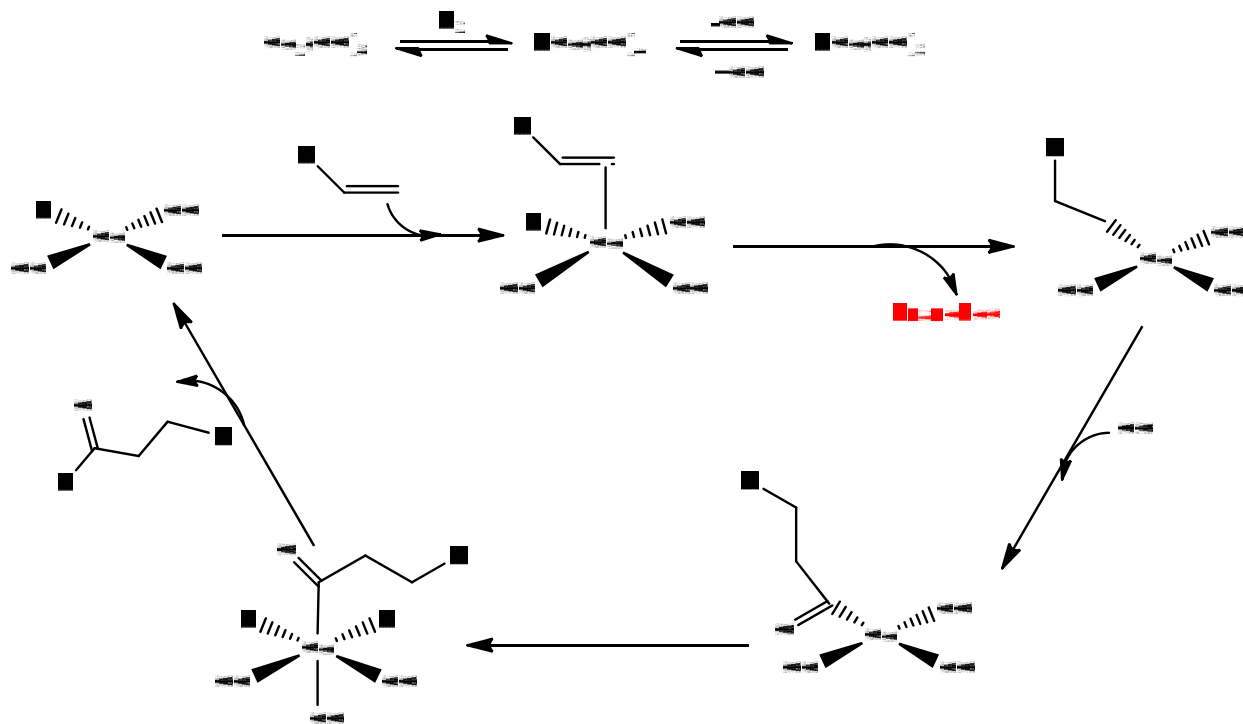


Figure 3.2 Unmodified cobalt hydroformylation cycle

The second step involves the hydride transfer from the metal to the alkene to give either the linear or branched alkyl species (linear is generally desired). CO coordination and migratory CO insertion follow this step. Lastly, the oxidative addition of H₂ and reductive elimination of the aldehyde regenerates the HCo(CO)₃ catalyst. It has also been postulated in the literature that when reactions are carried out under stoichiometric conditions using HCo(CO)₄ it will react directly with the acyl species to give the aldehyde and Co(CO)₇. The unsaturated species Co(CO)₇ can then go on to coordinate H₂ and regenerate the monomeric hydrides, HCo(CO)₄ and HCo(CO)₃. However, this only occurs when high concentrations of cobalt are present.^{3,5,6} This cycle is widely accepted as the general mechanism of cobalt catalyzed hydroformylation. However, it has not been clarified in every detail, and some aspects are still under investigation.⁷

3.1.2 Modified vs Unmodified Cobalt Hydroformylation

Conventional hydroformylation is often run using dicobalt octacarbonyl ($\text{Co}_2(\text{CO})_8$) as the catalyst precursor. This precursor is treated with 1:1 H_2/CO (syngas) under harsh conditions at temperatures of 100-180°C and pressures of 1500-4500 psi to convert it to the $\text{HCo}(\text{CO})_4$ catalyst. These extreme conditions are required to maintain the stability of $\text{HCo}(\text{CO})_4$ and prevent catalyst decomposition. At lower pressures and temperatures, $\text{HCo}(\text{CO})_4$ degrades to cobalt metal.^{8,9}

The hydrogenation activity of $\text{HCo}(\text{CO})_4$ is relatively low, with the aldehydes being the dominant species formed from the reaction, albeit with fairly low linear/branched (l/b) selectivity (Table 3.1). From this data, it is clear that changes in temperature and pressure have a dramatic effect on the selectivity of the catalyst.

Table 3.1 Hydroformylation of 1-pentene with $\text{Co}_2(\text{CO})_8$ as catalyst⁸

Expt No.	Temp (°C)	Max. Press. (psi)	H_2/CO ratio	% Yield (Alcoh./Aldeh.)	L/B selectivity	% Conv. of 1-pentene
6	100	400	1.0	2.8/96.7	50/50	67
7	120	1700	1.9	3.3/95.6	70/30	97.3
8	140	1700	1.9	9.7/84	64/36	100
9	150	400	1.0	4.5/90.5	50/50	47

For example, at lower maximum pressures of 400 psi (before catalyst decomposition) with a 1:1 H_2/CO ratio (experiments 16 and 19), the l/b selectivity is 50/50. At higher pressures of 1700 psi with a 2/1 H_2/CO ratio (experiments 17 and 18), the l/b selectivity is fairly higher at 70/30 and 64/36, respectively.⁸

In 1968, Slaugh and Mullineaux (Shell) reported that the addition of a phosphine ligand (called “modified” system), such as PBu_3 , could stabilize the catalyst to such an extent that reaction pressures lower than 1470 psi were feasible. These catalysts were formed in situ by combining

Co₂(CO)₈ with the appropriate phosphine ligand (1/1 or 2/1 ligand/cobalt) at 300-800 psi H₂/CO and 150-200°C.⁸ Though addition of the phosphine ligand allowed for lower temperatures and pressures, this modified system was actually less reactive and favored the formation of alcohols over aldehydes. However, the l/b selectivity was greatly enhanced while working with an excess of the phosphine ligand, at least 2/1 (ligand/cobalt).^{3,8,9}

Including trialkylphosphines such as PBu₃ and PEt₃, many bulky phosphines were also tested for the hydroformylation of 1-pentene. Table 3.2 shows a brief comparison of the effects of various phosphine and arsine ligands on the rates and isomeric compositions of the products at maximum pressures of 450-500 psi with an H₂/CO mole ratio of ~2. From this data it appears that tertiary arsines may be more active for hydroformylation but less selective than the phosphines.

Table 3.2 Hydroformylation of 1-Pentene with HCo(CO)₃L⁸

Expt No.	Ligand	Temp. (°C)	Initial Rate of Gas Consumption (mmole/h)	% Conv. of 1-pentene	% Yield (Alcoh./Aldehyd.)	L/B Selectivity
1	PEt ₃	195	220	100	79.8/0	80.9/19.1
2	PBu ₃	195	265	100	77.0/0	84.1/15.9
4	P(C ₆ H ₁₁) ₃	195	200	75.4	69.6/3.0	79.5/20.5
10	PPh ₃	195	19.8	39.9	60.7/10.3	66.0/34.0
11	dppe	195	57	96.2	67.7/1.3	56.5/43.5
14	AsBu ₃	150	206	82.8	51.9/28.7	67.8/32.2

The more basic phosphines lead to higher selectivities. For example, PBu₃ has a linear selectivity of up to 91%; while PPh₃, which is less basic, gives a much lower linear selectivity of 66%. Additionally, PPh₃ is a weakly binding ligand that must be used in higher concentrations during the catalysis to maintain some coordination to the metal centers. These ligands were used in a 1/1 cobalt/ligand ratio for these experiments. The bulkier phosphines used by Slauch and

Mullineaux give fairly moderate selectivities, but the bidentate ligands, such as dppe, gave a lower selectivity of 56.5%⁸

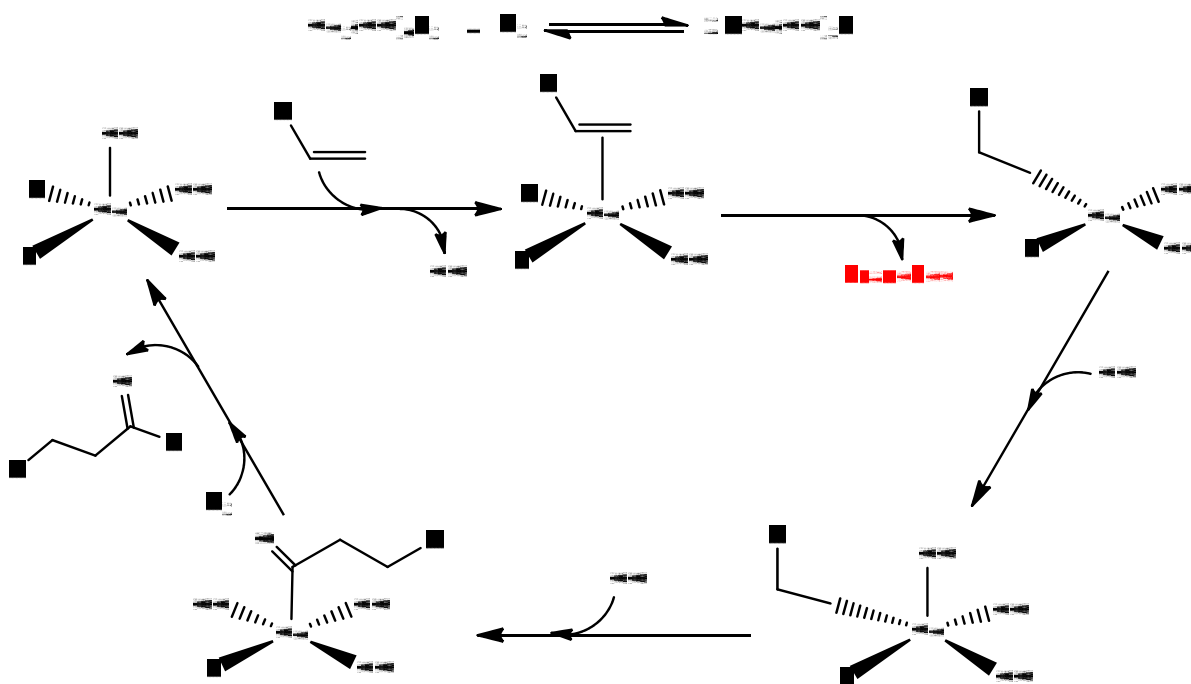


Figure 3.3 Modified cobalt hydroformylation cycle¹⁰

Since this discovery of the modified phosphine cobalt hydroformylation system, much research has been put into the study of various phosphine-containing ligands and their effects on the hydroformylation system. Research groups worldwide are still actively pursuing this area to obtain a highly selective catalyst without sacrificing reaction rate and reducing olefin hydrogenation and isomerization side reactions. The Heck and Breslow mechanism presented above has been modified to contain the phosphine substituent within the active species, $\text{HCo}(\text{CO})_3\text{L}$. Figure 3.3, shown above, is a scheme depicting the mechanism for the modified cobalt hydroformylation system.¹⁰

3.1.3 Commercial Hydroformylation and the Low Pressure Oxo Processes

Since the discovery of hydroformylation, almost 80 years ago, it has become one of the world's largest-scale industrial processes. The aldehyde production has increased constantly; in

2008, 10.4 million tons of aldehydes were produced.^{3,11} As previously stated, the majority of this capacity is absorbed by the polymer industry for plasticizers and the detergent industry. Industrial hydroformylation can be broken down into 3 generations of processes. The first generation was exclusively based on cobalt as the catalyst metal, without phosphine ligand. BASF, Exxon, ICI, Kuhlmann, and Ruhrchemie adapted this first generation process. Despite the harsh reaction conditions and low selectivity, reaction conditions were suited to ensure an acceptable rate of reaction. These processes only varied in the solution of how to separate products and catalyst. Various modes were developed to recover and recycle the catalyst and yielded comparable results.⁷

The second-generation processes combined the advantages of phosphine ligand modification with the transition from cobalt to rhodium as catalyst metal. Celanese Corporation and Union Carbide Corporation both adopted these low-pressure oxo (LPO) processes in 1974 and 1976 respectively, with many other companies following suit (Mitsubishi Chemical Corporation in 1978). Rhodium-phosphine catalysts afforded fairly high reaction rates, with better linear-branched selectivity and could be run at lower temperatures and pressures (85-130°C and 174-725 psi H₂/CO).^{12,13} The third generation, however, can be considered to be the basic idea of applying a water-soluble phosphine as ligand which transfers hydroformylation into the aqueous phase, such as the water-soluble rhodium-tppts (trisulfonated triphenylphosphine) system utilized since 1984 by Celanese.^{7,13,14}

As a result of this industrial success, commercial hydroformylation plants are run exclusively with catalysts based on Rh or Co. The primary advantage of cobalt catalysts over rhodium is their higher reactivity toward internal alkenes, which is due to their ability to isomerize. Rhodium based LPO processes are favored due to their mild reaction conditions, simpler and cheaper equipment, high efficiency, high yield of linear products, and easy recovery of the

catalyst.^{15,16} Because Co is relatively cheaper than Rh, it does not require complete recycling. However, the accumulation of Co decomposition products, such as clusters and metallic Co, can foul reactor surfaces and cause serious valve blockage problems that can result in the shutdown of a plant. The main disadvantages of Co systems are the high pressure conditions that result in high capital and operating costs.¹¹ Table 3.3 shows a brief comparison of the reaction parameters for Co and Rh based processes.^{15,16}

Table 3.3 Comparison of cobalt and rhodium based processes¹⁵

Catalyst	Cobalt (Classical) $\text{HCo}(\text{CO})_4$	Rhodium (ligand modified) $\text{HRh}(\text{CO})\text{L}_3$
Temperature ($^{\circ}\text{C}$)	130-190	85-130
Pressure (bar)	200-300	12-50
Metal concentration (%b.w.)	0.1-0.5	0.01-0.05
l/b ratio	80/20	>90/10
Formation of by products	High	Low
Catalyst recovery and recycle	Complicated	simple

*%b.w. means percent by weight

3.1.4 Hydroformylation Research Goals

The main research activities of hydroformylation are in the fields of ligand syntheses and modified catalysts. Phosphines are the most widely used and accepted ligands for hydroformylation. Since phosphine-modified hydroformylation has been so extensively studied, reactions can now be tuned by changing the electronics and steric effects of the ligand to yield different regioselectivities. In general, the linear/branched ratio of phosphine-modified catalysts increases with ligand/metal ratio. The coordination of the ligands to the metal center enhances the steric bulkiness and linear products are favored. Hydrogenation and isomerization side reactions are still possible, but they are typically suppressed with an excess of phosphine ligand.^{7,13,15}

In general, the phosphine-modified Co systems have lower reactivity than the unmodified version, though higher regioselectivity. This holds true for the Rh systems as well; the unmodified systems are much more active than the modified systems, albeit with almost no regioselectivity. Industrially, the price and long-term stability of the phosphine ligand are the most important factors for calculating the overall cost of the process. Short, high yield synthetic processes with cheap starting materials are desirable when a phosphine ligand is used. Due to the commercial success of Rh-phosphine systems, particularly the Rh-PPh₃ system for hydroformylation, much research has been put into understanding what role phosphines play in the catalysis.^{11,13}

The high selectivity of the Rh-P systems for linear aldehydes is a consequence of the *trans* configuration of two bulky groups on the P atom. These groups increase the coordinative unsaturation of the Rh metal center and lead to higher catalyst activity. The electron-donor properties of the ligand are best described in terms of the basicity of the free ligand. Based on the literature, it can be stated that in general, the strongly basic phosphines are less active for hydroformylation than less basic phosphines. Molecular orbital studies indicate that increased σ -electron donation from the phosphine ligand, which is directly related to the phosphine basicity, to the metal leads to stronger bonding of both the phosphine and the CO ligands. Increased bonding to the CO ligands is the result of an increased flow of electrons from the metal to the antibonding orbitals of the CO ligand, called π back-donation (or π -backbonding).¹⁷

The increased π -backbonding, however, can lead to slower hydroformylation catalysis because CO and phosphine dissociation are necessary steps in the mechanism of the reaction. The opening of a coordination site must occur to bind the alkene and start the reaction, as stated above. In general, electron-withdrawing ligands can lead to a decrease in π -backbonding to CO, an acceleration of the alkene complexation step, and faster catalysis. In terms of bulk, the highly

sterically demanding ligands can lead to more CO ligands, which makes the Rh center more electron-poor and enhances their dissociation. This effect can lead to higher l/b ratios.¹³ An example of the mechanism of Rh-catalyzed hydroformylation with three bulky phosphine groups can be found in Figure 3.4.

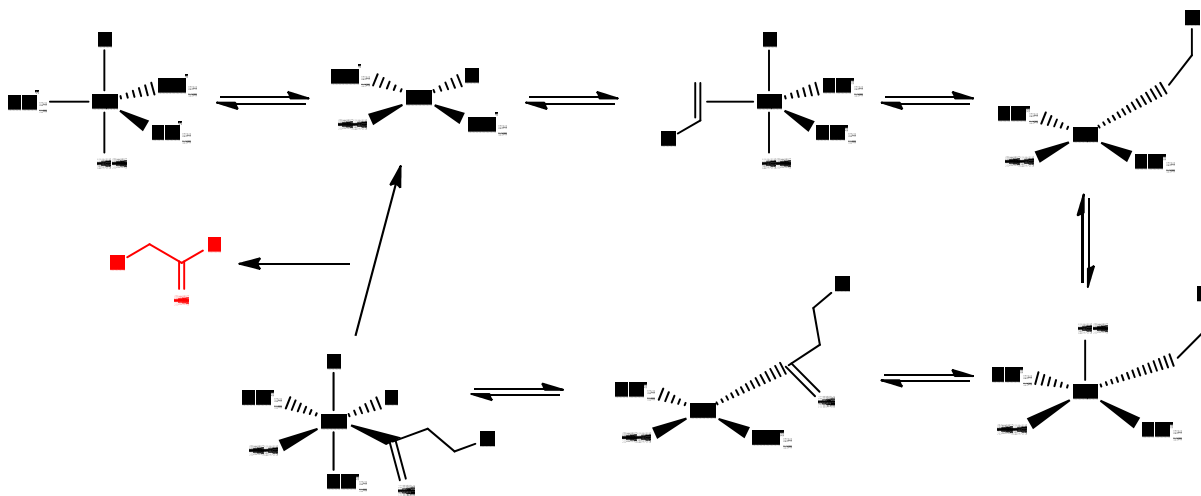
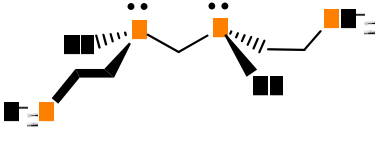
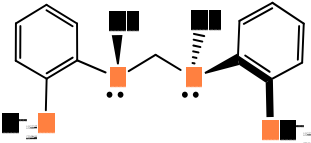
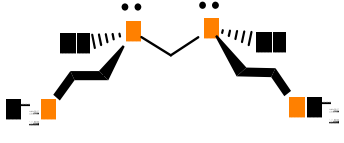
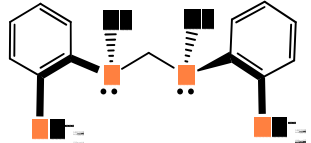


Figure 3.4 Mechanism of a rhodium-catalyzed hydroformylation reaction¹⁷

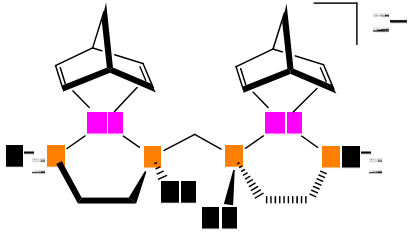
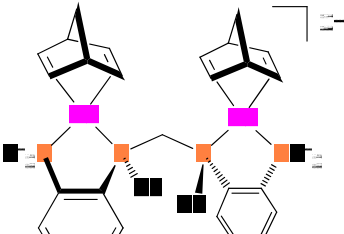
The most widely used Rh catalyst precursor is $\text{RhH}(\text{PPh}_3)_3\text{CO}$.¹³ Simple trialkylphosphines have been tested but are not practical for commercial hydroformylation as previously mentioned. Bulkier phosphines are preferred due to reduced volatility and catalyst stability.^{10,13} However, because of their initially low selectivities for hydroformylation,⁸ it was not until the late 1970s that the use of bidentate phosphine ligands in catalysis found some applications.^{13,18} The overall versatility of phosphine ligands is that it allows for tuning of the electronic properties of the ligand to be tailored to the type of desired catalysis. The Stanley research group has made use of this versatility through the development of two types of tetraphosphine ligands (Table 3.4) for a dirhodium-catalyzed hydroformylation system. The ligands were designed to bridge two metal centers together and lead to bimetallic cooperativity in catalysis. The dirhodium catalyst precursors are shown in Table 3.5.

Table 3.4 Stanley research group tetraphosphine ligands

“Old” Tetraphosphine Ligands	“New” Tetraphosphine Ligands
 <p data-bbox="414 514 592 556"><i>Rac</i>-eth,ph-P4</p>	 <p data-bbox="1015 535 1226 577"><i>Rac</i>-eth,ph-P4-Ph</p>
 <p data-bbox="397 819 609 861"><i>Meso</i>-eth,ph-P4</p>	 <p data-bbox="998 840 1242 882"><i>Meso</i>-eth,ph-P4-Ph</p>

Using these ligands, the Stanley research group has been able to demonstrate successful catalysis through bimetallic cooperativity. For example, the *rac* diastereomer of the “old” tetraphosphine ligand (eth,ph-P4) dirhodium catalyst precursor proved to be a very effective catalyst for the hydroformylation of 1-hexene with TOF of 60 min⁻¹ and l/b selectivity of 33/1.

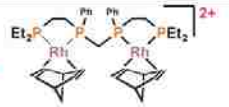
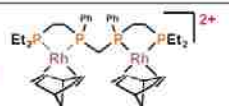
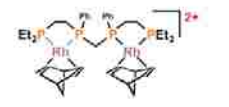
Table 3.5 Dirhodium-tetraphosphine catalyst precursors

<i>Rac</i> -Rh ₂ (nbd) ₂ (eth,ph-P4)	<i>Rac</i> -Rh ₂ (nbd) ₂ (eth,ph-P4-Ph)
	

The *meso* diastereomer, in comparison, was a much poorer hydroformylation catalyst with TOF of only 0.9 min⁻¹ with high isomerization and hydrogenation side reactions (24% and 10%,

respectively). Figure 3.5, below, shows the results of our catalyst systems compared to a standard industrial Rh-PPh₃ system.¹⁹

Hydroformylation of 1-Hexene (90 psig, 90°C)

Catalyst	Initial TOF (min ⁻¹)	L:B	iso	hydro
<i>rac</i> - 	20	25:1	2.5%	3.4%
<i>rac</i> - 	30-60	33:1	~1%	<0.1%
HRh(CO)(PPh ₃) ₂ (0.82 M PPh ₃)	9	17:1	1%	<0.5%
<i>meso</i> - 	0.9	14:1	24%	10%

*Result in blue used 30% H₂O/acetone as the solvent. All other results used acetone.

Figure 3.5 Hydroformylation results

Catalyst fragmentation issues lead to the design of the “new” tetraphosphine ligand also shown in Table 3.4. This ligand is more strongly coordinating due to the phenylene linkage between the internal and external phosphorous groups, which should make the catalyst more stable. Studies with this dirhodium catalyst (Table 3.5) are currently underway. Preliminary results have shown that this catalyst is more active than the older version.

Another type of reactivity, aldehyde-water shift catalysis, was discovered using our dirhodium system. This catalysis, shown in Figure 3.6, was discovered accidentally by a former group member, Dr. Novella Bridges, when there was a small leak that wasn't noticed in the autoclave.²⁰



Figure 3.6 Aldehyde-water shift catalysis reaction

This leak preferentially depleted H₂ in the autoclave, which shifted the catalyst equilibrium away from the Rh-hydride species. This increased the concentration of [Rh₂(μ-CO)₂(CO)₂(et,ph-P4)]²⁺ that catalyzed the reaction of aldehyde and H₂O to make the carboxylic acid and H₂. These results were surprising (Figure 3.7) and led to a new type of catalysis. However, this reactivity has not been very reproducible and has been shown to be very dependent on experimental conditions.

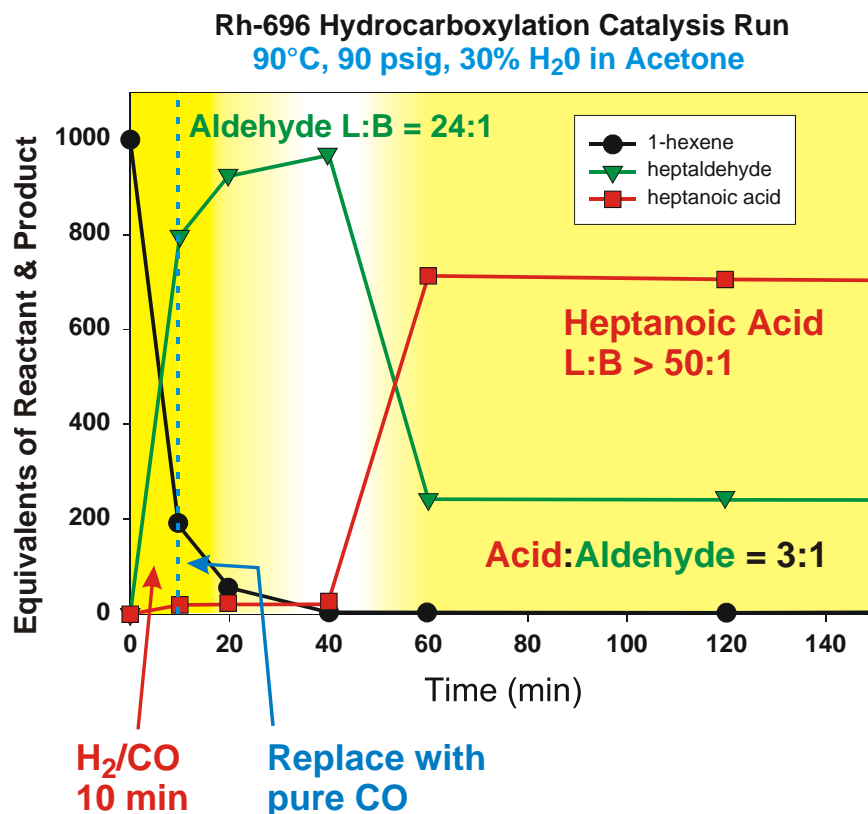


Figure 3.7 Aldehyde-water shift catalysis results²

Based on the success of the dirhodium systems in our group, the pursuit of a dicobalt system that could be active for both hydroformylation and aldehyde-water shift catalysis is the focus of this research. As previously stated, cobalt is still very relevant to industrial hydroformylation. In fact, Exxon, BASF, and Shell Chemical still use some form of HCo(CO)₄ for hydroformylation.^{7,15} A highly active and selective cobalt catalyst for hydroformylation could very useful and industrially profitable.

3.2 Results and Discussion

3.2.1 Background Research

The first dicobalt complex, shown in Figure 3.8, from the Stanley research group was synthesized by Dr. Fredric Askham using the hexaphosphine ligand system back in 1985. This complex was synthesized through a dicobalt tetrachloride precursor, which was then reduced by H_2/CO in an autoclave system.²¹ The next dicobalt complex, shown in Figure 3.9, was synthesized by Dr. Scott Laneman, who used our “old” *meso* tetraphosphine ligand and was generated through the use of a dicobalt-tetracarbonyl-bis(norbornadiene) starting material. This complex contains a unique “cradle” type geometry of the tetraphosphine ligand surrounding the metal centers. It is a neutral species that contains a single Co-Co bond.²² Synthetic schemes for both complexes can be found in Figures 3.10 and 3.11.

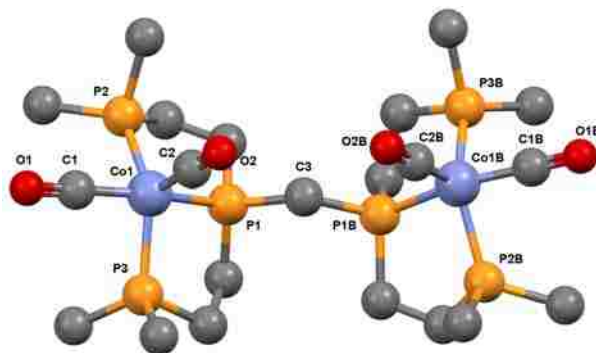


Figure 3.8 Ball-and-stick model for $[Co_2(CO)_4(eHTP)][PF_6]_2$. Hydrogen atoms, methyl groups on external P atoms, and counteranions have been omitted for clarity

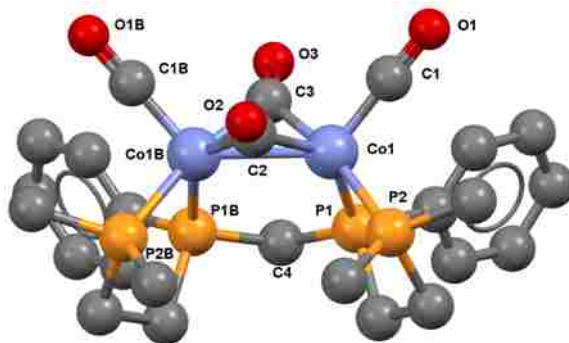


Figure 3.9 Ball-and-stick model for *meso*- $Co_2(\mu-CO)_2(CO)_2(et,ph-P_4)$. Hydrogen atoms and methyl groups on external P atoms omitted for clarity

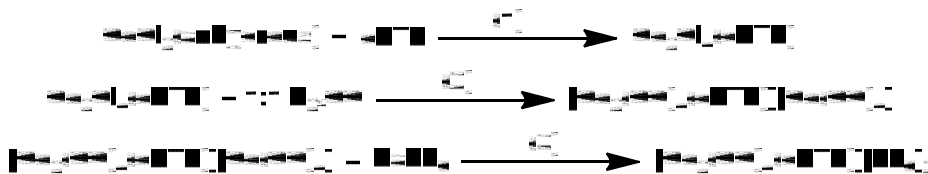


Figure 3.10 Synthesis of $[\text{Co}_2(\text{CO})_4(\text{eHTP})][\text{PF}_6]_2$



Figure 3.11 Synthesis of *meso*- $\text{Co}_2(\mu\text{-CO})_2(\text{CO})_2(\text{et,ph-P4})$

As a result of this previous work, several synthetic methods were developed and utilized in attempt to synthesize bimetallic cobalt complexes with both diastereomers of our “old” and “new” tetraphosphine ligands. The combination of a metal chloride starting material with our tetraphosphine ligand to form the bimetallic species *meso*- or *rac*- $\text{Co}_2\text{Cl}_4(\text{et,ph-P4})$ (or with the hexaphosphine ligand) has been utilized in our group to also obtain dinickel²³ and dichromium²⁴ complexes. Once the dicobalt tetrachloride species is formed, subsequent reduction in the presence of H_2/CO should make the appropriate carbonyl or carbonyl-hydride complex. This would make a more suitable hydroformylation catalyst to study for bimetallic cooperativity.

3.2.2 Attempted Reduction of *meso*- and *rac*- $\text{Co}_2\text{Cl}_4(\text{et,ph-P4})$ and (et,ph-P4-Ph)

As previously mentioned, the synthesis of $[\text{Co}_2(\text{CO})_4(\text{eHTP})][\text{PF}_6]_2$ was published by the Stanley research group in 1985.²¹ The synthesis first combined the hexaphosphine ligand with 2 equivalents of anhydrous cobalt chloride in EtOH. This step formed the dicobalt tetrachloride complex, $\text{Co}_2\text{Cl}_4(\text{eHTP})$. This dark green mixture of complex and solvent was then transferred to the Parr autoclave system, pressurized to 50 bar (~725 psig) H_2/CO (33.4% CO), and heated to 80°C for 12-36 hours. Upon removal from the autoclave, $\text{Co}_2(\text{CO})_4(\text{eHTP})\text{-CoCl}_4$ was isolated in vacuo. The final step involved an anion exchange using NaPF_6 to replace the $[\text{CoCl}_4]^{2-}$ dianion to

yield the final complex, $[\text{Co}(\text{CO})_4(\text{eHTP})][\text{PF}_6]_2$.²¹ Beginning with a design similar to this procedure, the reduction of both the new and old ligand dicobalt tetraphosphine complexes was attempted first with a 1:1 mixture of H_2/CO and then with various other reducing agents.

In addition to H_2/CO (syngas), sodium borohydride (NaBH_4), lithium aluminum hydride (LAH), lithium triethylborohydride (super hydride), sodium metal (Na), zinc metal (Zn), and magnesium turnings (Mg) were all utilized for this transformation. The interest in electron-transfer reactions of organometallic complexes has grown over the course of the last 20 years. As a result, the use of chemical redox agents to effect these transformations has grown as well. One main disadvantage of using chemical redox reagents in organometallic chemistry is the formation and separation of the byproducts formed during the reaction.²⁵ The formation and separation of byproducts proved to be a considerable problem for the cobalt reduction chemistry in this research.

3.2.3 Synthesis of *meso*- and *rac*- $\text{Co}_2\text{Cl}_4(\text{et,ph-P4})$ and (et,ph-P4-Ph)

The synthesis of $\text{Co}_2\text{Cl}_4(\text{et,ph-P4})$ for both the “old” P4 and “new” P4-Ph tetraphosphine ligands (Table 3.4) was performed by adding one equivalent of the ligand to two equivalents of cobalt chloride (CoCl_2) and the reaction mixture stirred overnight at room temperature. A scheme of this reaction can be found in Figure 3.12. Both the anhydrous and hydrated ($\text{CoCl}_2 \cdot 6\text{H}_2\text{O}$) forms were used for this synthesis, with the hydrated form being the better option because it is more soluble in polar organic solvents. The tetraphosphine ligands are soluble in most polar organic solvents and many non-polar solvents as well (i.e. benzene and hexane).



Figure 3.12 Synthesis of *meso*- $\text{Co}_2\text{Cl}_4(\text{et,ph-P4-Ph})$. Scheme shown here is with the new tetraphosphine ligand, but the same applies for the old tetraphosphine ligand, *et,ph-P4*

The choice of solvent turned out to be the most important variable for this reaction. Acetone, EtOH, THF, DCM, and CH_3CN were all used with acetone and CH_3CN the most suitable

solvents because both the ligands and CoCl_2 are soluble in them. THF and DCM worked fairly well, but the ligand is only moderately soluble in THF (it precipitates out of solution during the addition), and the CoCl_2 (both the hydrated and anhydrous forms) have poor solubility in DCM. In some cases where THF was used as the solvent for CoCl_2 , DCM was usually the chosen solvent for the ligand. Solvent combinations or concentrations did not seem to be a factor in the reaction. Typically, the reactions were run with about 20-30 mL of solvent and about 0.5 grams of ligand. A minimum amount of solvent appeared to be the most suitable for these reactions. The use of EtOH, however, proved to be problematic because it can act as a mild reducing agent and would cause the dicobalt tetrachloride complexes to degrade in solution if not removed within 24 hours. This degradation was noted by the color change of the reaction mixture from the usual dark green to brown/black and posed a problem for the next step of the synthesis, which involved the reduction of the dicobalt tetrachloride complexes with H_2/CO . The brown/black mixture is analogous with the formation of some cobalt metal, which leads to more “over-reduction” of the dicobalt tetrachloride complexes.

Typically these reaction mixtures were allowed to stir overnight under N_2 and the solvent removed to isolate *meso/rac*- $\text{Co}_2\text{Cl}_4(\text{et,ph-P4})$ or *meso/rac*- $\text{Co}_2\text{Cl}_4(\text{et,ph-P4-Ph})$. Once the addition of the ligand to the CoCl_2 solution began, the reaction mixture immediately took on a dark green color with a fine green precipitate; therefore, the length of reaction time to form this complex was not particularly important as we believe it occurred rapidly. As long as EtOH was not used as the solvent, the dicobalt complex was typically stable in solution for up to about 48 hours. Isolation of this complex worked better than using it in solution as done in the published synthesis²¹ because the concentrations of reducing agents could be more accurately deduced, which leads to better reductions and less degradation of the material. This complex appears unstable under H_2/CO

pressure, and it was found through much experimentation that it readily falls apart and degrades to form other monometallic cobalt species, such as *rac*-[CoCl₂(et,ph-P4-Ph)]³⁺, which was isolated and characterized by X-ray crystallography, and the [CoCl₄]²⁻ dianion, which was deduced from the blue color of the reaction mixture removed from the autoclave after the reductions.

Yields of the isolated dicobalt tetrachloride complexes were usually between 80-90%. On occasion when the *rac* diastereomers of the ligands were used, a purple precipitate, believed to be CoCl₂(κ³-et,ph-P4) based on other similarly related structures, such as CoCl₂(P(CH₃)₃)₃^{26a} and [(triphos)Co(μ-Cl)₂CoCl₂].^{26b} Both of these neutral complexes are violet in color and contain Co(II) metal centers that are 5-coordinate with two chloride ligands and three phosphine groups. Because of this degradation, the yield of the dicobalt tetrachloride complexes *rac*-Co₂Cl₄(et,ph-P4)/(et,ph-P4-Ph) would be lower, between 50-60%.

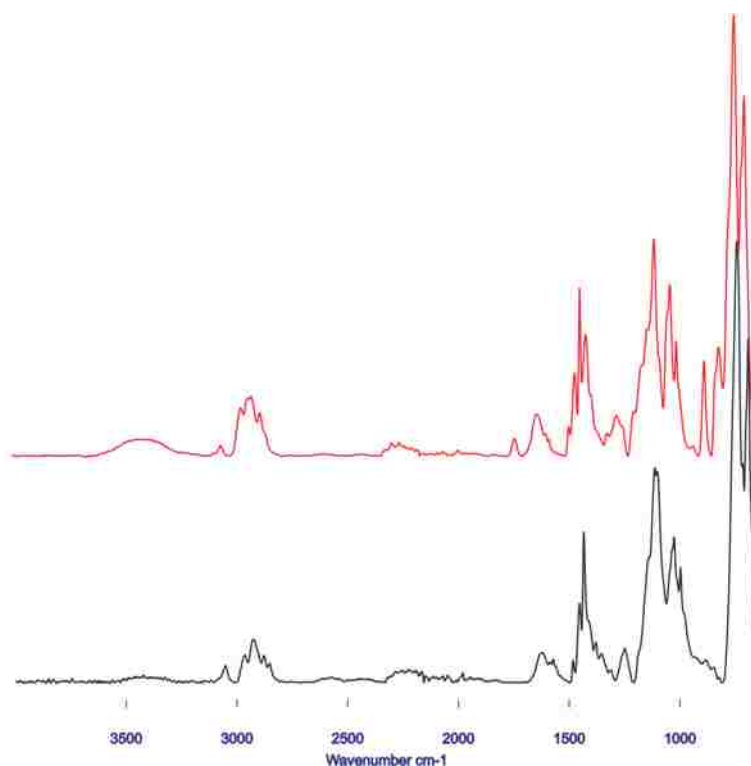


Figure 3.13 FT-IR Spectra of *meso*-Co₂Cl₄(et,ph-P4-Ph) (black spectrum) and *meso*-Co₂Cl₄(et,ph-P4) (red spectrum)

Analysis of the dicobalt tetrachloride complexes was performed using fourier transform-infrared spectroscopy (FT-IR). A comparison of the *meso* complexes can be found in Figure 3.13. As expected, there are no major differences between FT-IR spectra of the old and new ligand complexes. They are both very similar.

FT-IR analysis does not provide much information about the structure, but it serves as a background for the reduction step, which should include the coordination of carbonyl ligands, which are usually detected between 1800-2100 cm^{-1} . ^{31}P NMR is not useful for determining the structure of this paramagnetic Co(II) d^7 complex. To this date, there has been no success for obtaining crystals of *meso*- or *rac*- $\text{Co}_2\text{Cl}_4(\text{et,ph-P4})/(\text{et,ph-P4-Ph})$ for X-ray crystallography analysis. As previously mentioned, complexes similar to this one have been made and characterized in the Stanley research group such as our dinickel complexes.²³ The structures of these complexes can be found below in Figures 3.14 and 3.15, and we expect similar structures although with a tetrahedral geometry around the Co(II) metal centers.

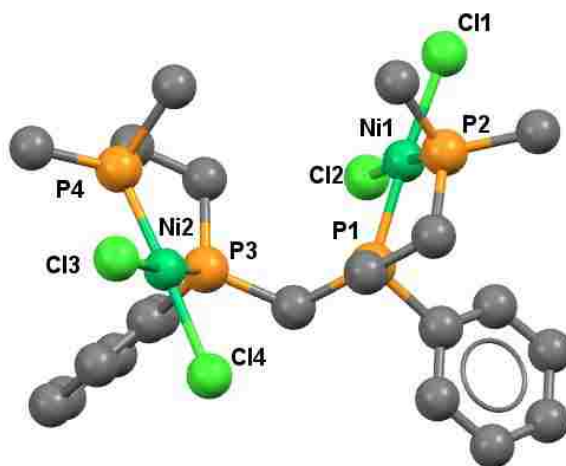


Figure 3.14 Ball-and-stick model for *rac*- $\text{Ni}_2\text{Cl}_4(\text{et,ph-P4})$. Hydrogen atoms and methyl groups on external P atoms have been omitted for clarity

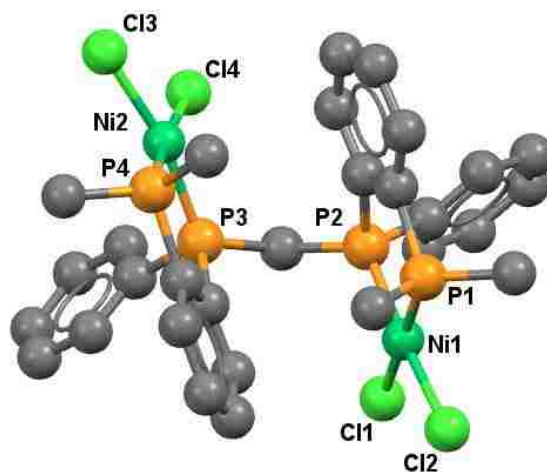


Figure 3.15 Ball-and-stick model for *rac*-Ni₂Cl₄(*et,ph*-P₄-Ph). Hydrogen atoms and methyl groups on external P atoms have been omitted for clarity

3.2.4 H₂/CO Reduction of *meso*- and *rac*-Co₂Cl₄(*et,ph*-P₄) and (*et,ph*-P₄-Ph)

Following the published method in the literature²¹, the formation of *meso*- and *rac*-[Co₂(CO)_x(*et,ph*-P₄)]²⁺ and new P₄-Ph complexes, *meso*- and *rac*-[Co₂(CO)_x(*et,ph*-P₄-Ph)]²⁺ for use as bimetallic hydroformylation catalysts was first attempted using syngas (1:1 H₂/CO) in the Parr autoclaves. A reaction scheme, based on the autoclave reduction from the hexaphosphine dicobalt paper²¹, can be found below in Figure 3.16.



Figure 3.16 Scheme for the H₂/CO Reduction of *meso*-Co₂Cl₄(*et,ph*-P₄-Ph). This scheme also applies to the old P₄ dicobalt tetrachloride complexes

The pressures of syngas were varied from 40 up to 250 psig with temperatures ranging from 50°C to 80°C. Reaction times were varied from 3 hours up to 24 hours with the latter being the better choice. Initial experiments revealed that 3 hours was not enough time to allow the complex to be completely reduced and ligand substitution from chloride to carbonyls to occur. This was deduced by the dark green color of the reaction mixture removed from the autoclave. As

previously stated, the combination of CoCl_2 and our tetraphosphine ligands in a polar organic solvent is usually dark green in color before its reaction with a reducing agent. The color changes of the reaction mixtures helped to identify whether a reduction was occurring or not. The absence of the dark green color meant the complex was reduced; however, the presence of a blue reaction mixture revealed the presence of $[\text{CoCl}_4]^{2-}$. Based on the literature results, a reduction under H_2/CO yielded some fragmentation of the hexaphosphine dicobalt tetrachloride complexes, to form the dicobalt-tetracarbonyl complex and the cobalt-tetrachloride dianion, which was still green in color. Isolation of the dicobalt-tetracarbonyl complex after counteranion exchange with NaPF_6 yielded a light yellow solid. The initial green color after the reduction was a result of the mixture of the blue $[\text{CoCl}_4]^{2-}$ and the yellow dicobalt-tetracarbonyl complex.²¹ We also had some H_2/CO reactions with this analogous color mixture.

Initial reactions began with the dicobalt tetrachloride complexes in solution transferred to the autoclave with 2-4 equivalents of trimethylamine (NEt_3). During the H_2/CO reductions, the $\text{Co(II)} d^7$ metal centers should get reduced to $\text{Co(I)} d^6$ centers. The chloride ligands can then be replaced by carbonyls or hydrides. NEt_3 is used to neutralize the HCl generated in the mixture as a byproduct by forming triethylammonium chloride (Et_3NHCl). The use of 4 equivalents of NEt_3 proved to be problematic because some of the Et_3NHCl (clear) co-crystallized along with a blue solid from the reaction mixture and the two solids could not be physically separated for further analyses. To combat this issue, the dicobalt tetrachloride complexes were isolated and characterized first (using FT-IR), and the appropriate amount of NEt_3 (2 equivalents) was added to the autoclave.

The solvent used in these reactions did not play a significant role in the results. The dicobalt tetrachloride complexes are most soluble in acetone, CH_3CN , and DCM . These were the main

solvents used for this reaction. The use of CH₃CN, however, led to a “sticky” material being removed from the autoclave. We think this is associated in some way with the ability of CH₃CN to act as a ligand and bind to the cobalt metal centers. This makes the product very difficult to isolate and use for further analyses by ³¹P NMR and FT-IR.

The temperatures also did not play a significant role in the results of these reactions. Most of the reactions were run at about 80°C. Temperatures were later lowered to about 50 or 60°C in attempt to prevent some of the over reduction to Co(0), deduced from the brown color removed from the autoclave, and in attempt to “cleanly” synthesize the desired complexes, [Co₂(CO)_x(et,ph-P4)/(et,ph-P4-Ph)]²⁺. However, through multiple experiments at different temperatures and pressures, we discovered that the pressure played the most important role during these reactions.

Initially, higher pressures (200-250 psig) were used for the reduction. The belief was that since cobalt is less reactive and previously published work used ~725 psi H₂/CO to achieve the desired complex²¹, higher pressures would be needed for this synthesis as well. As previously stated, though, the dicobalt tetrachloride complexes proved to be unstable under higher pressures for making [Co₂(CO)_x(et,ph-P4)/(et,ph-P4-Ph)]²⁺. Color changes led to the conclusion that complete degradation of the dicobalt tetrachloride complexes occurs leading to blue or brown/black mixtures of solid and solutions. In a few cases, an insoluble gray solid, believed to be Co metal, was removed from the autoclave system. Lower pressures from 100-150 psig yielded less degradation and better reductions but also led to some fragmentation (blue colored mixture), most likely associated with the formation of [Co₂(CO)_x(et,ph-P4)/(et,ph-P4-Ph)][CoCl₄].

In attempt to prevent this fragmentation and leaching of Co, pressures were eventually lowered to 90 and then 40 psig. At these lower pressures, it appeared that less degradation was occurring, but the reaction mixtures were still light green/blue in color, which suggested some

fragmentation was still occurring. We also assumed the presence of the green color meant the reduction was not fully occurring or we were forming unwanted by products.

FT-IR analyses were very unpredictable in these reactions. In some cases, usually with pressures at 200 psig or above, we would get three terminal CO bands at 1880, 1937, and 1995 cm^{-1} as shown in Figure 3.17. The CO band at 1880 cm^{-1} was only present in a few of the trials performed at pressures of about 200 psig and only from the reduction of the old P4 dicobalt tetraphosphine complexes.

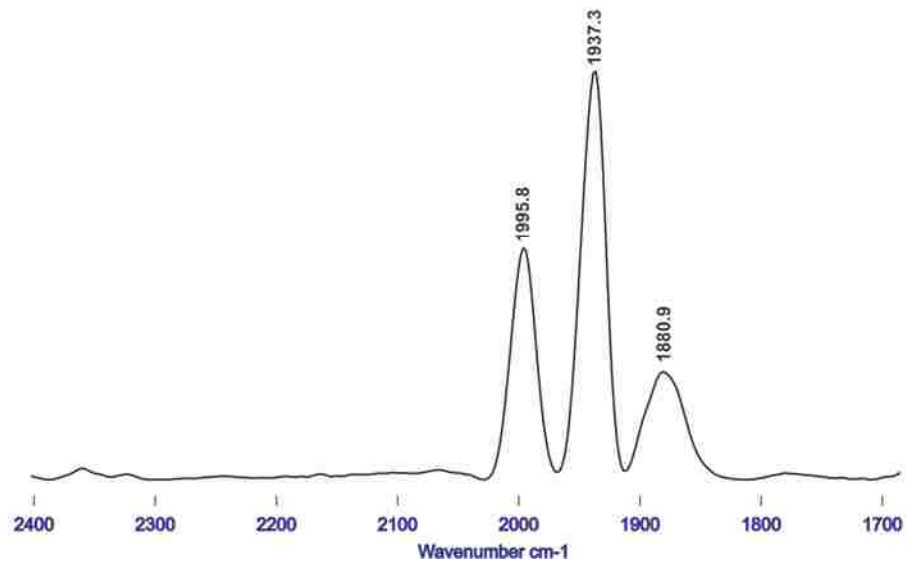


Figure 3.17 Partial FT-IR Spectrum of Autoclave Reduction of *meso*- $\text{Co}_2\text{Cl}_4(\text{et,ph-P4})$ in CH_3CN at 230 psig H_2/CO and 80°C

We have tentatively assigned this lower frequency band to be *meso*- $\text{Co}_2(\mu\text{-H})_2(\text{CO})_2(\text{et,ph-P4})$, shown in Figure 3.18, based on DFT studies performed by Dr. Stanley. This electron rich, neutral complex is very unique in that it contains a $\text{Co}=\text{Co}$ double bond and contains two bridging hydride ligands. According to the DFT studies, it should have a symmetrical ^{31}P NMR pattern with signals at 88 and 54 ppm. However, this species has not been isolated and characterized experimentally. Also, we do not see this low frequency CO band when we reduce the new P4-Ph

dicobalt tetracarbonyl complexes in the H₂/CO reduction at any pressure. This band was only present with the reduction of the old P4 dicobalt tetrachloride complexes, which led us to propose that the new P4-Ph tetraphosphine ligands were not electron rich enough to allow the formation of this neutral hydrido-carbonyl complex.

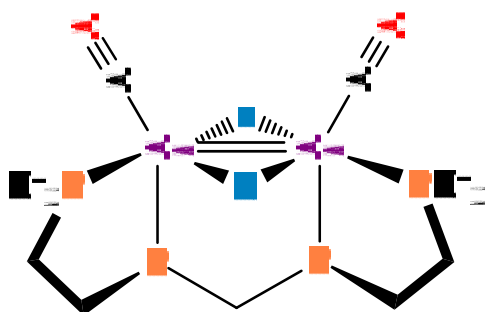


Figure 3.18 Structure of *meso*-Co₂(μ-H)₂(CO)₂(et,ph-P4)

The two higher frequency terminal CO bands at 1937 and 1995 cm⁻¹ have been assigned to a penta- or hexa-carbonyl dicobalt complex, *meso*-[Co₂(CO)₅₋₆(et,ph-P4)]²⁺, similar to Askham's dicobalt complex with the hexaphosphine ligand, [Co₂(CO)₄(eHTP)]²⁺.²¹ A scheme of the old P4 and new P4-Ph hexa-carbonyl dicobalt complexes can be found below in Figure 3.19.

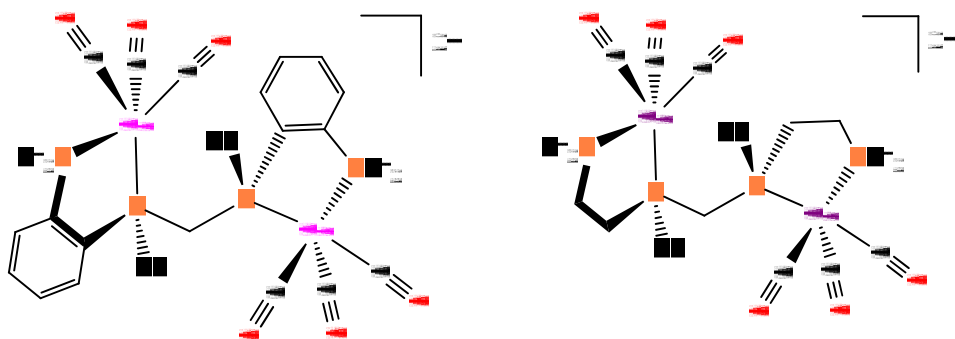


Figure 3.19 Structures of *rac*-[Co₂(CO)₆(et,ph-P4-Ph)]²⁺ (left) and *rac*-[Co₂(CO)₆(et,ph-P4)]²⁺ (right)

When the pressures were lowered to about 100 psig, we would only get the two terminal CO bands, as shown in Figure 3.20, usually at roughly the same wavenumbers of about 1930 and 1990 cm⁻¹. These bands were consistent throughout most of the experiments at both higher and

lower pressures, and as previously stated, we believe them to be associated with the most stable species formed during the reduction, either the penta-carbonyl or hexa-carbonyl dicobalt complex.

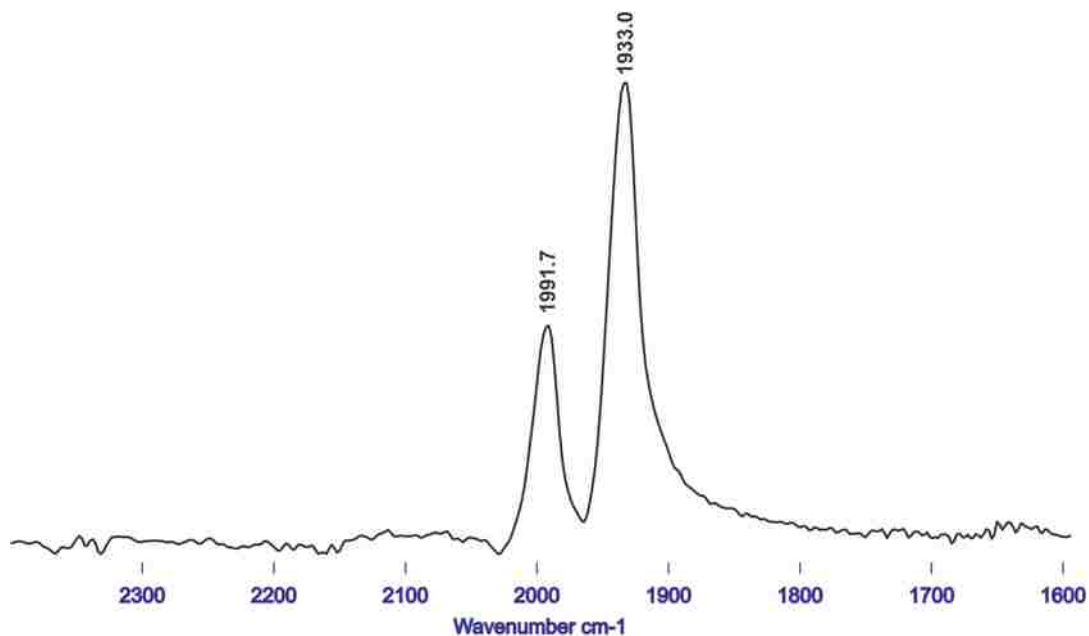


Figure 3.20 Partial FT-IR spectrum of autoclave reduction of *rac*-Co₂Cl₄(*et*,*ph*-P₄) in DCM/CH₃CN at 100 psig H₂/CO and 60°C

With pressures lower than 100 psig, we would get the same two terminal CO bands, but with much lower intensities, especially with pressures around 40 psig as seen in Figure 3.21. The lower intensities and light green/blue mixtures were determined to be the result of loss of the cobalt and formation of [CoCl₄]²⁻. The higher wavenumbers of the new P₄-Ph dicobalt-carbonyl complexes versus the old P₄ complexes is also evident in this figure. The carbonyl frequencies in the new P₄-Ph dicobalt-carbonyl complexes are higher in wavenumber because the new P₄-Ph tetraphosphine ligands are less electron rich than the old P₄ ligands. Thus, less electron density is available for π -backbonding between the Co metal centers and the carbonyl ligands, resulting in higher stretching frequencies.

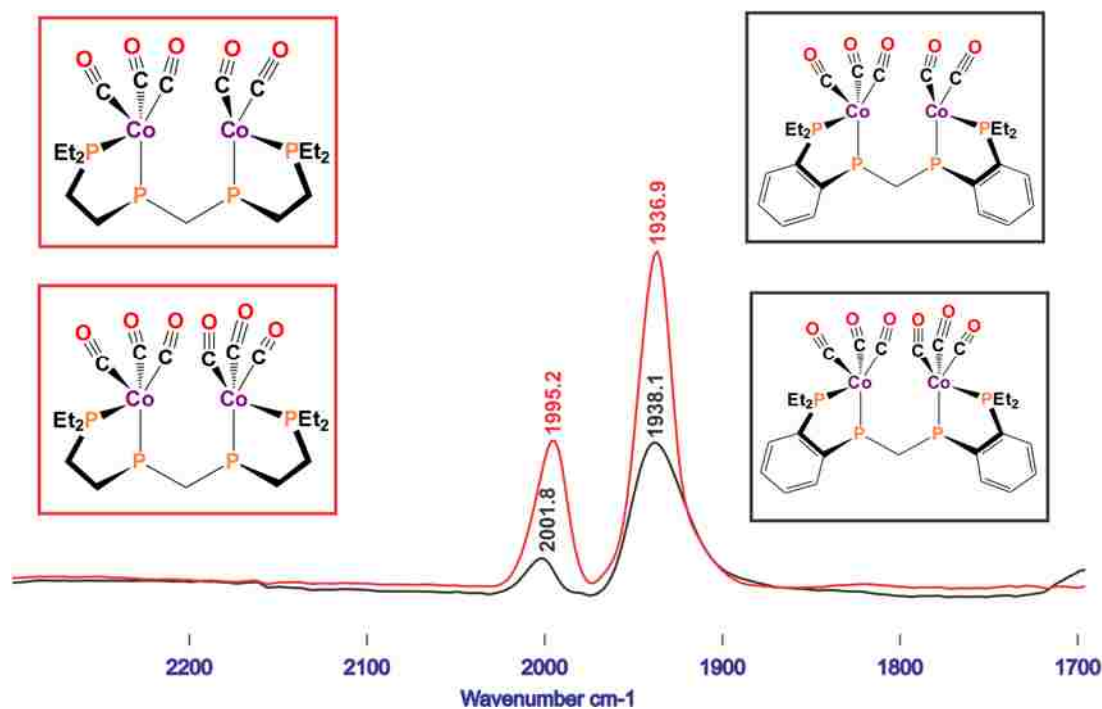


Figure 3.21 Comparison of the partial FT-IR spectra of autoclave reductions of *meso*-Co₂Cl₄(*et,ph*-P₄) in DCM at 50 psig H₂/CO and 60°C (red spectrum) and *meso*-Co₂Cl₄(*et,ph*-P₄-Ph) in acetone at 40 psig H₂/CO and 50°C (black spectrum). The figures in the red boxes are the proposed complexes for the old *meso* dicobalt tetrachloride reductions, and the figures in the black boxes are the proposed complexes for the new *meso* dicobalt tetrachloride reductions

³¹P NMR analysis was another useful tool to track the reduction of these complexes. As previously stated the dicobalt tetrachloride complexes are paramagnetic. However, once the reduction from a Co (II) d⁷ to Co(I) d⁸ oxidation state occurs, the complex should no longer be paramagnetic and can be analyzed by NMR. Similar to the FT-IR results, the ³¹P NMR results were also highly unpredictable. In most cases, no signals were detected after about 1500-2000 scans, probably a result of the mixture of species (some paramagnetic) produced in these reactions. Since diamagnetic cobalt complexes have a quadrupole moment (non-spherical electric and magnetic fields), their NMR spectra suffer from severe line broadening, shallow signals, and difficulties with phasing and integration. Whenever a mixture of complexes with Co(II) impurities was present in any of our experiments, we would need to run a multitude of scans, at least 3000, to detect the signals from a Co(I)-phosphine complex.²⁷

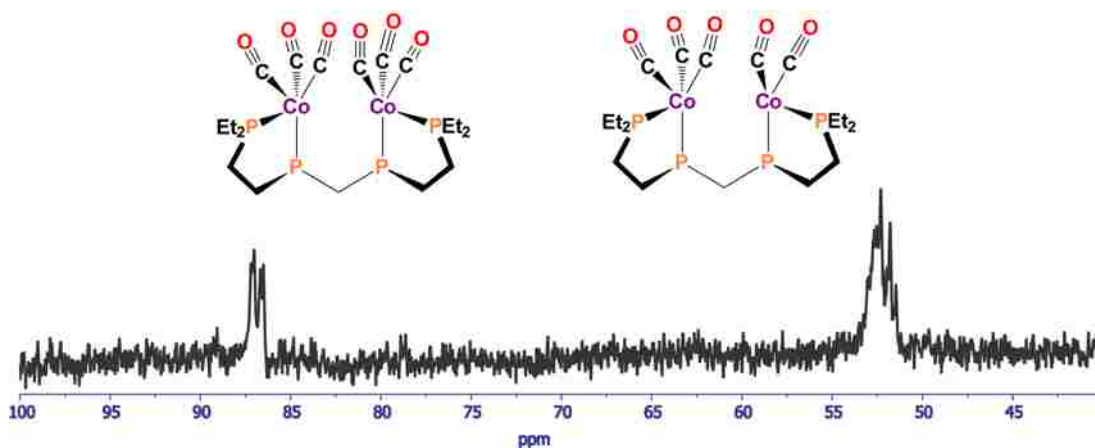


Figure 3.22 ^{31}P NMR spectrum of autoclave reduction of *meso*- $\text{Co}_2\text{Cl}_4(\text{et,ph-P4})$ in CH_3CN at 230 psig H_2/CO and 80°C

There were a few experiments that yielded what appeared to be two symmetrical patterns at 52 and 86 ppm, shown above in Figure 3.22. We believe this distorted doublet of doublets at 86 ppm and multiplet at 52 ppm to most likely be associated with the penta- or hexacarbonyl dicobalt complexes previously described. These signals are somewhat similar to Askham's ^{31}P NMR for the tetracarbonyl dicobalt complex, $[\text{Co}_2(\text{CO})_4(\text{eHTP})]^{2+}$. He observed a quintet pattern at 127 ppm and a doublet at 83.4 ppm.²¹

We postulated that some unreacted dicobalt tetrachloride complex was still present after the reactions were complete as well as some leaching of cobalt to form the dianion, $[\text{CoCl}_4]^{2-}$. This led us to the conclusion that even at lower pressures, the complex was still falling apart. There were even a few reactions where certain isolated solids from the autoclave reductions with H_2/CO would contain no CO signals. Attempts to separate the mixture of species being formed using the pure solvents or a mixture of solvents, such as DCM, acetone, CH_3CN , hexanes, THF, or MeOH, and/or crystallize either of the proposed complexes, $[\text{Co}_2(\text{CO})_{5-6}(\text{et,ph-P4})]^{2+}$ or $\text{Co}_2(\mu\text{-H})_2(\text{CO})_2(\text{et,ph-P4})$ were unsuccessful.

A few experiments were also run using 2-4 equivalents of NaPF_6 or NaBF_4 at 90-100 psig and $50\text{-}60^\circ\text{C}$. The presence of these counter anions (PF_6^{1-} and BF_4^{1-}) should have served as a

replacement for the $[\text{CoCl}_4]^{2-}$ dianion. However, a similar mixture of species was still obtained as previous experiments. In fact, an unexpected result was obtained through recrystallization attempts of the mixtures.

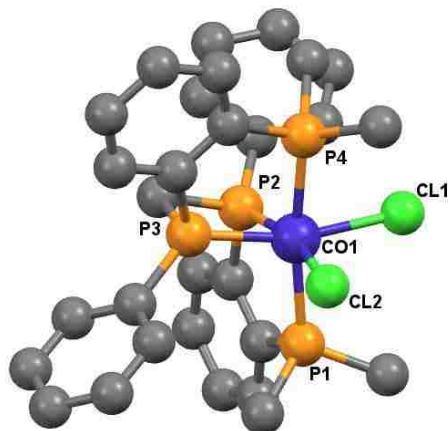


Figure 3.23 Ball-and-stick model for $\text{rac}-[\text{CoCl}_2(\text{et,ph-P4-Ph})]^+$. Hydrogen atoms and methyl groups on the external P atoms have been omitted for clarity

Using MeOH as the recrystallization solvent, deep orange/red crystals were obtained from the results of one of the autoclave reduction mixtures. These crystals were identified as $\text{rac}-[\text{CoCl}_2(\text{et,ph-P4-Ph})][\text{PF}_6]$ (Figure 3.23) via X-ray crystallography.

This result was the most concrete evidence for the instability of $\text{meso}/\text{rac}-\text{Co}_2\text{Cl}_4(\text{et,ph-P4})$ and the new P4-Ph ligand dicobalt tetrachloride complexes, $\text{meso}/\text{rac}-\text{Co}_2\text{Cl}_4(\text{et,ph-P4-Ph})$, under H_2/CO pressures. The formation of this Co(III) d^6 monometallic complex could be from the degradation of the bimetallic complexes during the autoclave reduction experiments. During these reactions, it is possible that Co(II) is disproportionating to form Co(III) and Co(I), and this Co(III) complex provides evidence for this phenomenon.

The Stanley group isolated and characterized a similar monometallic Fe complex using the hexaphosphine ligand system from its bimetallic counterpart, $[\text{Fe}_2\text{Cl}_2(\text{eHTP})][\text{Cl}]_2$ in 1987.²⁸ This distorted octahedral Fe complex, $[\text{FeCl}(\text{CO})(\eta^4\text{-eHTP})][\text{Cl}]$, shown in Figure 3.24, was isolated

from the exposure of the bimetallic species to an atmosphere of CO.²⁸ The X-ray structure revealed that the two internal P atoms were in a 4-membered chelate ring *trans* to the CO and Cl⁻ ligands.

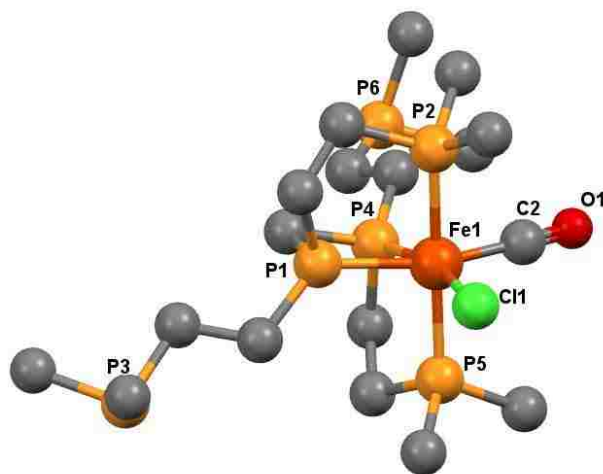


Figure 3.24 Ball-and-stick model for $[\text{FeCl}(\text{CO})(\text{eHTP})]^{1+}$. Hydrogen atoms and methyl groups on the external and dangling P atoms have been omitted for clarity

This is very similar to our mononuclear, distorted octahedral cobalt complex in which the internal P atoms of the old P4 tetraphosphine ligand are in a 3-membered chelate ring *trans* to the two Cl⁻ ligands. The Co-Cl and Fe-Cl bond distances are roughly the same for both complexes as well with the Co-Cl distances at 2.29 Å and the Fe-Cl distance at 2.36 Å, which are typical single bond distances for these metal centers.²⁸

A few experiments were run with pure CO instead of the H₂/CO mixture, since CO itself can act as a reducing agent, usually in the presence of oxygen. We proposed that the lack of H₂ may lead to a more direct synthetic route to the desired complex, $[\text{Co}_2(\text{CO})_{5-6}(\text{et,ph-P4})]^{2+}$. Our initial hypothesis was that the H₂ was causing some of the over-reduction and fragmentation, and the inseparable mixture of complexes produced was from the presence of hydride impurities. As previously discussed, at 1:1 H₂/CO pressures of 200 psig or higher, we proposed the lower frequency terminal CO band at 1882 cm⁻¹ to be the neutral dibridged-hydride complex, $\text{Co}_2(\mu\text{-H})_2(\text{CO})_2(\text{et,ph-P4})$, but we were not able to isolate it and further characterize the likely structure.

Experiments conducted at ~120 psig CO at 80°C yielded a blue colored reaction mixture that contained a single carbonyl signal at 1940 cm⁻¹ by FT-IR analysis. This signal was very weak in intensity, which led to the belief that this was a mixture with the carbonyl species being the minority. The second experiment was conducted at ~220 psig CO and 80°C with 2 equivalents of NEt₃. This experiment again yielded a mixture of species and some degradation of the material. With the instability of the dicobalt tetrachloride complexes under H₂/CO and CO high pressures (even at 40 psig), other reducing agents were explored in hopes of yielding a cleaner, and better reduction method.

3.2.5 NaBH₄ Reduction of *meso*- and *rac*-Co₂Cl₄(*et,ph*-P₄) and (*et,ph*-P₄-Ph)

NaBH₄ is commonly used as a mild reducing agent in organic and organometallic chemistry.²⁵ However, the reduction of metal ions with NaBH₄ has been often shown to yield either metal borides or zero-valent metals. The formation of cobalt boride (Co₂B) particles results from the combination of NaBH₄ and CoCl₂.²⁹ An example of this reaction can be found in Figure 3.25.

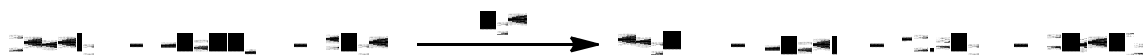


Figure 3.25 Synthesis of Cobalt Boride (Co₂B)²⁹

The literature shows that the reduction of Co²⁺ with NaBH₄ and the reactions between Co²⁺, bis(diphenylphosphino)methane (dppm), and NaBH₄ are very complex and slight changes in reaction conditions, such as concentration, ratio of the two, and rate of mixture of the two can change the identity of the product.^{29,30,31,32} Co₂B and the corresponding nickel boride (Ni₂B) have found some application in heterogeneous hydrogenation and can also be used as reducing agents.³³

For the attempted reduction of *meso*- and *rac*-Co₂Cl₄(*et,ph*-P₄) and *meso*- and *rac*-Co₂Cl₄(*et,ph*-P₄-Ph), 2 or 2.5 equivalents of NaBH₄ were used per mole of CoCl₂. All reactions were run between 2-24 hours usually at room temperature under CO balloon pressure in a polar

organic solvent or solvent mixture (EtOH, EtOH/C₆H₆, THF, or acetone). Each reaction was conducted by adding the appropriate amount of NaBH₄ to the dicobalt tetrachloride complex and then adding a CO-filled balloon. The time of reactivity or choice of solvent did not play a significant role in the results; all reactions using both the old P4 and new P4-Ph dicobalt tetrachloride complexes resulted in a green/brown mixture. This color change led us to conclude that the dicobalt tetrachloride complexes were only being partially reduced with some over reduction to Co(0), due to the presence of the brown color. A few of the experiments resulted in a black precipitate, presumably some cobalt-boride species²⁹ being formed. No ³¹P NMR signals were detected in any of these experiments, and FT-IR analyses yielded three low intensity CO bands (Figure 3.26) at 1932 with a shoulder at 1949, 1990 and 2058 cm⁻¹. As previously mentioned, we can most likely associate these signals with the penta- or hexacarbonyl dicobalt complexes. However, the presence of multiple CO bands probably means there was a mixture of other cobalt carbonyl complexes as well. Additionally, the higher frequencies of the carbonyl bands are analogous with the new P4-Ph tetraphosphine ligands as discussed above.

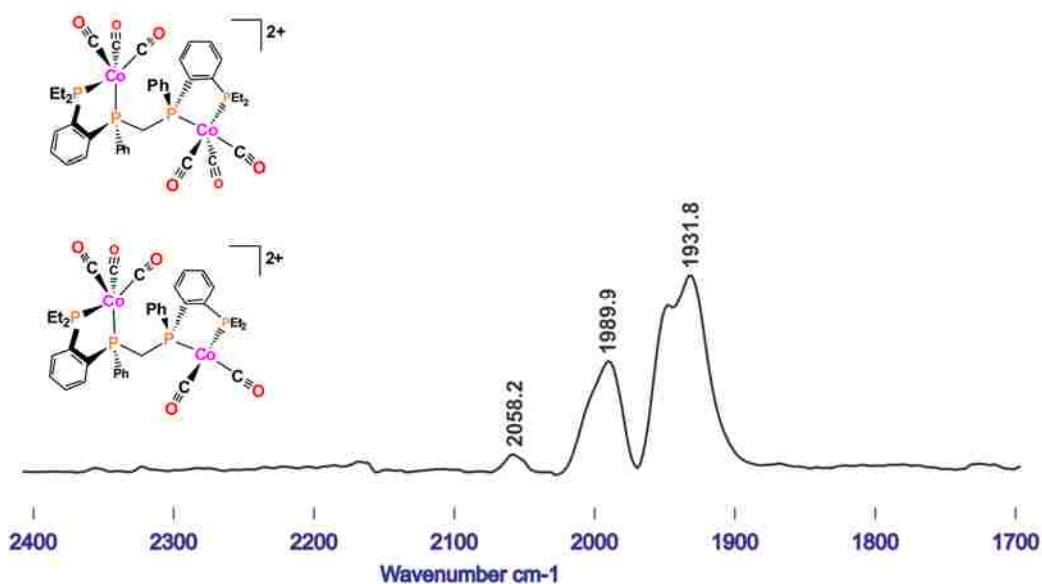


Figure 3.26 Partial FT-IR spectrum of NaBH₄ reduction of *rac*-Co₂Cl₄(et,ph-P4-Ph) at room temperature for 2 hours in a mixture of C₆H₆/EtOH

One experiment was conducted using 2 equivalents of NaBH₄ with 100 psig CO autoclave pressure at 80°C to reduce the old P4 *racemic* dicobalt tetrachloride complex. This reaction resulted in a purple/blue mixture being removed from the autoclave. The purple portion was believed to be *rac*-CoCl₂(κ³-et,ph-P4), while the blue portion was the [CoCl₄]²⁻ dianion. The FT-IR spectrum from this experiment can be found in Figure 3.27. It contains two larger intensity terminal CO bands at 1944 and 2002 cm⁻¹, which is most likely the penta- or hexacarbonyl dicobalt complex, *rac*-[Co₂(CO)₅₋₆(et,ph-P4)]². The reaction colors in this experiment, however, led us to believe that the complex was still partially degrading and leaching Co under pressure.

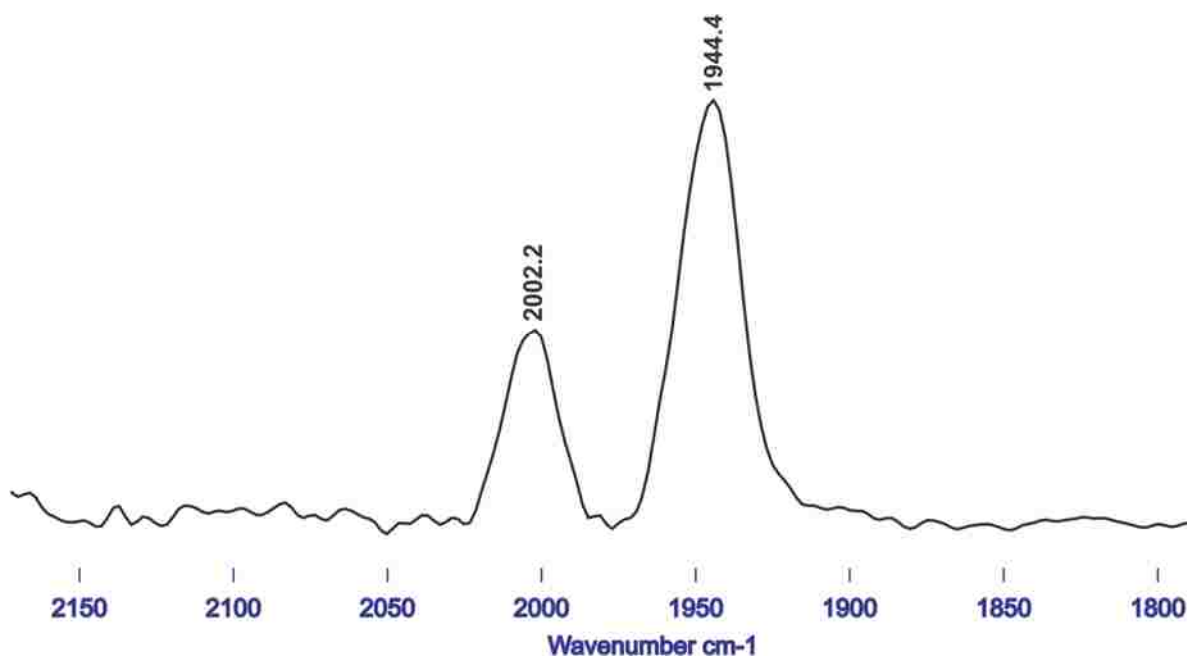


Figure 3.27 Partial FT-IR spectrum of NaBH₄ reduction of *rac*-Co₂Cl₄(et,ph-P4) with 100 psig CO (autoclave) at 80°C overnight in acetone

3.2.6 Lithium Aluminum Hydride (LAH) Reduction of *meso*-Co₂Cl₄(et,ph-P4-Ph)

LAH can also act as a one-electron reducing agent for organometallic complexes. Reductions with LAH have been shown to yield mixtures of products for a molybdenum (Mo) complex, however, and the removal of aluminum salt byproducts can be difficult.^{25,34} Also, transition metals have been shown to assist with LAH reductions in the literature.³⁵ One reduction

attempt using LAH with the new P4-Ph *meso* dicobalt tetrachloride complex was performed at room temperature, under CO balloon pressure, with THF as the solvent. Two equivalents of LAH under these conditions, however, did not appear to reduce the complex. The final color of the reaction mixture was dark green, which is the same as the initial color. There was a small amount of black precipitate present as well which we believed to be associated with some degradation of the dicobalt tetrachloride complex. FT-IR analysis did not yield any carbonyl signals. A lower temperature reduction might have led to a better result due to the higher reduction ability of LAH vs NaBH₄.

3.2.7 Super Hydride Reduction *meso*- and *rac*-Co₂Cl₄(*et,ph*-P4-Ph)

Studies have proven LiEt₃BH, or super hydride, to be one of the most effective reagents for the rapid reduction of alkyl halides. It is also commercially available as a 1M solution in THF and relatively inexpensive. The high reactivity of LiEt₃BH can lead to over reduction, which posed a problem in some systems.^{36,37,38} Due to its inexpensive commercial availability, it was used as a reducing agent for our dicobalt tetrachloride complexes. Experiments were conducted with 2 or 3 equivalents of super hydride, at 0°C or room temperature, between 2-24 hours, in THF (since the super hydride is a 1 M solution in THF), and under CO balloon pressure. Based on the results, however, we propose super hydride is too powerful a reducing agent for this system. This made it very difficult to control the reduction, which yielded a mixture of cobalt complexes. Also, the use of 3 equivalents of the super hydride was an experimental error, even at short reaction times of about 1 hour. Only 1 equivalent of super hydride per Co(II) center was needed for this reduction.

Experiments conducted for 2 hours yielded green or red/brown reaction mixtures. Attempted characterization of isolated species always led to no ³¹P NMR signals. FT-IR analyses contained a large, broad CO signal at 1940 cm⁻¹ with shoulders at 1884 and 1968 cm⁻¹, and two

small, low intensity CO signals at 2002 and 2041 cm^{-1} as shown in Figure 3.28. This mixture of CO bands at high and lower wavenumbers points to a mixture of cationic and neutral cobalt-carbonyl and/or carbonyl-hydride complexes, with, perhaps, one of these complexes being the dicationic penta- or hexacarbonyl dicobalt complex. Additionally, experiments conducted for 24 hours gave some blue/gray precipitates believed to be cobalt metal.

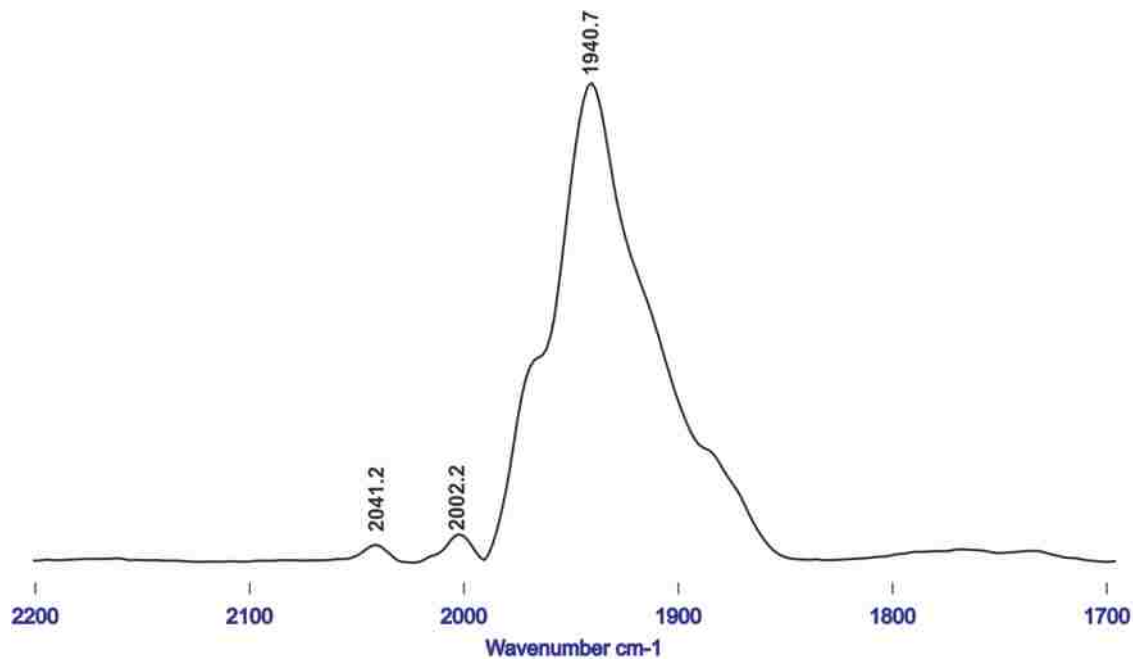


Figure 3.28 Partial FT-IR spectrum of super hydride reduction of *meso*- $\text{Co}_2\text{Cl}_4(\text{et,ph-P4-Ph})$ under CO atmosphere at room temperature for 2 hours in THF

3.2.8 Mg and Zn Reductions of *meso*- and *rac*- $\text{Co}_2\text{Cl}_4(\text{et,ph-P4})$ and (et,ph-P4-Ph)

Mg and Zn are widely used reducing reagents in organic chemistry. The Mg in methanol reduction of diphenylethylenes offers the advantages of being efficient, economical, and convenient, while being applicable to systems incorporating nuclear halogen substituents and heteroatoms.³⁹ Elemental Zn has been used as a reducing agent for nitroaromatics⁴⁰ and unsaturated 1,4-diketones⁴¹ under very mild conditions.

We decided to attempt the reduction of our old P4 and new P4-Ph dicobalt tetrachloride complexes with the use of Zn and Mg as mild reducing agents. The Mg reduction experiments

were run with the new P4-Ph *meso* dicobalt tetrachloride complex, 2 equivalents of Mg, ~50 mL of acetone or CH₃CN, at room temperature, and under CO balloon pressure. After running for 24 hours in either solvent, the color of the reaction mixture had only changed from dark green to a slightly lighter green. This led to the conclusion that the reduction did not occur using Mg. One hypothesis is that the oxide coating of Mg was not permeated enough to facilitate the reduction. Mg contains a thin layer of oxide coating that makes it air stable but sometimes difficult to remove. A solution to this problem could have been to allow the Mg turnings to stir vigorously for at least 24 hours or activation with iodine (I₂), but further experiments were not performed due to the success of the Zn reduction.

FT-IR analyses detected two weak CO signals (Figure 3.29) from the light green solid isolated from the Mg reduction experiments at around 1950 cm⁻¹ with a shoulder at 1975 cm⁻¹ and 2013 cm⁻¹, which are most likely from the dicationic penta- or hexacarbonyl dicobalt complexes.

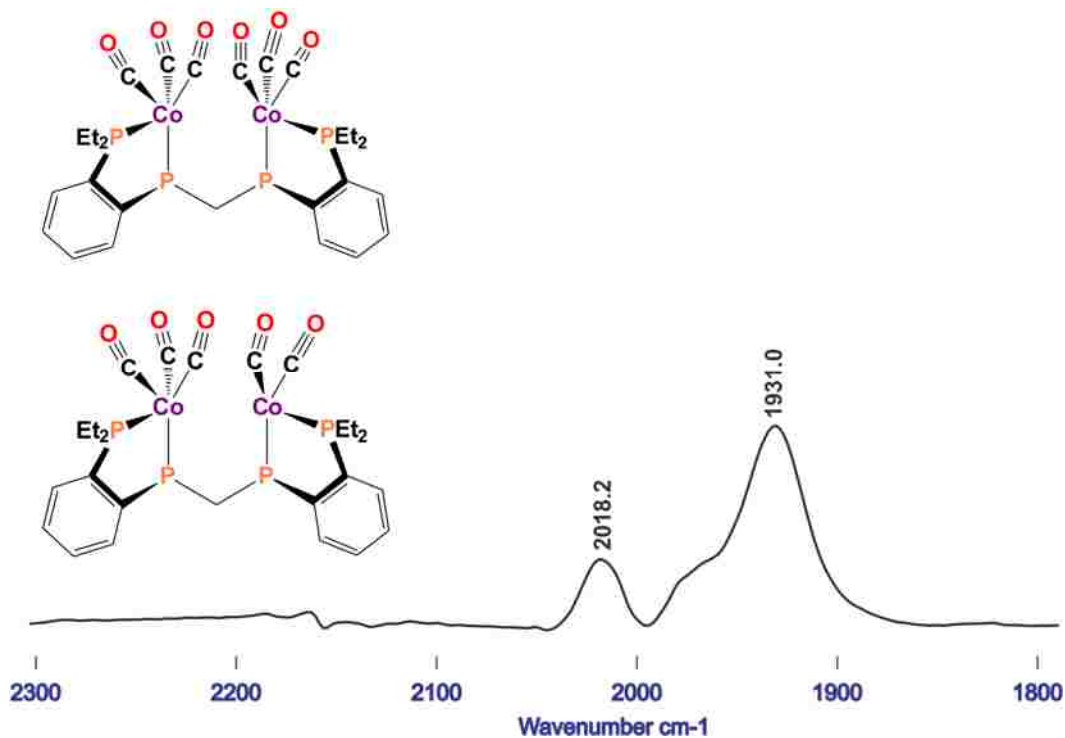


Figure 3.29 Partial FT-IR spectrum of attempted Mg reduction of *meso*-Co₂Cl₄(et,ph-P₄-Ph) in acetone

These carbonyl bands are typical for the new P4-Ph cobalt carbonyl complexes, and they are analogous with other reduction experiments performed using H₂/CO as well. There were no signals detected by ³¹P NMR due to the paramagnetic dicobalt tetrachloride complex most likely still present in the material.

Of all of the reducing agents used, Zn appeared to give the most effective and “cleanest” reduction for our system via FT-IR analyses. The reductions were run similar to the Mg experiments with the combination of the dicobalt-tetrachloride complex, 2-4 equivalents of Zn granules or dust, ~50 mL of acetone, CH₃CN, DCM, or DMF, at room temperature, and under CO balloon pressure. A few experiments were run in the autoclave at 40 psig CO and 50°C. The Zn dust resulted in faster reductions over the granules, which can be attributed to the larger surface area of the dust over the granules; the larger surface area leads to higher reactivity. Zn dust reductions were usually complete in about 3 hours, but experiments with the granules had to be run for at least 24 hours. The results after 24 hours for either would be the same. Any unreacted Zn (if more than 2 equivalents were used) could be filtered after the reactions were complete.

The choice of solvent played the most significant role in these reactions. It was discovered that the reduction only occurs with acetone, CH₃CN, and DMF. DCM is not a good solvent for this reaction. One hypothesis for why the reaction does not occur in DCM could be associated with the penetration of the Zn oxide coating. Perhaps, the more polar solvents like CH₃CN, acetone, and DMF help penetrate the oxide coating of Zn dust to enhance its reduction potential. Of the three solvents that the reaction did occur, CH₃CN was the most suitable choice. The byproduct produced in these reactions is ZnCl₂ formed from the combination of Zn and the chloride ligands free in solution after the reduction occurred. When acetone was used as a solvent, the ZnCl₂ was mostly soluble making its removal problematic. Partial solubility of the ZnCl₂ also occurs in

CH₃CN but to a lesser extent, and isolation of the orange/gold dicobalt complex was more facile. DMF was not chosen as a suitable solvent due to its high boiling point, which makes it difficult to evaporate from the final complex.

FT-IR analyses of the orange/gold material isolated from the Zn reductions of the old P4 and new P4-Ph dicobalt tetrachloride complexes usually yielded two sharp terminal carbonyl signals at 1938 and 1998 cm⁻¹ and three terminal carbonyl signals at 1934, 1971, and 2016 cm⁻¹, respectively. A comparison of these spectra can be found below in Figure 3.30.

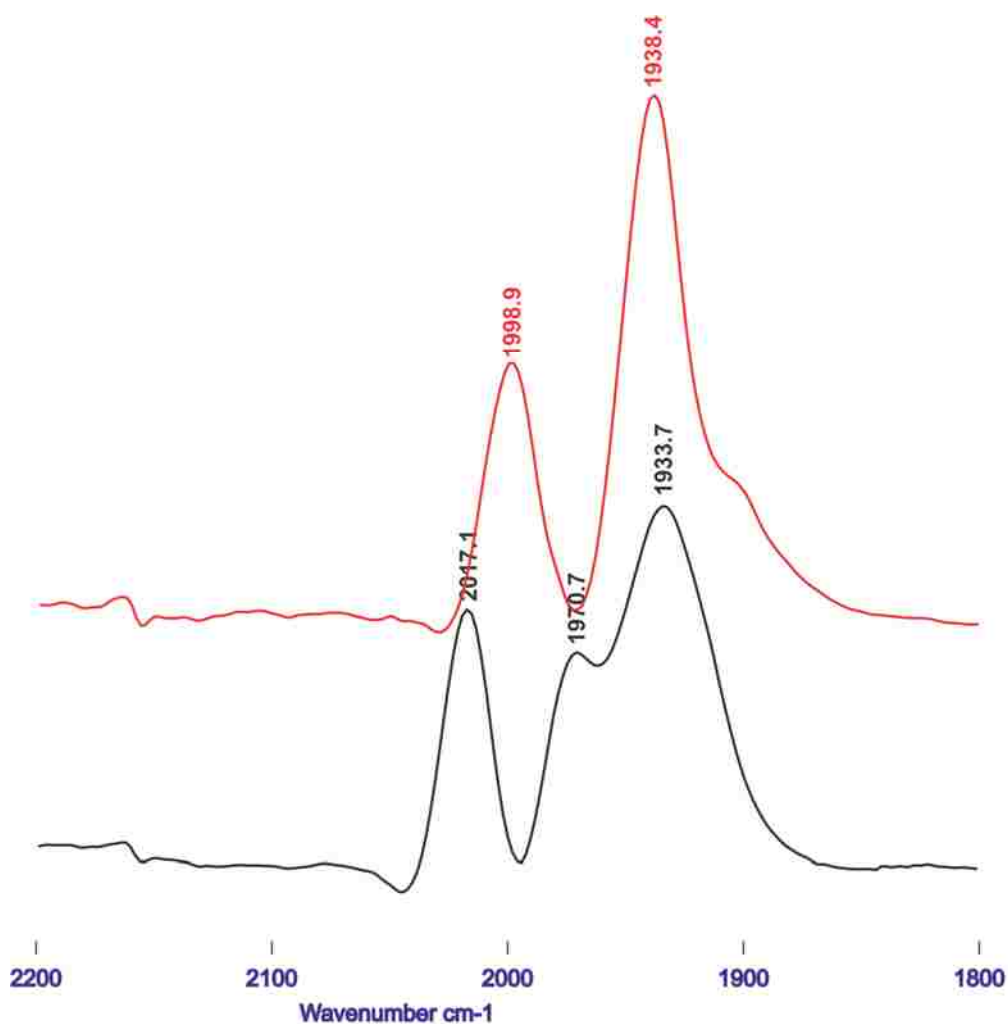


Figure 3.30 Comparison of partial FT-IR spectra of Zn reductions of *meso*-Co₂Cl₄(et,ph-P4-Ph) (black spectrum) and *rac*-Co₂Cl₄(et,ph-P4) (red spectrum) in CH₃CN at room temperature under CO atmosphere overnight

As previously discussed, the carbonyl bands shift to higher wavenumbers in the new P4-Ph cobalt carbonyl complexes. These signals remained consistent for most of the reactions and are comparable to the H₂/CO reduction experiments. We propose these terminal carbonyl bands to be a mixture of the dicationic penta- and hexacarbonyl dicobalt complexes for both the old P4 and new P4-Ph tetraphosphine ligands, as shown in Figure 3.31. No bridging carbonyl signals were ever detected in any of these experiments.

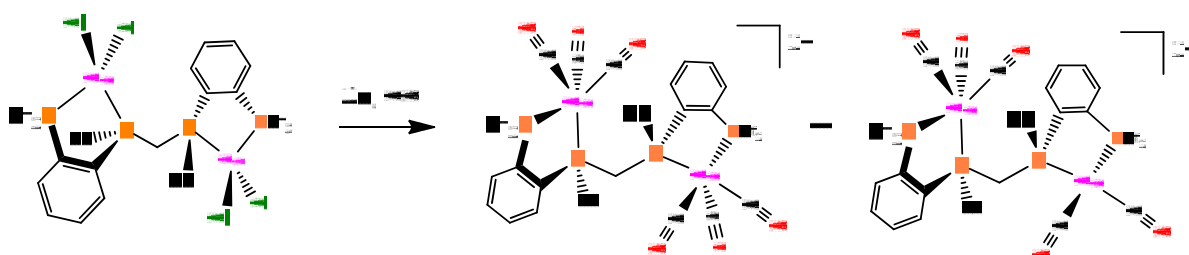


Figure 3.31 An example scheme showing the Zn reduction of *rac*-Co₂Cl₄(*et,ph*-P4-Ph) to form both the dicationic penta- and hexacarbonyl complexes under CO atmosphere

A few experiments performed in the autoclave at a higher temperature and pressure (50°C and 40 psig CO) did not give the same results as the milder conditions with the exception of the one reaction performed using acetone. The autoclave experiment in acetone yielded the same orange/gold mixture with the off-white ZnCl₂ precipitate. However, as mentioned before, most of the ZnCl₂ could not be removed from this reaction mixture. The reactions using CH₃CN and DCM under these conditions did not work as well; a light green mixture was removed from the autoclave using these solvents. An example of the FT-IR spectrum from one of these experiments using *meso*-Co₂Cl₄(*et,ph*-P4-Ph) in CH₃CN overnight can be found in Figure 3.32. The carbonyl signals at 1931 and 2010 cm⁻¹ are much lower in intensity than the experiments under CO balloon pressure at room temperature. Our hypothesis is that since both the old P4 and new P4-Ph dicobalt tetrachloride complexes are not stable under higher pressures (even at 40 psi), as discovered in the H₂/CO reductions, the complex falls apart before it can be reduced by the Zn.

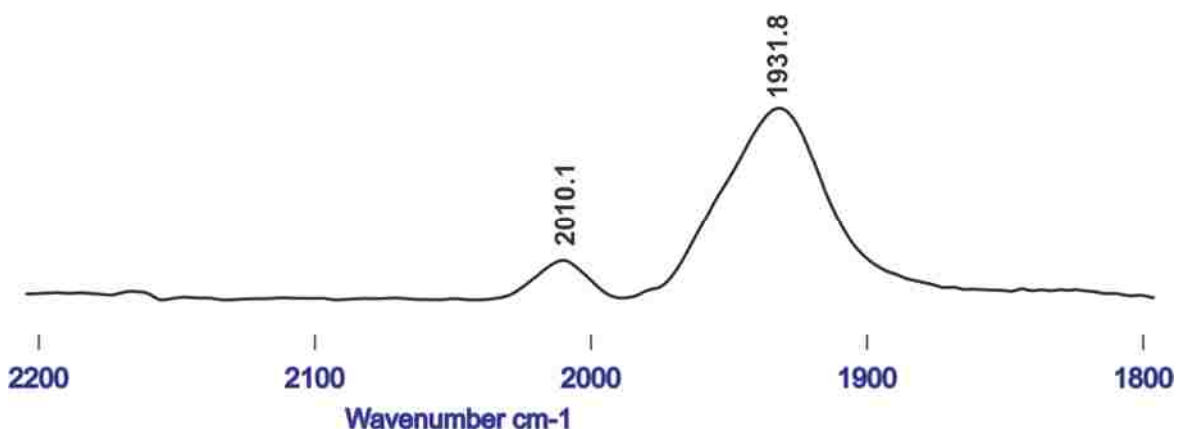


Figure 3.32 Partial FT-IR spectrum of Zn autoclave reduction of *meso*-Co₂Cl₄(*et,ph*-P4-Ph) in CH₃CN overnight at 50°C and 40 psig CO

Despite “clean” FT-IR results, ³¹P NMR analyses of the orange/gold material isolated from the Zn reductions revealed a mixture of complexes. As shown in Figure 3.33, several signals were detected from the reduction of the new P4-Ph *meso* dicobalt tetrachloride complex with Zn. This spectrum was collected by running 91,000 scans over the course of about 72 hours in attempt to collect better data. However, the quadrupolar relaxation effect still led to poor signal-to-noise ratios and difficulties with phasing. With such poor quality signals and no COSY NMR experiments, we are not able to identify the multitude of complexes obviously present in this spectrum. Additionally, we believe the complex may have degraded in solution over the long reaction time leading to these multiple impurities. We have proposed that the distorted doublets at 21 and 81 ppm correlate to penta- or hexacarbonyl dicobalt complex, *meso*-[Co₂(CO)₅₋₆(*et,ph*-P4-Ph)], based on the FT-IR analyses. Unfortunately, another possibility for the multiple signals could be that the dicobalt tetrachloride complexes are still degrading to some extent under the mild Zn reduction conditions.

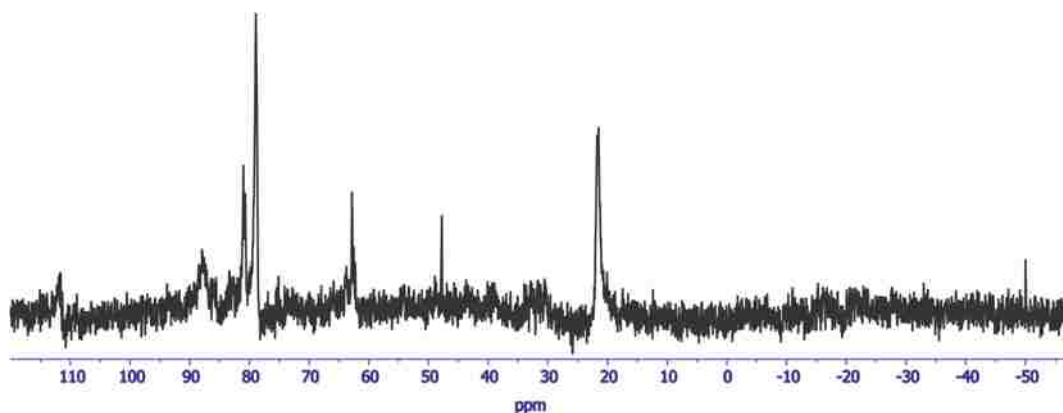


Figure 3.33 ^{31}P NMR spectrum of orange/gold material in d_6 -acetone from the Zn reduction of *meso*- $\text{Co}_2\text{Cl}_4(\text{et,ph-P4-Ph})$ in CH_3CN at room temperature under CO atmosphere overnight

3.2.9 Attempted Chloride Abstractions of *meso*- $\text{Co}_2\text{Cl}_4(\text{et,ph-P4-Ph})$ with AgBF_4 or AgPF_6

Silver(I) salts (Ag^+), such as AgBF_4 and AgPF_6 , are widely used as mild one-electron oxidants and halide abstractors. Despite their wide use, their reactivity can be quite unpredictable. Solutions of silver(I) salts are sometimes air and moisture sensitive, but the removal of the byproduct AgCl is typically straightforward with filtration over celite or some other filter aid. Under certain conditions, the formation of silver metal as a byproduct is also possible.²⁵

As a result of some of the failed attempts at reducing the new P4-Ph dicobalt tetrachloride complexes and removing all of the chloride ligands, a few halide abstraction experiments were conducted under CO balloon pressure to directly remove the halides before the reduction. The experiments were conducted with 4 or 5 equivalents of AgBF_4 or AgPF_6 at room temperature for 24 hours in acetone or CH_3CN . Both abstraction reagents and solvent systems yielded the same results, an orange/brown/off-white mixture that contained no CO character via FT-IR analyses.

Additionally, the byproduct(s), AgCl and/or Ag metal, formed in these reactions could not be fully removed even after multiple filtrations over celite. We hypothesized that since AgBF_4 and AgPF_6 can act as mild oxidizing agents to facilitate the transformation from Co(II) to Co(III) , the complex was actually being partially oxidized, which inhibited the binding of the carbonyl ligands.

3.2.10 Reactions with $\text{Co}_2(\text{CO})_8$

The second strategy explored for this synthesis was taken from Laneman's method for his dicobalt tetraphosphine complex, *meso*- $\text{Co}_2(\text{CO})_4(\text{et,ph-P4})$. As previously stated, this complex was synthesized through the direct reaction of a $\text{Co}_2(\text{CO})_4(\text{nbd})_2$ precursor and the tetraphosphine ligand, *meso*-*et,ph-P4*.²² The dicobalt precursor was synthesized using an old Wilkinson method by the direct reaction of $\text{Co}_2(\text{CO})_8$ and *nbd*. This reaction, however, is highly irreproducible and the product is unstable in solution.⁴² Stemming from the work done by Laneman, the direct combination of $\text{Co}_2(\text{CO})_8$ and *et,ph-P4* in solution was another synthetic strategy explored for this method.

3.2.11 Ligand Substitution Reactions of $\text{Co}_2(\text{CO})_4(\text{nbd})_2$ with *meso*- and *rac*-*et,ph-P4*

As previously stated, the synthesis of the precursor, $\text{Co}_2(\text{CO})_4(\text{nbd})_2$ was performed via an adaptation of Wilkinson's method.⁴² According to Wilkinson's method excess norbornadiene was refluxed with one equivalent of $\text{Co}_2(\text{CO})_8$ for 2 hours in light petroleum. The product was isolated by removal of solvent and excess norbornadiene under vacuum and recrystallized using ether.⁴² Our synthetic adaptation used a 2 hour reflux at 65-70°C in hexane. We isolated about a 58% yield of the orange product. According to Wilkinson, however, the complex is highly unstable in solution and could only be characterized by IR.⁴² An example of the FT-IR spectrum obtained in these experiments can be found in Figure 3.34.

According to Wilkinson, only three CO signals were detected during his experiments, two terminal at 2021 and 1996 cm^{-1} and one bridging at 1798 cm^{-1} .⁴² In our case, the spectrum was much more complex, and we propose that multiple cobalt carbonyl complexes are present in the final product. Wilkinson briefly discussed that the monosubstituted-norbornadiene complex, $\text{Co}_2(\text{CO})_6(\text{nbd})$, can also be produced in low yields along with the disubstituted version.⁴²

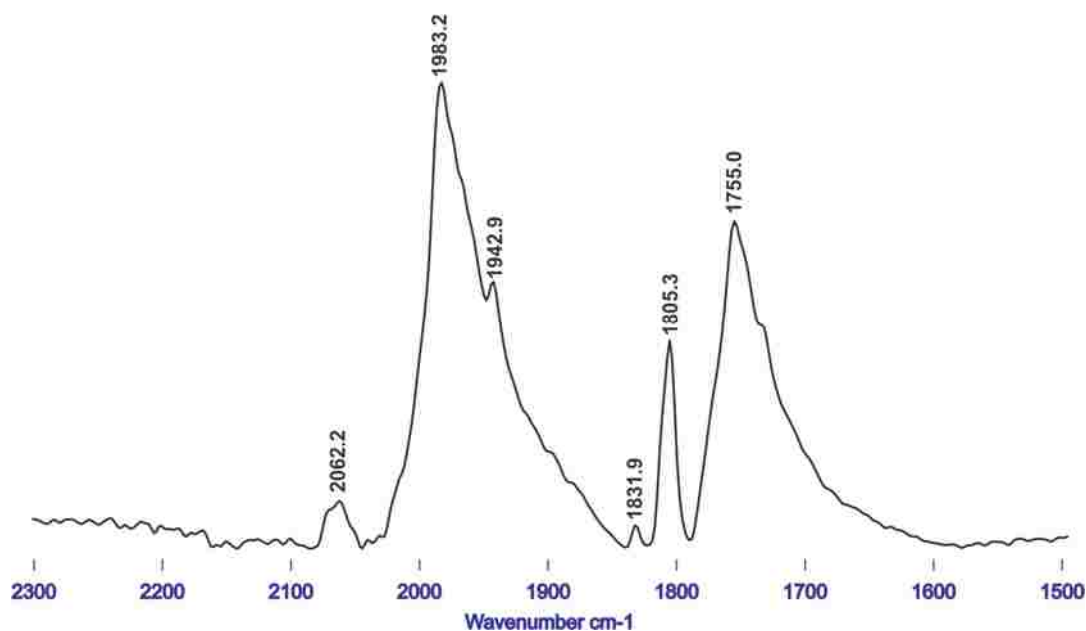


Figure 3.34 Partial FT-IR spectrum from the attempted synthesis of $\text{Co}_2(\text{CO})_4(\text{nb})_2$

The smaller signals in our spectrum at 2062 (with a shoulder at 2072 cm^{-1}) and 1832 cm^{-1} are most likely from the monosubstituted-norbornadiene cobalt carbonyl complex. The large intensity of the signals at 1755 (with a shoulder at 1733 cm^{-1}), 1943, and 1983 are most likely from a mixture of the desired disubstituted complex with some unreacted dicobalt octacarbonyl. This theory is based on the large size and broadness of the signals. Figure 3.35 compares the FT-IR spectra of pure $\text{Co}_2(\text{CO})_8$ and our experimental $\text{Co}_2(\text{CO})_4(\text{nb})_2$. The large signals at 1755 and 1983 cm^{-1} appear to somewhat overlap, albeit with lower frequencies, further indicating some $\text{Co}_2(\text{CO})_8$ is present in this mixture of complexes.

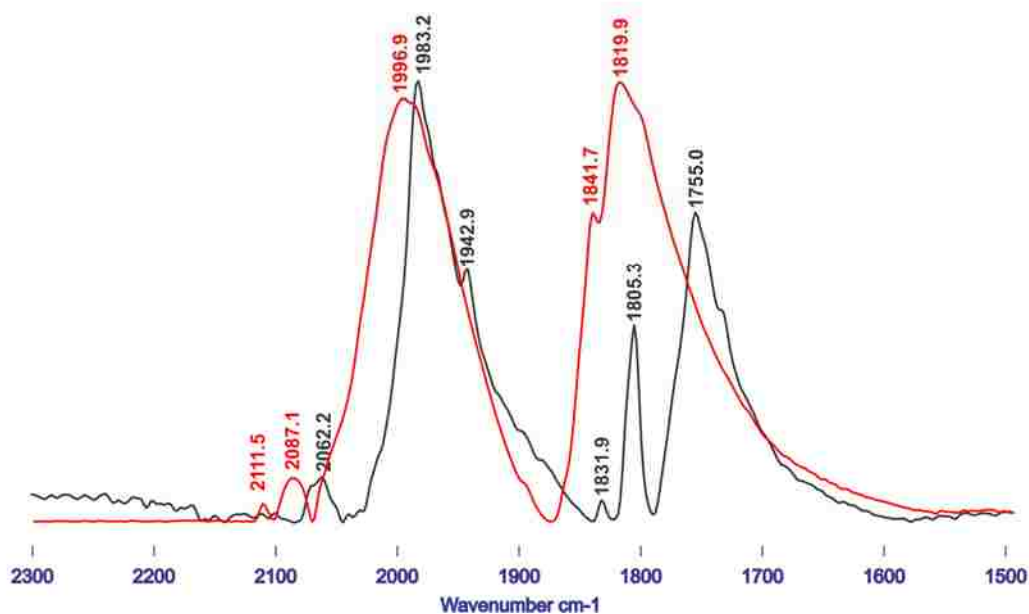


Figure 3.35 Comparison of partial FT-IR spectra of product from attempted synthesis of $\text{Co}_2(\text{CO})_4(\text{nbd})_2$ (black spectrum) and pure $\text{Co}_2(\text{CO})_8$ (red spectrum)

Using a 1:1 combination of $\text{Co}_2(\text{CO})_4(\text{nbd})_2$ from our syntheses and *meso*- or *rac*-*et*,*ph*-P4, attempts to synthesize the neutral dicobalt carbonyl complexes, *meso*- and *rac*- $\text{Co}_2(\text{CO})_4(\text{et},\text{ph}-\text{P4})$ were performed using a 60-70°C reflux between 3-24 hours in DCM or hexanes. All experiments, regardless of solvent or length of reaction time, yielded the same type of dark green/brown mixture. Upon isolation, FT-IR analyses and ^{31}P NMR experiments verified the irreproducibility of this method. Some experiments revealed a mixture of complexes present by FT-IR analyses (Figure 3.36) and no ^{31}P NMR signals; other experiments resulted in the same mixture of complexes by FT-IR analyses and rather “clean” ^{31}P NMR spectra (Figure 3.37).

According to Laneman’s results, there should be one terminal CO signal at 1925 cm^{-1} and one bridging CO signal at 1720 cm^{-1} .²² However, there appear to be no bridging carbonyl signals in our spectrum and four broad terminal carbonyl signals at 1885, 1898, 1936, and 1996 cm^{-1} .

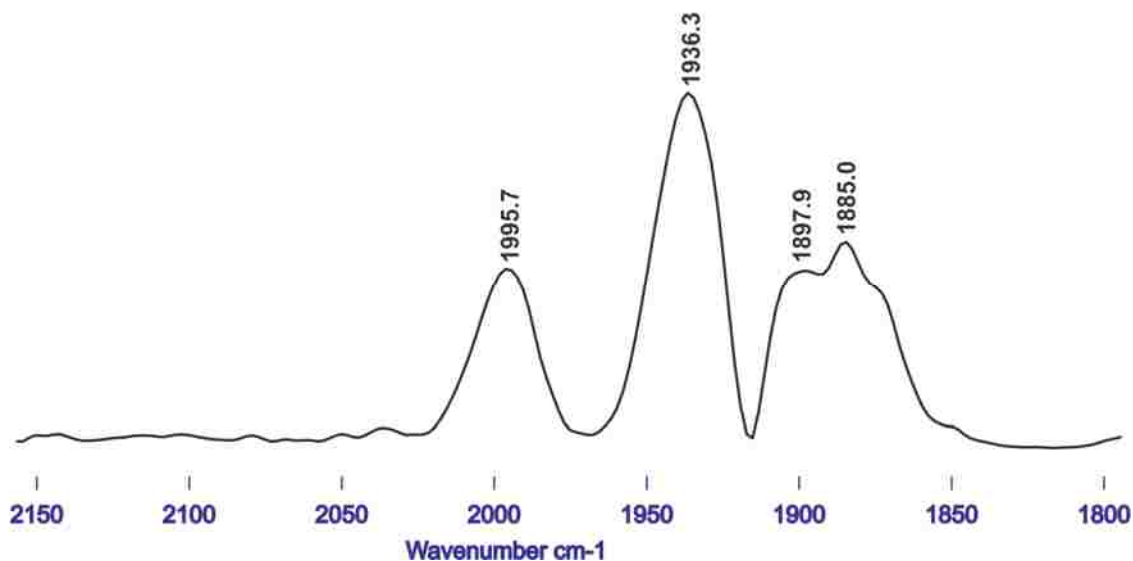


Figure 3.36 Partial FT-IR spectrum of the reaction of $\text{Co}_2(\text{CO})_4(\text{nbid})_2$ and *meso*-*et*,*ph*-P4 in hexane

We have proposed that the higher frequency bands at 1936 and 1996 cm^{-1} are from the dicationic tetra- and/or penta/hexacarbonyl complex, *meso*- $[\text{Co}_2(\text{CO})_{4-6}(\text{et},\text{ph-P4})]^{2+}$ because they are similar to the bands from the reduction experiments with the old P4 dicobalt tetrachloride complexes. The broadness of these bands, though, suggests they could be a mixture of both the tetra- and pentacarbonyl (or hexacarbonyl) dicobalt complexes. The lower frequency bands at 1898 and 1885 cm^{-1} can most likely be associated with the tetracarbonyl cobalt anion, $[\text{Co}(\text{CO})_4]^-$, which has a stretching frequency of 1890 cm^{-1} . These bands are also very broad which suggests they are the result of multiple carbonyl signals.

Even though we are starting with a neutral complex, $\text{Co}(0)$ can disproportionate to $\text{Co}(\text{I})$ and $\text{Co}(-\text{I})$. We noticed similar disproportionation in our H_2/CO reduction experiments with $\text{Co}(\text{II})$ to give $\text{Co}(\text{I})$ and $\text{Co}(\text{III})$ products, as identified through the X-ray crystallography analysis of *rac*- $[\text{CoCl}_2(\text{et},\text{ph-P4-Ph})]^+$ (Figure 3.22). This disproportionation of $\text{Co}(0)$ to $\text{Co}(\text{I})$ and $\text{Co}(-\text{I})$ explains the presence of the dicationic tetra-, penta-, and/or hexacarbonyl dicobalt complexes, which contain $\text{Co}(\text{I})$ centers, and $[\text{Co}(\text{CO})_4]^-$, which contains a $\text{Co}(-\text{I})$ center.

^{31}P NMR analyses were dominated by the presence of doublets at 33 and 49 ppm (shown in Figure 3.37), most likely from the same complex. We believe this complex is the dicationic tetra, penta, or hexacarbonyl dicobalt complex based on the similarity of this pattern to NMR results from the reduction experiments. Also, since these complexes are diamagnetic, we should see ^{31}P NMR signals. There is another small set of signals at 37 and 82 ppm, which provides more evidence for the mixture of carbonyl complexes proposed from our FT-IR analyses.

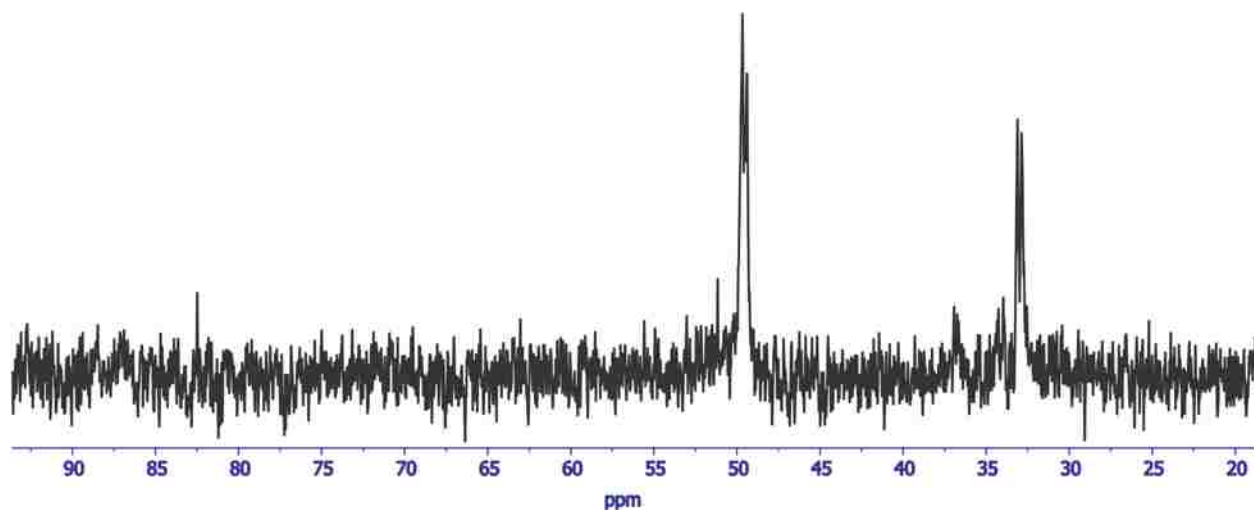


Figure 3.37 ^{31}P NMR spectrum of dark green material in d_2 -DCM from the reaction of $\text{Co}_2(\text{CO})_4(\text{nbd})_2$ and *meso*-*et*,*ph*-P4 in hexane

Laneman reported his complex, *meso*- $\text{Co}_2(\text{CO})_4(\text{et},\text{ph}-\text{P}_4)$, to contain two broad signals at 20 and 80 ppm on the ^{31}P NMR. However, since our starting material $\text{Co}_2(\text{CO})_4(\text{nbd})_2$ contains a mixture of complexes, including the monosubstituted-norbornadiene complex and some unreacted $\text{Co}_2(\text{CO})_8$, it is plausible that we would get a range of different cobalt carbonyl complexes. Though the ^{31}P NMR appears to be “clean,” FT-IR analysis suggests otherwise. Because of the instability of the starting complex in solution and the irreproducibility of both synthetic methods, a direct approach of reacting our old P4 *meso* tetraphosphine ligand with $\text{Co}_2(\text{CO})_8$ was also attempted.

3.2.12 Direct Reaction of *meso*-et,ph-P4 with $\text{Co}_2(\text{CO})_8$

The mechanism of substitution of dicobalt octacarbonyl has been the study of much challenging research since it is one of the more reactive simple binary carbonyls and it itself serves as a catalyst for hydroformylation (as discussed in the introduction). The substitution with phosphines is also well established in the literature and usually gives rise to a Co(I)/Co(-I) disproportionation product, $[\text{Co}(\text{CO})_3\text{L}_2][\text{Co}(\text{CO})_4]$ (Figure 3.38).⁴³⁻⁴⁸



Figure 3.38 Direct reaction of phosphines with $\text{Co}_2(\text{CO})_8$

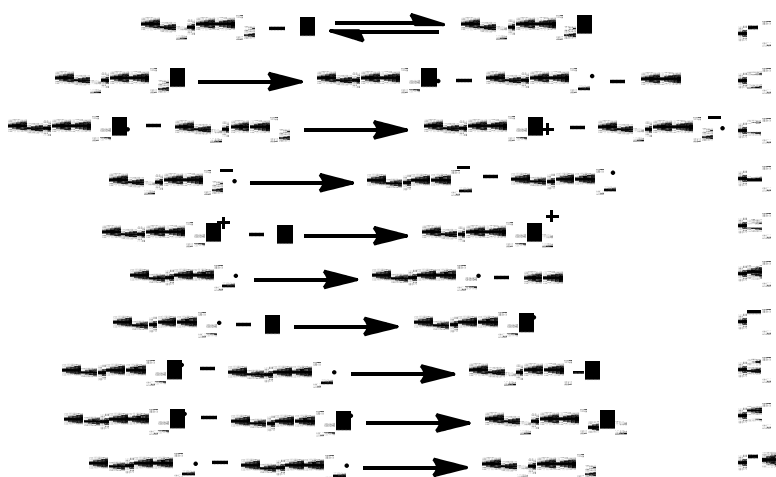


Figure 3.39 Radical pathway of substitution for $\text{Co}_2(\text{CO})_8$ ⁴⁷

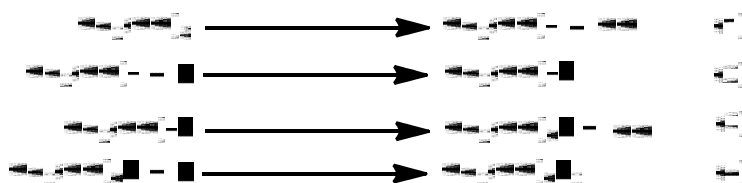


Figure 3.40 Direct substitution mechanism for $\text{Co}_2(\text{CO})_8$ ⁴⁷

The more basic phosphines typically lead to the disproportionation product. The rise of the disproportionation product over the direct substituted product proceeds through a radical pathway, shown in Figure 3.39. For comparison, the direct substituted mechanism is shown in Figure 3.40.

The rate determining step in this reaction is the initial loss of CO to form the intermediate $\text{Co}_2(\text{CO})_7$.⁴⁷

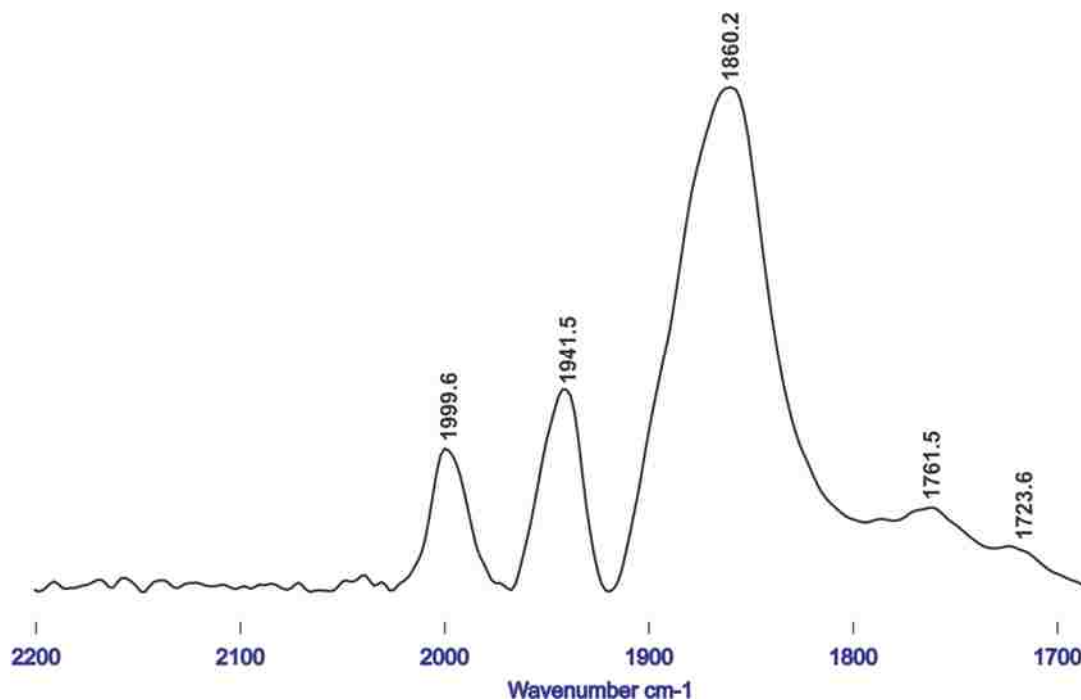


Figure 3.41 Partial FT-IR spectrum of the direct reaction of $\text{Co}_2(\text{CO})_8$ with *meso*-et,ph-P4 in THF

The direct reaction of our old *meso* tetraphosphine ligand with $\text{Co}_2(\text{CO})_8$ was performed using a 1:1 molar ratio of ligand to complex, at room temperature, between 2-24 hours, and using acetone, DCM, or THF as solvent. All experiments, regardless of time or solvent, yielded a brown/gold solid. FT-IR and ^{31}P NMR analyses revealed a mixture of cobalt carbonyl complexes, shown in Figures 3.41 and 3.42. Three terminal CO signals were detected at 1860, 1941, and 1999 cm^{-1} , and most likely two bridging CO signals were detected at 1723 and 1761 cm^{-1} by FT-IR.

The three terminal CO signals at 1860, 1941, and 1999 cm^{-1} are most likely the result of the dicationic penta- or hexacarbonyl dicobalt complex, *meso*- $[\text{Co}_2(\text{CO})_{5-6}(\text{et,ph-P4})][\text{Co}(\text{CO})_4]$, which has been consistent in most of our experiments. This disproportionation, as stated above, is very common in direct substitution reactions between phosphines and $\text{Co}_2(\text{CO})_8$. The larger

terminal CO signal at 1860.2 cm^{-1} is most likely the result of the tetracarbonyl cobalt dianion, $[\text{Co}(\text{CO})_4]^{2-}$. As previously stated, this dianion typically has a stretching frequency of about 1860 cm^{-1} . We are proposing that the extremely dominant signal at 1860 cm^{-1} could also contain some $[\text{Co}(\text{CO})_3]^-$, which has a CO stretching frequency of about 1830 cm^{-1} .⁴⁹ The combination of the two signals at 1890 for $[\text{Co}(\text{CO})_4]^-$ and at 1830 for $[\text{Co}(\text{CO})_3]^-$ could result in the large band at 1860 cm^{-1} . There are also two low intensity bridging CO signals at 1723 and 1761 cm^{-1} which are the result another cobalt carbonyl complex present in a small quantity. We could not propose a structure for this species, however.

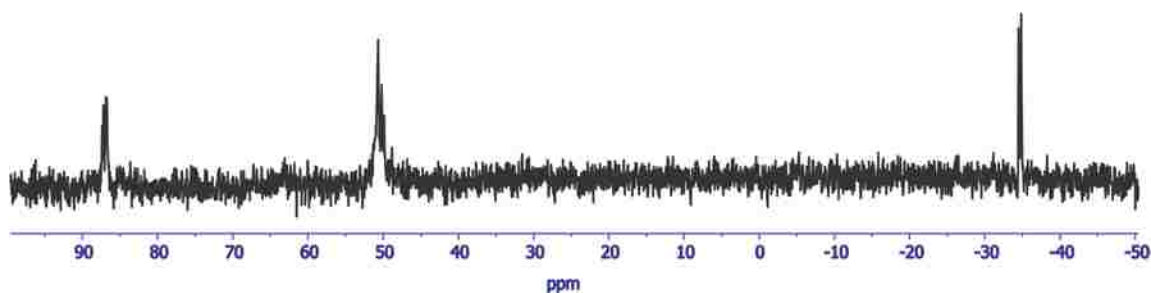


Figure 3.42 ^{31}P NMR spectrum of the direct reaction of $\text{Co}_2(\text{CO})_8$ with *meso*-*et*,*ph*-P4 in THF in d_6 -acetone

The multiplets at 50 and 86 ppm on the ^{31}P NMR spectrum are most likely from the proposed dicationic penta- or hexacarbonyl dicobalt complex, but there is most likely another complex overlapping with these signals. The presence of the dangling phosphine signal at -34 ppm is puzzling. Originally, we assigned it to a cobalt carbonyl κ^3 -tetrphosphine complex, such as $[\text{Co}_2(\text{CO})_x(\kappa^3\text{-et,ph-P4})]^{2+}$, but a complex like this should have at least four ^{31}P NMR signals, one for each phosphine as noted with our dinickel complexes' reactivity with H_2O to produce a monometallic nickel complex with a dangling phosphine atom (Chapter 2). However, we have now tentatively assigned this signal to be a tricarbonyl-dicobalt- κ^1 -tetrphosphine ligand complex, shown below in Figure 3.43, in which the internal P atoms are dangling and should be detected as a downfield doublet. One example for this type of complex is the $[\text{Co}(\text{CO})_3\text{P}(\text{ptol})_3]^-$ species shown

in Figure 3.44. According to the literature, this complex should also have an FT-IR stretching frequency of 1830 cm^{-1} ,⁴⁹ which is consistent with our FT-IR assignment.

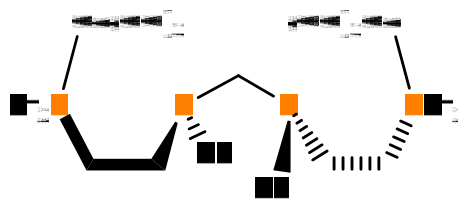


Figure 3.43 Proposed structure for FT-IR band at 1830 cm^{-1} and ^{31}P NMR dangling phosphine signal

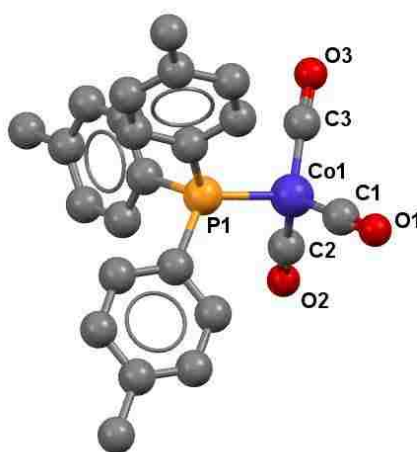


Figure 3.44 Ball-and-stick model for $[\text{Co}(\text{CO})_3\text{P}(\text{ptol})_3]$. Hydrogen atoms have omitted for clarity (Ptol = C_7H_7)

3.2.13 Exploration of Non-Halide Containing Starting Materials

The final synthetic strategy for producing a bimetallic cobalt system for hydroformylation and aldehyde-water shift catalysis was through the exploration of some monometallic cobalt precursors. Two $\text{Co}(\text{II})$ precursors discovered in the literature with labile ligands are $[\text{Co}(\text{H}_2\text{O})_6][\text{BF}_4]_2$ and the CH_3CN version, $[\text{Co}(\text{CH}_3\text{CN})_6][\text{BF}_4]_2$.^{50a,b} The hexaaqua species was attempted first because its procedure was rather simple. It involved the direct neat reaction of refluxing cobalt metal and fluoroboric acid solution (HBF_4 in 48% H_2O) for 3 hours at about 90°C , shown in Figure 3.45.^{50a,b} After several experiments, the synthesis of this complex could be performed with yields up to about 90% (from the amount of cobalt metal used). The material was

a bright pink solid as described in the literature^{50b} and was used directly for experiments with the tetraphosphine ligands.

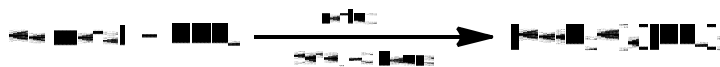


Figure 3.45 Synthesis of $[\text{Co}(\text{H}_2\text{O})_6][\text{BF}_4]_2$

3.2.14 Reaction of $[\text{Co}(\text{H}_2\text{O})_6][\text{BF}_4]_2$ with *rac*-*et,ph*-P4 and *et,ph*-P4-Ph

To date, three experiments have been performed to react the hexaaqua cobalt species with the old and new *racemic* tetraphosphine ligands. All experiments used 2 equivalents of cobalt complex for every 1 equivalent of the ligand as shown below in Figure 3.46.



Figure 3.46 Synthesis of $[\text{Co}_2(\text{H}_2\text{O})_x(\text{et,ph-P4})][\text{BF}_4]_4$

The reactions were performed by the cannula addition of the ligand to the cobalt complex in either THF or acetone at room temperature and were allowed to stir overnight. All experiments resulted in a dark red/green “sticky” solid which could not be analyzed via FT-IR or ³¹P NMR successfully. FT-IR analysis resulted in a large, broadened signal due to the large amount of H₂O present. ³¹P NMR analyses could not be performed because the cobalt metal centers are each in a +2 oxidation state, which makes the highly cationic (+4) complex paramagnetic. Additionally, some of the H₂O ligands could deprotonate to form some, possibly bridging, OH⁻ ligands. We see this type of behavior in the reaction of our dinickel tetrachloride complexes with H₂O to form the bridging-hydroxide complex $[\text{Ni}_2(\mu\text{-OH})\text{Cl}_2(\text{et,ph-P4})]^+$ (Chapters 1 and 2).

3.2.15 H₂/CO and Zn Reduction Attempts of *rac*- $[\text{Co}_2(\text{H}_2\text{O}/\text{OH})_x(\text{et,ph-P4})/(\text{et,ph-P4-Ph})]^{4+}$

The attempted reduction of the new P4-Ph complex, *rac*- $[\text{Co}_2(\text{H}_2\text{O})_x(\text{OH})_x(\text{et,ph-P4-Ph})][\text{BF}_4]_4$, was first performed using 1:1 H₂/CO balloon pressure at room temperature in DCM

for 24 hours. This experiment resulted in a light orange/red reaction mixture. Analysis of isolated solid by FT-IR revealed no CO character in the material, however. Additionally, the color did not change much from the initially dark orange/red, which could mean the reduction did not occur. Perhaps, higher H₂/CO pressures are required for a reduction to occur.

The second experiment to reduce the old P4 complex, *rac*-[Co₂(H₂O)_x(OH)_x(*et,ph-P4*)] [BF₄]₄, was performed using 2 equivalents of Zn dust in acetone for 24 hours under CO balloon pressure. Within about two hours, the reaction mixture had turned from a deep red/brown color to an orange color. FT-IR analyses revealed the presence of 3 terminal CO signals at 1947, 2008, and 2084 cm⁻¹ (Figure 3.47).

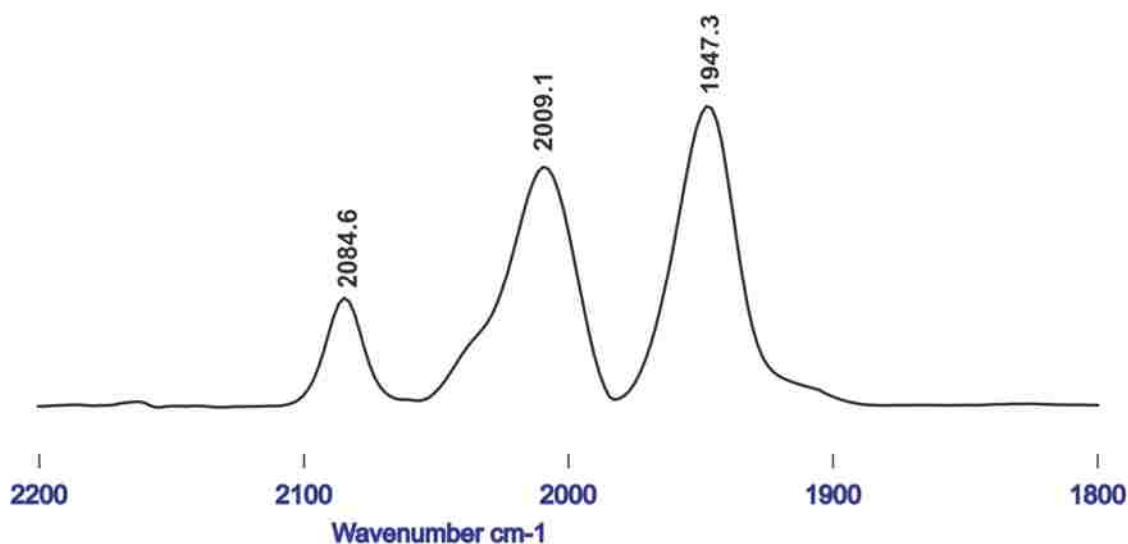


Figure 3.47 Partial FT-IR spectrum of attempted Zn reduction of *rac*-[Co₂(H₂O)_x(*et,ph-P4*)] [BF₄]₄ under CO atmosphere.

However, there were no signals detected on the ³¹P NMR analysis. This could be the result of the complex being partially reduced to form a paramagnetic mixture of Co(I)/Co(II) complexes, such as *rac*-[Co₂(CO)₅(*et,ph-P4*)]²⁺ and [Co₂(OH)₂(CO)₂(*et,ph-P4*)]²⁺. A tricationic mixed Co(I)/Co(II) complex containing both CO and OH⁻ ligands, such as [Co₂(CO)_x(OH)_x(*et,ph-P4*)]³⁺, is also possible and is supported by the carbonyl bands' shift to higher wavenumbers with the old

P4 tetraphosphine ligand. As previously discussed, cobalt carbonyl complexes with the old P4 ligand normally have lower CO wavenumbers than complexes with new P4-Ph ligand. This shift to higher wavenumbers, which means less π -backbonding is occurring, and partial reduction of the complex, could be evidence for the presence of a tricationic species. In addition, attempted removal of the $[\text{Zn}(\text{H}_2\text{O})_x]$ byproduct and/or crystallization using acetone resulted in a pink/white colored solid isolated from the mixture. We presumed this solid to be the Zn byproduct, but it could not be fully removed from the mixture, even by multiple filtration attempts.

3.2.16 Hydroformylation of 1-Hexene Attempts with Dicobalt Complexes

Two attempts to perform the hydroformylation of 1-hexene have been performed using these dicobalt complexes. The first attempt was performed with a 1 mM solution of *rac*- $\text{Co}_2\text{Cl}_4(\text{et,ph-P4-Ph})$ in DCM at ~ 150 psig H_2/CO and 100°C . Four equivalents of NEt_3 and 5 equivalents of NaBF_4 were added to assist in the removal of Cl ligands by the reduction of the complex. No aldehyde was formed from the reaction after 3 hours via GC-MS analysis.

The second attempt was performed with the product from one of the Zn reductions, presumably *rac*- $[\text{Co}_2(\text{CO})_{5-6}(\text{et,ph-P4})]^{2+}$. The reaction was run using 1 mM of the material in acetone at ~ 150 psi H_2/CO and 100°C . No aldehyde was produced after 2 hours of reaction time as determined via GC-MS. The reaction mixture was initially orange but turned a light yellow/green color upon removal from the autoclave. FT-IR and ^{31}P NMR analyses were conducted after the experiment to try to determine the structure of this material.

FT-IR analysis (Figure 3.48) revealed the presence of two, terminal CO signals at 1947 and 2004 cm^{-1} . These signals were very sharp in intensity and similar to the spectra of many of the reduction attempts using Zn and H_2/CO indicating the *rac*- $[\text{Co}_2(\text{CO})_{5-6}(\text{et,ph-P4})]^{2+}$ complex.

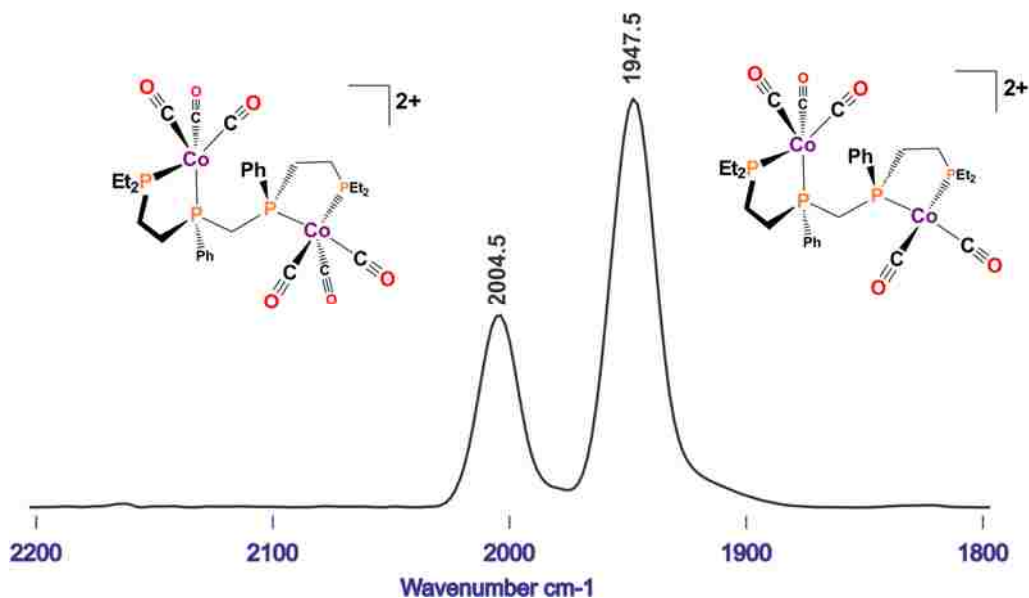


Figure 3.48 Partial FT-IR spectrum of isolated material from hydroformylation of 1-hexene using a dicobalt complex

^{31}P NMR analysis revealed a mixture of species as shown in Figure 3.49. From this data, it appears the two distinct doublets of doublets at 52 and 85 ppm are from the same complex, most likely $\text{rac-}[\text{Co}_2(\text{CO})_{5-6}(\text{et,ph-P4})]^{2+}$.

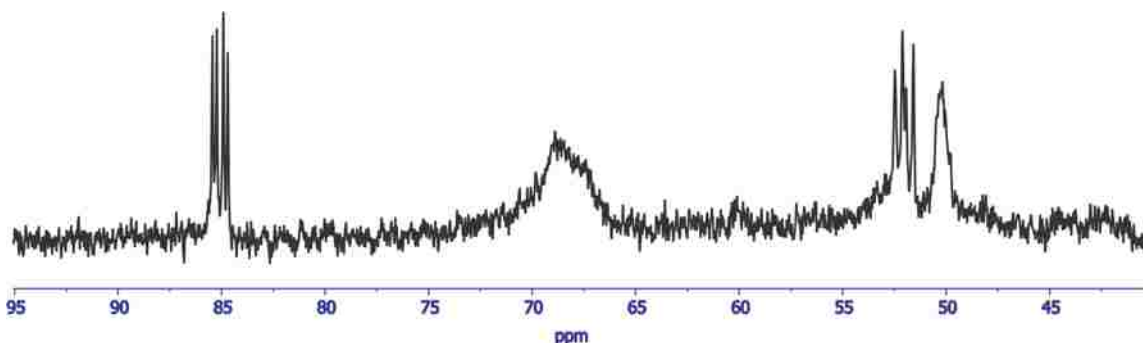


Figure 3.49 ^{31}P NMR spectrum of isolated material from hydroformylation of 1-hexene using a dicobalt complex

The two very broad signals at 50 and 68 ppm may be some exchange with another complex, perhaps the tentatively assigned dibridged-hydride species, $\text{Co}_2(\mu\text{-H})_2(\text{CO})_2(\text{et,ph-P4})$. Additionally the ^{31}P analysis is cleaner than any of the other spectra collected which provides further evidence for our proposed penta- or hexacarbonyl dicobalt complexes.

3.3 Conclusion

The pursuit of a bimetallic cobalt system for hydroformylation and aldehyde-water shift catalysis has been by far one of the most challenging research endeavors encountered in my graduate school career. At least three years of challenging work went into pursuing this project with ill-defined results. The numerous synthetic strategies presented here are the results of multiple experiments performed changing multiple variables in attempt to yield successful results. There were some small victories, but the majority of the results are failed reactions that taught the lessons of what does not work for this system.

Cobalt is not a very reactive metal; it does not form particularly strong metal-ligand bonds, which can be expected for a first row transition metal. Most of the reduction attempts using the multitude of reducing agents either resulted in partial decomposition of the starting material (1:1 H₂/CO autoclave reduction) or some over-reduction of the complex to Co⁰ and even cobalt metal (super hydride). In a few of the H₂/CO autoclave reduction experiments, some black material formed during the reactions was believed to cobalt metal.

When this project first began, we attempted the reduction of the dicobalt tetrachloride complexes with both the old P4 and new P4-Ph tetraphosphine ligands with a 1:1 H₂/CO mixture (syngas). However, it did not occur to myself nor Dr. Stanley that this mixture contains too much H₂ for the formation of a dicobalt carbonyl complex. Not only are the dicobalt tetrachloride complexes unstable under high pressures, even at 40 psig, the presence of 50% H₂ turned out to be very problematic for the system. The hexaphosphine paper published in 1985,²¹ used 33.4%/66.6% CO/H₂ mixture, which led to fragmentation of their dicobalt tetrachloride complex. They were still able to isolate the desired dicobalt tetracarbonyl complex because their system needed less CO ligands. Our 50/50 mixture of H₂/CO led to over reduction and an inseparable mixture of

complexes. A better method would have been to use much less H₂ and excess CO to achieve the desired transformation. In future studies, this reduction will be performed with a 1:6 mixture of H₂/CO in hopes of isolating the dicationic penta- or hexacarbonyl dicobalt complex in higher yield.

Several solvents and solvent combinations were also used over the three year span to either crystallize a bimetallic cobalt complex or separate the multiple species formed during the H₂/CO autoclave reductions. The only crystals analyzed from these mixtures were the *rac*-[CoCl₂(*et*,*ph*-P4-Ph)]⁺ complex, shown in Figure 3.23, and the byproduct, trimethylammonium chloride (HNEt₃Cl). Attempts to separate the mixtures of species using DCM usually gave a blue colored material and a green colored material. EPR studies indicated that both of these complexes both had cobalt metal centers in the +2 oxidation state. FT-IR data showed the same two terminal CO bands as shown in Figure 3.17, and no ³¹P NMR signals were detected for either solid.

The removal of byproducts formed during the reduction experiments was another huge problem to tackle with this project. Though the Zn reduction appeared to give the best experimental results based on FT-IR analyses, the removal of the ZnCl₂ byproduct proved to be a major issue. Different solvents were used for the reduction in an attempt to combat this problem, but since the dicobalt tetrachloride complexes are only soluble in a few polar organic solvents (acetone, DCM, CH₃CN, and DMF, for the most part), we were severely limited by the different solvent systems we could use. Additionally, attempted removal of ZnCl₂ using these solvents in combination with non-polar solvents such as hexanes was unsuccessful. In most cases, both the ZnCl₂ and the desired complex, [Co(CO)₅₋₆(*et*,*ph*-P4)]²⁺, would partially precipitate out of the mixture.

Experiments with Co₂(CO)₈ proved to be just as problematic. A direct substitution or ligand exchange experiments should have ideally been the quickest and most facile route to yield a neutral cobalt (0) species. This neutral species could have been oxidized to yield a cationic complex,

similar to the dirhodium cationic system shown to be an excellent hydroformylation catalyst. However, $\text{Co}_2(\text{CO})_8$ is very unstable and degrades over the course of a few weeks, even when stored in cold temperatures unexposed to air or moisture. It is my belief that the instability of $\text{Co}_2(\text{CO})_8$ is the major reason why any experiments using it are highly irreproducible. FT-IR studies, shown in Figures 3.34-3.36, clearly indicate that a mixture of cobalt carbonyl complexes was being formed, and in some cases, the starting material was still present after the reaction appeared to be complete.

The exploration of a non-halide containing starting material appears to be the best route for the synthesis of this complex. Previous synthetic routes showed the halides were not as easily removed as we originally believed and direct experiments to remove them were unsuccessful. The two simple complexes, $[\text{Co}(\text{H}_2\text{O})_6][\text{BF}_4]_2$ and $[\text{Co}(\text{CH}_3\text{CN})_6][\text{BF}_4]_2$, are relatively inexpensive to synthesize and the methods are well documented in the literature.⁴⁸ Work began with the hexaaqua species because the synthetic route was simpler than the acetonitrile version. Thus far, the two attempts using H_2/CO and Zn to reduce the complexes formed from the combination of the hexaaqua species with the tetraphosphine ligands, $[\text{Co}_2(\text{H}_2\text{O})_x(\text{et,ph-P4})][\text{BF}_4]_4$, have been unsuccessful. It is my belief, however, that use of another mild reducing agent, with an easily isolable by product, would be the most suitable choice for the reduction of this complex. These studies are currently underway in the Stanley group.

3.4 References

1. Kim, J. H.; Howe, P. D. Cobalt and Inorganic Cobalt Compounds. Concise International Chemical Assessment Document 69. World Health Organization, 2006.
2. Cobalt Development Institute: Catalysts. <http://www.thecdi.com/general> (accessed May 4, 2016).
3. Hebrard, F.; Kalck, P. Cobalt-Catalyzed Hydroformylation of Alkenes: Generation and Recycling of the Carbonyl Species, and Catalytic Cycle. *Chem. Rev.* **2009**, *109*, 4272-4282.

4. Breslow, D. S.; Heck, R. F. Mechanism of the Hydroformylation of Olefins. *Chemistry and Industry*. **1960**, 467.
5. Alemdaroglu, N. H.; Penninger, J. L. M.; Oltay, E. Study of the Mechanism of Hydroformylation at Industrial Conditions. *Monatshefte fur Chemie*. **1976**, *107*, 1153-1165.
6. Tannenbaum, R.; Dietler, U. K.; Bor, G.; Ungvary, F. Fundamental metal carbonyl equilibria, V: Reinvestigation of the equilibrium between dicobalt octacarbonyl and cobalt tetracarbonyl hydride under hydrogen pressure. *J. Organomet. Chem*. **1998**, *570*, 39-47.
7. Cornils, B.; Herrmann, W. A., Eds. Carbon Monoxide and Synthesis Gas Chemistry. In *Applied Homogeneous Catalysis with Organometallic Compounds: Volume 1*; Wiley-VCH: Weinheim, Germany, 2002; pp 29-85.
8. Slauch, L. H.; Mullineaux, R. D. Novel Hydroformylation Catalysts. *J. Organomet. Chem*. **1968**, *13*, 469-477.
9. Crause, C.; Bennie, L.; Damoense, L.; Dwyer, C. L.; Grove, C.; Grimmer, N.; van Rensburg, W. J.; Kirk, M. M.; Mokheseng, K. M.; Otto, S.; Steyberg, P. J. Bicyclic phosphines as ligands for cobalt-catalysed hydroformylation. *Dalton Trans*. **2003**, 2036-2042.
10. Rosi, L.; Bini, A.; Frediani, P.; Bianchi, M.; Salvini, A. Functionalized phosphine substituted cobalt carbonyls. Synthesis, characterization, and catalytic activity in the hydroformylation of olefins. *J. Mol. Catal. A*. **1996**, *112*, 367-383.
11. Franke, R.; Selent, D.; Borner, A. Applied Hydroformylation. *Chem. Rev*. **2012**, *112*, 5675-5732.
12. Beller, M.; Cornils, B.; Frohning, C. D.; Kohlpaintner, C. W. Progress in hydroformylation and carbonylation. *J. Mol. Catal. A*. **1995**, *104*, 17-85.
13. Leeuwen, P. W. N. M.; Claver, C., Eds. *Rhodium Catalyzed Hydroformylation*; Kluwer Academic Publishers: Dordrecht, The Netherlands, 2000; pp 1-284.
14. Markiewicz, M. K.; Baird, M. C. Olefin Hydroformylation Catalyzed by a Cobalt Carbonyl Complex Containing a Water-soluble Phosphine. *Inorg. Chim. Acta*. **1986**, *113*, 95-99.
15. Beller, M.; Cornils, B.; Frohning, C. D.; Kohlpaintner, C. W. Progress in hydroformylation and carbonylation. *J. Mol. Catal. A*. **1995**, *104*, 17-85.
16. Klinger, R. J.; Chen, M. J.; Rathke, J. W.; Kramarz, K. W. Effect of Phosphines on the Thermodynamics of the Cobalt-Catalyzed Hydroformylation System. *Organometallics*. **2007**, *26*, 352-357.
17. Oswald, A. A.; Hendriksen, D. E.; Kastrup, R. V.; Mozeleski, E. J. Electronic Effects on the Synthesis, Structure, Reactivity, and Selectivity of Rhodium Hydroformylation Catalysts. *Advances in Chemistry*. **1992**, *230*, 395-418.

18. Van Leeuwen, P. W. N. M.; Casey, C. P.; Whiteker, G. T. Phosphines as Ligands. In *Rhodium Catalyzed Hydroformylation*; Van Leeuwen, P. W. N. M.; Claver, C., Eds.; Kluwer Academic Publishers: Dordrecht, The Netherlands, 2000; pp 63-105.
19. Broussard, M. E.; Juma, B.; Train, S. G.; Peng, W. J.; Laneman, S. A.; Stanley, G. G., *Science* **1993**, *260* (5115), 1784-1788.
20. Bridges, N. Ph.D. Dissertation, Louisiana State University, Baton Rouge, May **2001**.
21. Askham, F. R.; Stanley, G. G.; Marques, E. C. A New Type of Transition-Metal Dimer Based on a Hexaphosphine Ligand System: $\text{Co}_2(\text{CO})_4(\text{eHTP})^{2+}$ (eHTP = $(\text{Et}_2\text{PCH}_2\text{CH}_2)_2\text{PCH}_2\text{P}(\text{CH}_2\text{CH}_2\text{PEt}_2)_2$). *J. Am. Chem. Soc.* **1985**, *107*, 7423-7431.
22. Laneman, S. A.; Fronczek, F. R.; Stanley, G. G. A Ligand-Imposed Cradle Geometry for a Dicobalt Tetracarbonyl Tetratertiary Phosphine Complex. *Inorg. Chem.* **1989**, *28*, 1206-1207.
23. Laneman, S. A.; Stanley, G. G. An Open-Mode Nickel Dimer Based on a Binucleating Hexaphosphine Ligand System. Solid-State and Solution Conformations. *Inorg. Chem.* **1987**, *26*, 1177-1181.
24. Askham, F. R.; Maverick, A. W.; Stanley, G. G. Synthesis and Structural Characterization of *mer*, *mer*- $\text{Cr}_2\text{Cl}_6(\text{eHTP})$ (eHTP = $(\text{Et}_2\text{PCH}_2\text{CH}_2)_2\text{PCH}_2\text{P}(\text{CH}_2\text{CH}_2\text{PEt}_2)_2$). A New Binuclear Coordination Mode for eHTP. *Inorg. Chem.* **1987**, *26*, 3963-3966.
25. Connelly, N. G.; Geiger, W. E. Chemical Redox Agents for Organometallic Chemistry. *Chem. Rev.* **1996**, *96*, 877-910.
26. Heinze, K.; Huttner, G.; Zsolnai, L.; Schober, P. Complexes of Cobalt(II) Chloride with the Tripodal Trisphosphane triphos: Solution Dynamics, Spin-Crossover, Reactivity, and Redox Activity. *Inorg. Chem.* **1997**, *36*, 5457-5469.
27. Kuhl, O. *Phosphorus-31 NMR Spectroscopy*; Springer-Verlag: Berlin, Germany, 2008; pp 1-131.
28. Askham, F. R.; Saum, S. E.; Stanley, G. G. A Chiral Mononuclear Complex of eHTP. Structure and Paramagnetically Decoupled ^{31}P NMR of $\text{FeCl}(\text{CO})(\eta^4\text{-eHTP})^+$. *Organometallics*. **1987**, *6*, 1370-1372.
29. Glavee, G. N.; Klabunde, K. J.; Sorenson, C. M.; Hadjapanayis, G. C. Borohydride Reductions of Metal Ions. A New Understanding of the Chemistry Leading to Nanoscale Particles of Metals, Borides, and Metal Borates. *Langmuir*. **1992**, *8*, 771-773.
30. Elliot, D. J.; Holah, D. G.; Hughes, A. N.; Maciaszek, S. Reactions between Co (II) and bis(diphenylphosphino)methane in the presence of NaBH_4 or NaBH_3CN . *Can. J. Chem.* **1988**, *66*, 81-85.
31. Heinzman, S. W.; Ganem, B. The Mechanism of Sodium Borohydride-Cobaltous Chloride Reductions. *J. Am. Chem. Soc.* **1982**, *104*, 6801-6802.

32. Glavee, G. N.; Klabunde, K. J.; Sorenson, C. M.; Hadjipanayis, G. C. Borohydride Reductions of Cobalt Ions in Water. Chemistry Leading to Nanoscale Metal, Boride, or Borate Particles. *Langmuir*. **1993**, *9*, 162-169.
33. Wade, R. C.; Holah, D. G.; Hughes, A. N.; Hui, B. C. Catalytically Active Borohydride-Reduced Nickel and Cobalt Systems. *Cataly. Rev.* **1976**, *14*, 211-246.
34. Blough, B. E.; Carroll, F. I. Reduction of Isoquinoline and Pyridine-containing Heterocycles with Lithium Triethylborohydride (Super-Hydride©). *Tetrahedron Lett.* **1993**, *34*, 7239-7242.
35. Osby, J. O.; Heinzman, S. W.; Ganem, B. Studies on the Mechanism of Transition-Metal-Assisted Sodium Borohydride and Lithium Aluminum Hydride Reductions. *J. Am. Chem. Soc.* **1986**, *108*, 67-72.
36. Brown, H. C.; Kim, S. C.; Krishnamurthy, S. Selective Reductions. 26. Lithium Triethylborohydride as an Exceptionally Powerful and Selective Reducing Agent in Organic Synthesis. Exploration of the Reactions with Selected Organic Compounds Containing Representative Functional Groups. *J. Org. Chem.* **1980**, *45*, 1-12.
37. Sievert, A. C.; Muetterties, E. L. Arene Transition-Metal Chemistry. 6. Hydride Reduction of η^6 -Arene Iridium (I) Complexes. *Inorg. Chem.* **1981**, *20*, 2276-2278.
38. Krishnamurthy, S.; Brown, H. C. Selective Reductions. 31. Lithium Triethylborohydride as an Exceptionally Powerful Nucleophile. A New and Remarkably Rapid Methodology for the Hydrogenolysis of Alkyl Halides under Mild Conditions. *J. Org. Chem.* **1983**, *48*, 3085-3091.
39. Profitt, J. A.; Ong, H. H. Reduction of Diphenylethylenes and Related Compounds with Magnesium in Methanol. *J. Org. Chem.* **1979**, *44*, 3972-3974.
40. Kelly, S. M.; Lipshutz, B. H. Chemoselective Reductions of Nitroaromatics in Water at Room Temperature. *Org. Lett.* **2014**, *16*, 98-101.
41. Lutz, R. E.; Love, L.; Palmer, F. S. The Reductions of Unsaturated 1,4-Diketones with Zinc Combinations. The Formation of the Cyclic Dimolecular Products. *J. Am. Chem. Soc.* **1935**, *57*, 1953-1957.
42. Winkhaus, G.; Wilkinson, G. Some Diolefin Carbonyl Complexes. *Royal Society of Chemistry*. **1961**, *120*, 602-605.
43. Elliot, D. J.; Holah, D. G.; Hughers, A. N. New Cobalt-Carbonyl-Phosphine Complexes. *Inorganica Chimica Acta*. **1988**, *142*, 195-196.
44. Moreno, C.; Macazanga, M. J.; Delgado, S. Reactions of $\text{Co}_2(\text{CO})_8$ with potentially polydentate phosphines. *Inorganica Chimica Acta*. **1991**, *182*, 55-58.
45. Thornhill, D. J.; Manning, A. R. Reactions of Octacarbonyldicobalt with some Ditertiary Phosphines and Arsines. *J. Chem. Soc., Dalton Trans.* **1973**, 2086-2090.
46. Brown, D. A.; Lyons, H. J.; Sane, R. T. Solvent and Structural Effects in Substitution Reactions of Metal Carbonyl Halides. *Inorganica Chimica Acta*. **1970**, *4*, 621-625.

47. Forbus, N. P.; Brown, T. L. Effects of Steric Requirement and Ligand Basicity in Phosphine Substitution Reactions of Dicobalt Octacarbonyl. *Inorg. Chem.* **1981**, *20*, 4343-4347.
48. Absi-Halabi, M.; Atwood, J. D.; Forbus, N. P.; Brown, T. L. The Mechanism of Substitution of Dicobalt Octacarbonyl. *J. Am. Chem. Soc.* **1980**, *102*, 6248-6254.
49. Brammer, L.; Rivas, J. C. M.; Zhao, D. Unexpectedly Lengthened N-H...Co Hydrogen Bonds?. *Inorg. Chem.* **1998**, *37*, 5512-5518.
50. (a) Holt, D. G. L.; Larkworthy, L. F.; Povey, D. C.; Smith, G. W.; Leigh, G. J. Facile Synthesis of Complexes of Vanadium(II) and the Crystal and Molecular Structures of Hexaaquavanadium(II) Trifluoromethylsulphonate. *Inorg. Chim. Acta.* **1990**, *169*, 201-205. (b) Coucouvanis, D. Useful Reagents and Ligands. In *Inorganic Syntheses: Volume 33*; John Wiley & Sons: New York, NY, 2002; pp 75-121.

Chapter 4: Experimentals

4.1 General Comments

Unless otherwise noted, all reactions were carried out under a nitrogen atmosphere by using glovebox or Schlenk line techniques. All solvents and their deuterated versions and most of the chemicals used in the reactions were purchased from Sigma-Aldrich, unless stated otherwise. *Trans*-4-nonene and 1-dodecene were purchased from GFS Chemicals. Oleic acid was purchased from Alfa Aesar. Both tetraphosphine ligands, *et,ph*-P4 and *et,ph*-P4-Ph, were synthesized and their diastereomers were separated by previous methods.¹⁻³ The dinickel complexes, *meso*-/*rac*-Ni₂Cl₄(*et,ph*-P4) and *meso*-/*rac*-Ni₂Cl₄(*et,ph*-P4-Ph) were also synthesized by previously published methods.^{1,4} Solvents were obtained dry and packaged under N₂ or degassed with N₂ and used without further purification. All ¹H and ³¹P NMR spectra were recorded on one of three instruments: Bruker DPX 250 MHz spectrometer, Bruker Avance 400 MHz spectrometer, or Avance III 400 MHz spectrometer. All FT-IR data was collected on one of two instruments: Bruker Alpha FT-IR or Bruker Tensor 27 FT-IR. NMR data was analyzed and simulated using MestRenova (v. 10.0) and FT-IR data was analyzed and simulated using Bruker Opus 7.2 Software. ¹H NMR shifts are reported relative to TMS, and ³¹P NMR shifts are reported relative to the shift of the external 85% H₃PO₄. LC-MS ESI data was collected by Dr. Connie David on Agilent 6210 LC electrospray system. GC-MS data was collected on Agilent Technologies 6890N Network GC system/5975 B VL MSD. Column = HP-5MS (30m x 0.25mm x 0.25μm).

X-ray crystallography analyses were performed by Dr. Frank Fronczek using a Nonius KappaCCD diffractometer using Mo K α radiation and graphite crystal monochromators or Bruker Kappa APEX-II DUO diffractometer using Mo K α or Cu K α radiation and graphite crystal monochromators.

4.2 Oxidative Cleavage Reactions

Two types of oxidative cleavage reactions were run, with air or with O₂ balloon pressure. All reactions were run on the benchtop exposed to air, except when otherwise noted. The reactions were run the same, regardless of the alkene. The reactions analyzed by ¹H NMR were run in the deuterated solvents with 10% D₂O.

4.2.1 Type I

A small schlenk flask was charged with 10 mM metal complex or phosphine ligand, typically 10% H₂O and polar organic solvent system (either 5 or 10mL total), and 30 equivalents of alkene. The reaction mixture was either stirred or put on the sonicator for 5-10 minutes to ensure the metal complex or phosphine ligand was fully dissolved in solution. A latex balloon was wired to the top of the flask and filled with O₂ using an O₂ gas tank with regulator set at 30 psig. The reaction mixture was rapidly stirred overnight. The next day the stirring was stopped and the remaining O₂ in the balloon was vented and removed from the flask. A small aliquot was removed from the mixture, diluted with the appropriate organic solvent, and analyzed by GC-MS. In some cases, another small aliquot of the reaction mixture was transferred to an NMR tube and analyzed by ¹H NMR for the detection of the aldehyde signal.

4.2.2 Type II

A small round bottom was charged with 10 mM metal complex or phosphine ligand, typically 10% H₂O and polar organic solvent system (either 5 or 10mL total), and 30 equivalents of alkene. The reaction mixture was either stirred or put on the sonicator for 5-10 minutes to ensure the metal complex or phosphine ligand was fully dissolved in solution. A rubber septum or glass stopper was added to the flask, and the reaction mixture was rapidly stirred overnight. The next day the stirring was stopped and the rubber septum or glass stopper was removed. A small aliquot

was removed from the reaction mixture, diluted with the appropriate organic solvent, and analyzed by GC-MS. In some cases, another small aliquot of the reaction mixture was transferred to an NMR tube and analyzed by ¹H NMR for the detection of the aldehyde signal.

4.2.3 Reaction Tables

The following three tables contain the majority of the oxidative cleavage reactions performed with acetone, CH₃CN, and other solvents or solvent combinations. All reactions used 10mM metal complex or ligand, except reactions in which the new tetraphosphine ligands, et,ph-P4-Ph, were used. Most of the reactions were repeated multiple times to verify the results, and most were run at room temperature, except otherwise noted. The *meso* and *racemic* dinickel complexes are abbreviated as follows: *meso*-Ni₂Cl₄(et,ph-P4) — Ni(1M), *rac*-Ni₂Cl₄(et,ph-P4) — Ni(1R), *meso*-Ni₂Cl₄(et,ph-P4-Ph) — Ni(2M), and *rac*-Ni₂Cl₄(et,ph-P4-Ph) — Ni(2R).

Table 4.1 Oxidative Cleavage Reactions with Acetone

Substrate	Complex/Ligand	Amount of H ₂ O	Additives	Type
1-hexene	Ni(1M)	15%	None	I
Cyclohexene	Ni(1M)	15%	None	I
α-methylstyrene	Ni(1M)	15%	None	I
Cyclopentene	Ni(1M)	15%	None	I
<i>Trans</i> -5-decene	Ni(1M)	15%	None	I
<i>Trans</i> -4-nonene	Ni(1M)	15%	None	I
<i>Cis</i> -3-octene	Ni(1M)	15%	None	I
Oleic acid	Ni(1M)	15%	None	I
Styrene	Ni(1M)	15%	None	I
Oleic acid	Ni(1R)	15%	None	I
Oleic acid	Ni(1R)	10%	None	I
Oleic acid methyl ester	Ni(1M)	10%	None	I
Oleic acid	Ni(1M)	10%	None	I
Oleic acid methyl ester	Ni(1R)	10%	None	I

(Table 4.1 continued)

Substrate	Complex/Ligand	Amount of H ₂ O	Additives	Type
Oleic acid	Ni(1M)	No H ₂ O	None	I
Oleic acid	Ni(1R)	No H ₂ O	None	I
Oleic acid methyl ester	Ni(1R)	No H ₂ O	None	I
Ricinoleic acid	Ni(1M)	10%	None	I
Ricinoleic acid	Ni(1R)	10%	None	I
Oleic acid	Ni(2M)	15%	None	I
Styrene	Ni(2M)	15%	None	I
Oleic acid	Ni(2M)	20%	None	I
1-hexene	Ni(2M)	15%	None	I
Styrene	Ni(2M)	20%	None	I
Oleic acid	Ni(2M)	10%	None	I
Oleic acid	<i>Meso</i> -et,ph-P4	15%	None	II
Oleic acid	<i>Meso</i> -et,ph-P4	10%	None	II
Oleic acid	<i>Meso</i> -et,ph-P4	10%	60°C oil bath	II
Oleic acid	Ni(2M)	10%	None	II
Oleic acid	<i>Rac</i> -Co ₂ Cl ₄ (et,ph-P4)	10%	None	II
Oleic acid	[Co(H ₂ O) ₆][BF ₄] ₂	No H ₂ O	None	II
Oleic acid	NiCl ₂ ·6H ₂ O	No H ₂ O	None	II
Oleic acid	CoCl ₂ ·6H ₂ O	No H ₂ O	None	II
Oleic acid	[Co(H ₂ O) ₆][BF ₄] ₂	10%	None	II
Oleic acid	[Co(H ₂ O) ₆][BF ₄] ₂	No H ₂ O	None	I
Oleic acid	[Co(H ₂ O) ₆][BF ₄] ₂	No H ₂ O	4 eq <i>rac</i> -et,ph-P4	II
Oleic acid	<i>Rac</i> -et,ph-P4	10%	65°C oil bath	II
Oleic acid	Dppm	10%	None	II
Oleic acid	P(C ₆ H ₁₁) ₃	10%	None	II
Oleic acid	[<i>Rac</i> -CoCl ₂ (et,ph-P4-Ph)] ¹⁺	10%	None	II

(Table 4.1 continued)

Oleic acid	<i>Meso</i> -et,ph-P4-Ph	10%	None	II
Oleic acid	<i>Meso</i> -et,ph-P4-Ph	No H ₂ O	None	II
Oleic acid	<i>Rac</i> -Co ₂ Cl ₄ (et,ph-P4-Ph)	10%	None	II
Oleic acid	<i>Meso</i> -Co ₂ Cl ₄ (et,ph-P4-Ph)	10%	None	II

Table 4.2 Oxidative Cleavage Reactions with Acetonitrile

Substrate	Complex/Ligand	Amount of H ₂ O	Additives	Type
1-octene	Ni(1M)	15%	None	I
1-dodecene	Ni(1M)	10%	None	I
Oleic acid	Ni(1R)	15%	None	I
1-dodecene	Ni(1R)	10%	None	I
α -methylstyrene	Ni(1R)	15%	None	I
<i>Trans</i> -5-decene	Ni(1R)	10%	None	I
<i>Trans</i> -4-nonene	Ni(1R)	10%	None	I
Styrene	Ni(1R)	15%	None	I
Oleic acid methyl ester	Ni(1R)	10%	None	I
<i>Cis</i> -3-octene	Ni(1R)	10%	None	I
Oleic acid methyl ester	Ni(1R)	10%	None	I
Cyclopentene	Ni(1R)	15%	None	I
Oleic acid	Ni(1M)	10%	None	I
Oleic acid	Ni(1M)	No H ₂ O	None	I
Oleic acid	Ni(1R)	No H ₂ O	None	I
Oleic acid methyl ester	Ni(1M)	No H ₂ O	None	I
Ricinoleic acid	Ni(1M)	10%	None	I
Ricinoleic acid	Ni(1R)	10%	None	I
Oleic acid	Ni(2M)	15%	None	I
Styrene	Ni(2M)	15%	None	I

(Table 4.2 continued)

Oleic acid	Ni(2M)	10%	None	I
Oleic acid	Ni(2M)	20%	None	I
1-hexene	Ni(2M)	15%	None	I
Oleic acid	<i>Meso</i> -et,ph-P4	10%	None	II
Oleic acid	<i>Rac</i> - Ru ₂ Cl ₄ (cod) ₂ (et,ph-P4-Ph)	10%	None	II

Table 4.3 Oxidative Cleavage Reactions with Other Solvents

Substrate	Complex/Ligand	Solvent System	Additives	Type
Oleic acid	Ni(1M)	10%H ₂ O/THF	None	I
Oleic acid	Ni(1R)	10%H ₂ O/THF	None	I
Oleic acid	Ni(1M)	10%H ₂ O/MeOH	None	I
Oleic acid	Ni(1M)	10%H ₂ O/DMSO	None	I
Oleic acid	Ni(1M)	DMSO only	None	I
Oleic acid	Ni(1M)	10%H ₂ O/DCM	None	I
Oleic acid	Ni(1R)	10%H ₂ O/DCM	None	I
Oleic acid methyl ester	Ni(1M)	10%H ₂ O/MeOH	None	I
Oleic acid	Ni(1M)	H ₂ O/CH ₃ CN/AcOEt	None	I
Oleic acid	Ni(1R)	H ₂ O/CH ₃ CN/AcOEt	None	I
Oleic acid	<i>Meso</i> - Co ₂ Cl ₄ (et,ph-P4)	MeOH only	None	II

4.3 ¹H NMR Oxidative Cleavage Quantification Experiments

The oxidative cleavage of oleic acid reactions were run as stated above with 10 mM dinickel complex or tetraphosphine ligand in 5 mL of a 10% D₂O/d₆-acetone solution and 30 equivalents of oleic acid combined in a small round bottom. Two trials were performed for each dinickel complex and tetraphosphine ligand. After stirring each reaction overnight, a serial dilution

of 0.188 g of 1,1,2,2-tetrachloroethane was added to d₆-acetone to make a 10 mL total volume. Adding 1 mL of this solution to d₆-acetone to make another 10 mL total volume was performed for the second dilution. To each reaction mixture, 1 mL of the second dilution was added and 1 mL of the reaction mixture was transferred to an NMR tube. These dilutions yielded 1.73×10^{-6} mol of the internal standard in each trial. All NMR tubes were analyzed by ¹H NMR, and a comparison of the integration of the aldehyde signal to the internal standard signal was made to determine the amount of aldehyde produced in each trial.

4.4 Esterification of Oleic Acid

The esterification of oleic acid was performed using a solid heterogeneous catalyst in an adapted procedure.⁵ A 50 mL schlenk flask was charged with 0.050 g of Amberlyst-15, 1.000 g of oleic acid, and 8 mL of methanol with a magnetic stirbar in the presence of air/oxygen. The mixture was stirred on a 65°C oil bath for 17 hours. After 17 hours, the mixture was removed from the oil bath and the unreacted acid catalyst was filtered from the reaction mixture by gravity filtration, washing with 10-15 mL of CH₃OH. The crude mixture was analyzed by GC-MS to confirm the presence of oleic acid methyl ester. The methyl ester was extracted from the organic phase of the mixture three times using hexane. Hexane was removed from the methyl ester by a simple distillation. ¹H NMR was used to analyze the isolated oleic acid methyl ester, specifically for the detection of the methyl group. The presence of the methyl group distinguishes it from the oleic acid. (90% yield).

4.5 Attempted Isolation of Ricinoleic Acid

The saponification of castor oil was performed through an adapted mixed saponification/acidification technique.⁶ A schlenk flask was charged with 10.167 g of castor oil, 2.436 g of KOH and 50 mL of EtOH in the presence of air/oxygen. The mixture was refluxed at

80-100°C for 1 hour and allowed to cool to room temperature. While cooling, a white salt precipitated out of the yellow mixture. 60 mL of H₂O was added while vigorously stirring to dissolve the precipitate. The mixture was then acidified with 50 mL of concentrated HCl to pH=1 (tested using pH paper). The fatty acid was next extracted once using 30 mL of ethyl acetate and dried over Na₂SO₄. A small amount of aluminum oxide was added to decolorize the yellow oil and filtered using gravity filtration. Filtrate was transferred to a schlenk flask and about 90% of the ethyl acetate was removed under vacuum. Exact yield could not be determined due to solvent and oleic and ricinoleic acid impurities still present. The yellowish, viscous solution, believed to be mostly ricinoleic acid, was analyzed by ¹H NMR.

4.6 ³¹P NMR Studies of the Dinickel Complexes' Reactivity with H₂O

Under N₂ atmosphere (in the glovebox), a small vial was charged with 10 mM of dinickel complex. 1.8 mL of d₇-DMF was added to fully dissolve the complex. A small aliquot of this mixture was transferred to an NMR tube. 0.2 mL of D₂O was then added to the vial, and the solution was lightly swirled to mix. Another small aliquot of the mixture was removed and transferred to an NMR tube. The contents of both tubes were analyzed by ³¹P NMR. The sample containing the D₂O was covered with parafilm, and analyzed again by ³¹P NMR after 2-3 hours. The tube was then stored and analyzed by ³¹P NMR over the course of 7 days or longer. We propose the old P4 *rac* dinickel complex forms the OH-bridged complex *rac*-[Ni₂(μ-OH)Cl₂(et,ph-P4)]¹⁺: ³¹P {¹H} NMR (400 MHz, d₇-DMF) δ 28 ppm (t) and 46 ppm (t). This complex later falls apart to form a monometallic nickel complex, shown in Figure 2.18: ³¹P {¹H} NMR (400 MHz, d₇-DMF) δ 76 ppm (dd, *J* = 267, 58 Hz), 54 ppm (dd, *J* = 64, 58 Hz), 37 ppm (d, *J* = 7 Hz), and 5 ppm (ddd, *J* = 267, 64, and 7 Hz). All coupling constants were reported previously by Dr. Schreiter.⁴ We also propose the new P4-Ph *meso* dinickel complex reacts with H₂O to form the

OH-bridged complex *meso*-[Ni₂(μ-OH)Cl₂(*et,ph*-P4-Ph)]: ³¹P {¹H} NMR (400 MHz, d₇-DMF) δ 63 ppm (s) and 64 ppm (s). No coupling constants have been determined for this data yet.

4.7 Synthesis of Drago's Catalyst, CoSMDPT

Drago's catalyst, CoSMDPT, was synthesized according to the published literature procedure.⁷ A 250 mL schlenk flask was charged with 5.00 g of N-methyl-bis (3-aminopropyl)-amine, 30 mL EtOH, and 8.3 g salicylaldehyde. In a separate 100 mL schlenk flask, 8.6 g Co(CH₃-CO₂)₂-4H₂O was suspended in solution with 30 mL EtOH. The amine solution was added to the cobalt solution via dropwise cannula addition. This mixture was refluxed for 2 hours at 80°C. The mixture was allowed to cool to room temperature and the brown solid was filtered in the glovebox, washing 3 times with diethyl ether. The brown solid was dried under vacuum (>80% yield).

4.8 Oxidative Cleavage of Isoeugenol using Drago's Catalyst

Under N₂ atmosphere (in the glovebox), 0.10 grams of CoSMDPT, 46.5 mL of toluene, and 3.72 grams of isoeugenol were combined in a 125 mL Erlenmeyer flask. This mixture was poured into the Parr autoclave system, pressurized to 75 psi O₂, and heated to 60°C. After 2 hours of reactivity, the reaction was stopped, and the autoclave was depressurized and allowed to cool to room temperature. A deep brown solution was removed from the autoclave and transferred to a 250 mL beaker. A small aliquot was removed from the solution, diluted with d₆-benzene and transferred to an NMR tube. The sample was analyzed by ¹H NMR for the detection of the aldehydes. ¹H NMR (400 MHz): δ 9.6 (s, vanillin), 9.14 (q, acetaldehyde).

4.9 Synthesis of *meso*-/*rac*-Co₂Cl₄(*et,ph*-P4) and *meso*-/*rac*-Co₂Cl₄(*et,ph*-P4-Ph)

This procedure was performed similar to the published method.⁸ The amounts of reactants and solvents described here are general and can be altered to suit the reaction conditions. To a solution of CoCl₂-6H₂O (0.512 g, 2.15 mmol) in acetone (25.0 mL), a solution of *et,ph*-P4 or *et,ph*-

P4-Ph (0.5 g, 1.08 mmol) in acetone (25.0 mL) was added dropwise via cannula over the course of 30 minutes. The dark green mixture was allowed to stir overnight under N₂ at room temperature. The mixture was filtered in the glovebox using gravity filtration to remove any impurities. The filtrate was transferred to a clean, preweighed schlenk flask and the solvent was removed under vacuum with a warm water bath. The product was isolated as a dark green solid (80-90% yield), analyzed by FT-IR, and stored in the glovebox.

4.10 Reduction of *meso*-/*rac*-Co₂Cl₄(*et*,*ph*-P4) and *meso*-/*rac*-Co₂Cl₄(*et*,*ph*-P4-Ph)

The reduction of both the old P4 and new P4-Ph dicobalt tetrachloride complexes was performed using various reducing agents with either the crude mixture of the dicobalt tetrachloride complex in solution before it was isolated or the isolated complex dissolved in a polar organic solvent. The reactions typically worked better with the isolated complex dissolved in a polar organic solvent because a more accurate amount of the reducing agent could be used to perform the transformation. A general procedure for each type of reduction is described below. The amounts of reactants and solvents are general amounts used for each reduction and can be altered to suit the reaction conditions. All manipulations were performed in the glovebox or using Schlenk line techniques unless otherwise stated. All solid products were checked for their solubility in most polar organic solvents and analyzed by FT-IR and ³¹P NMR (in most cases).

4.10.1 H₂/CO Reduction Experiments

A 250 mL Erlenmeyer flask was charged with 0.528 g (0.729 mmol) of old P4 *meso* dinickel tetrachloride complex dissolved in 70 mL DCM in the glovebox. The mixture was transferred to the sonicator for 10-15 minutes to ensure the complex completely dissolved in solution. A separate small round bottom was charged with 0.148 g (1.46 mmol) NEt₃ and a few mL of DCM. If any other additives were used, such as NaPF₆, a separate round bottom was charged

with the appropriate amount. All reactants were poured in the Parr autoclave system, exposing them to air for a few seconds, and washed with DCM. The mixture was then pressurized to 100 psig 1:1 H₂/CO (syngas) (or desired pressure) and heated to 60°C (or desired temperature) overnight while stirring at 1000 rpm. This mixture was removed from the autoclave and filtered in the glovebox. The filtrate was transferred to a schlenk flask and the solvent was removed under vacuum. The solid was analyzed by FT-IR for the detection of carbonyl signals. In most cases, the solid was dissolved in a deuterated solvent and analyzed by ³¹P NMR (usually in d₆-acetone) to determine if some reduction had occurred. ³¹P {¹H} NMR (400 MHz, CD₃CN) δ 86 ppm (distorted dd) and 52 ppm (distorted m).

4.10.2 NaBH₄ Reduction Experiments

With the new P4-Ph *meso* dicobalt tetrachloride complex suspended in 30 mL solution of 1:1 C₆H₆ and EtOH in a separate 250 mL schlenk flask, a small round bottom was charged with 0.21 g (5.55 mmol) NaBH₄ (2 equiv. for 1 equiv. CoCl₂·6H₂O, 0.509 g, 2.14 mmol). The NEt₃ was added via cannula to the cobalt mixture while stirring. A latex balloon was wired to the top of the schlenk flask and filled with CO using the Parr autoclave system. This mixture was allowed to stir for 2 hours. Upon removal of the CO balloon, the mixture was filtered in the glovebox, and the filtrate was transferred to a clean schlenk flask. The solvent was removed under vacuum, and a dark green/brown solid was isolated. The solid was analyzed by FT-IR and ³¹P NMR in CD₃CN (no signals detected in ³¹P NMR analyses).

4.10.3 Attempted LAH Reduction Experiment

A schlenk flask contained the new P4-Ph *meso* dicobalt tetrachloride complex suspended in a solution of THF and DCM (30 mL). LAH solution (0.20 g in 12 mL THF) was added dropwise via cannula to the cobalt solution. Immediately following the addition, a latex balloon was wired

to the top of the flask and filled with CO using the Parr autoclave system. The mixture was stirred at room temperature for about 2 hours. The CO balloon was then removed and the mixture was filtered by gravity filtration in the glovebox. Solvent removal from the filtrate under vacuum isolated the dark green solid. No signals were present on the ^{31}P NMR analysis, and due to the lack of color change, the reaction was believed to have failed.

4.10.4 Super Hydride Reduction Experiments

A 3-neck round bottom flask contained the new P4-Ph *rac* dinickel complex suspended in a solution of THF (10 mL). A latex balloon was wired to one neck of the flask and filled with CO using the Parr autoclave system. This mixture was allowed to stir for 20 minutes. Another small round bottom flask was charged with 2.114 mL of 1M LiEt_3BH in THF (3 equiv. for 1 equiv. *et*, *ph*-P4-Ph, 0.395 g, 0.705 mmol). The LiEt_3BH solution was added to the cobalt solution via cannula in a quick addition. The reaction mixture was stirred rapidly for 2 hours. After 2 hours, the CO balloon was removed, and the solution (no precipitate) was transferred to a clean schlenk flask. The solvent was removed under vacuum. The deep red/brown solid was analyzed by FT-IR and ^{31}P NMR in d_2 -DCM. No ^{31}P NMR signals were ever detected.

4.10.5 Attempted Mg Reduction Experiments

A 100 mL schlenk flask was charged with 0.340 g (0.415 mmol) dicobalt tetrachloride complex, 0.09 g (3.70 mmol) Mg turnings, and 40 mL CH_3CN . A latex balloon was wired to the flask and filled with CO using the Parr autoclave system. The reaction mixture was stirred rapidly overnight. The CO balloon was then removed and the mixture was filtered by gravity filtration to remove excess Mg turnings and/or MgCl_2 . The filtrate was transferred to a clean schlenk flask and the solvent was removed under vacuum. The light green solid was analyzed by FT-IR.

4.10.6 Zn Reduction Experiments

The Zn reductions were performed similar to the attempted Mg reductions with either Zn dust or powder. The amounts of Zn were kept the same as with the Mg experiments, with the use of excess reducing agent. Filtration of excess Zn and/or Zn chloride was performed by filtration over celite and washing with the appropriate organic solvent. Analyses were also performed by FT-IR and ^{31}P NMR in d_6 -acetone. ^{31}P $\{^1\text{H}\}$ NMR (400 MHz, d_6 -acetone) δ 111 ppm (broad), 88 ppm (broad), 81 ppm (distorted d), 62 (s), 47 (s), 21 ppm (distorted d), -50 ppm (s). No COSY experiments have been performed on this material.

A few of the Zn reductions were performed in the autoclave with higher pressures of CO. These experiments began with similar technique, but the mixture was transferred to the autoclave (minimal exposure to air) instead, pressurized to 40 psig CO only, heated to 50°C, and stirred at 1000 rpm overnight. The reaction mixture was then removed from the autoclave, filtered to remove byproducts, and dried under vacuum. The solid product was analyzed by FT-IR.

4.10.7 Attempted Chloride Abstractions using $\text{AgBF}_4/\text{AgPF}_6$

A 3-neck round bottom was charged with 0.407 g (0.497 mmol) dicobalt tetrachloride complex dissolved in 10 mL acetone using the sonicator (10-15 minutes). In a separate round bottom, 0.502 g (1.99 mmol) AgPF_6 was dissolved in 10 mL acetone using the sonicator (10-15 minutes). A latex balloon was wired to the 3-neck flask and filled with CO using the Parr autoclave system. The AgPF_6 solution was added via cannula in a quick addition, and the mixture was stirred for 2 hours. The CO balloon was then removed and the mixture was filtered over celite, washing with a small amount of acetone. Much of the precipitate was still present in the filtrate, so the mixture was filtered over celite several times to remove about 90% of the byproducts. The filtrate was concentrated in vacuo, and the product was analyzed by FT-IR.

4.11 Reactions with $\text{Co}_2(\text{CO})_8$

The dicobalt octacarbonyl used in these experiments was purchased from Sigma-Aldrich, used as was received with no further purification, and stored at cold temperatures, exposed to no air or moisture. The reagent was used within a few days of receiving it and was disposed of after about 1 month, due to its high instability. Subsequent reactions were performed with a fresh bottle after analysis by FT-IR. Unless otherwise noted, all manipulations were performed with glovebox and schlenk line techniques.

4.11.1 Synthesis of $\text{Co}_2(\text{CO})_4(\text{nbd})_2$

The synthesis of $\text{Co}_2(\text{CO})_4(\text{nbd})_2$ was performed according to the literature procedure.⁹ A 100 mL schlenk flask was charged with 0.890 g (2.60 mmol), 4.793 g (52.0 mmol) norbornadiene, and 30 mL hexanes. The mixture was refluxed for 2 hours at 60°C. The reaction mixture was allowed to cool to room temperature and the solvent and excess norbornadiene were removed under vacuum. Attempted recrystallization in diethyl ether did not work so the orange/red solid was re-isolated (67% yield) and analyzed by FT-IR.

4.11.2 Reactions of $\text{Co}_2(\text{CO})_4(\text{nbd})_2$ with et,ph-P4

This procedure was performed according to the literature.¹⁰ A small schlenk flask was charged with 0.271 g (0.583 mmol) et,ph-P4 dissolved in 20 mL hexanes using sonicator (10-15 minutes). A second schlenk flask was charged with 0.244 g (0.589 mmol) $\text{Co}_2(\text{CO})_4(\text{nbd})_2$ and 30 mL hexanes. The et,ph-P4 solution was added in a dropwise cannula addition to the cobalt solution. The mixture was refluxed overnight at 70°C. The mixture was allowed to cool to room temperature, and the brown solid was filtered by gravity filtration, washing with hexanes. The brown solid was dried under vacuum (40% yield) and analyzed by FT-IR and ^{31}P NMR in d_2 -DCM. ^{31}P { ^1H } NMR (400 MHz, d_2 -DCM) δ 49 ppm (distorted d) and 33 ppm (distorted d).

4.11.3 Reactions of $\text{Co}_2(\text{CO})_8$ with *meso*-et,ph-P4

A small schlenk flask was charged with 0.510 g (1.10 mmol) *meso*-et,ph-P4 dissolved in 15 mL acetone. Another small schlenk flask was charged with 0.375 g (1.10 mmol) $\text{Co}_2(\text{CO})_8$ dissolved in 20 mL acetone. The et,ph-P4 solution was added in a cannula dropwise addition to the cobalt solution over the course of 10-15 minutes. The mixture was stirred at room temperature for 3 hours (or longer). Acetone was removed under vacuum to yield a gold colored solid (80% yield). The solid was analyzed by FT-IR and ^{31}P NMR in d_2 -DCM. ^{31}P $\{^1\text{H}\}$ NMR (400 MHz, d_2 -DCM) δ 86 ppm (broad), 50 ppm (broad), and -34 ppm (distorted d).

4.12 Synthesis of $[\text{Co}(\text{H}_2\text{O})_6][\text{BF}_4]_2$

The synthesis of $[\text{Co}(\text{H}_2\text{O})_6][\text{BF}_4]_2$ was performed according to the procedure in the literature.¹¹ A schlenk flask was charged with 1.000 g Co metal and 8 mL HBF_4 (48% H_2O) and refluxed at 90°C for 3 hours. The reaction mixture was allowed to cool to room temperature and filtered by gravity filtration in the glovebox, washing once with diethyl ether. Filtrate was transferred to a schlenk flask and solvent was removed under vacuum to isolate a deep pink solid (90% yield, based on the amount of Co metal).

4.13 Synthesis of *rac*- $[\text{Co}_2(\text{H}_2\text{O})_x(\text{et,ph-P4})][\text{BF}_4]_4$ and *rac*- $[\text{Co}_2(\text{H}_2\text{O})_x(\text{et,ph-P4-Ph})][\text{BF}_4]_4$

A schlenk flask was charged with 0.422 g (0.753 mmol) et,ph-P4-Ph dissolved in 20 mL THF using sonicator (10-15 minutes). A second schlenk flask was charged with 0.516 g (1.51 mmol) $[\text{Co}(\text{H}_2\text{O})_6][\text{BF}_4]_2$ dissolved in 25 mL THF using sonicator (10-15 minutes). The ligand was added to the cobalt solution via cannula in a dropwise addition. The dark green/red mixture was stirred overnight at room temperature. The mixture was filtered in the glovebox by gravity filtration, and the filtrate was transferred to a schlenk flask. The solvent was removed under vacuum to yield a sticky dark green/red paste (exact yield could not be determined).

4.14 Attempted H₂/CO Reduction of *rac*-[Co₂(H₂O)_x(*et*,*ph*-P4-Ph)][BF₄]₄

A small schlenk flask was charged with 0.132 g dicobalt complex dissolved in 20 mL DCM to form a pink solution. A latex balloon was wired to the schlenk flask and filled with 1:1 H₂/CO (syngas) using the Parr autoclave system. The mixture was stirred vigorously overnight. The balloon was then removed, and the mixture was filtered by gravity filtration in the glovebox, washing with a few mL of DCM. The filtrate was transferred to a schlenk flask and the solvent was removed under vacuum. The solid was analyzed by FT-IR but no carbonyl signals were detected.

4.15 Attempted Zn Reduction of *rac*-[Co₂(H₂O)_x(*et*,*ph*-P4)][BF₄]₄

A 250 mL schlenk flask was charged with 0.942 g (0.822 mmol) of the dicobalt complex, 0.14 g (2.14 mmol) Zn dust, and 50 mL acetone. A latex balloon was wired to the flask and filled with CO using the Parr autoclave system. The mixture was stirred overnight. The balloon was then removed, and the mixture was filtered over celite in the glovebox. The filtrate was dried under vacuum to yield an orange solid. The solid was analyzed by FT-IR and ³¹P NMR in d₆-acetone. No ³¹P NMR signals were detected in this experiment.

4.16 Hydroformylation of 1-Hexene Attempts with Dicobalt Complexes

Hydroformylation experiments were attempted for both *rac*-Co₂Cl₄(*et*,*ph*-P4-Ph) (Attempt 1) and the proposed product of the Zn reductions *rac*-[Co₂(CO)₅₋₆(*et*,*ph*-P4)]²⁺ (Attempt 2) using 1-hexene as the substrate. Attempt 1 was run by combining a 1 mM solution of the cobalt complex in 100 mL of DCM. Four equivalents of NEt₃ and 5 equivalents of NaBF₄ were also added to the mixture. The entire mixture was transferred to the Parr autoclave system, pressurized to 150 psig H₂/CO and heated to 100°C for 3 hours. No aldehyde was produced according to GC-MS analyses. Attempt 2 was performed by combining a 1mM solution of the cobalt complex in 100 mL of

acetone. The mixture was transferred to the Parr autoclave system, pressurized to 150 psig H₂/CO and heated to 100°C for 2 hours. No aldehyde was produced according to GC-MS analyses. The reaction mixture was removed from the autoclave and the solvent was removed under vacuum. The remaining solid was analyzed by FT-IR and ³¹P NMR. ³¹P {¹H} NMR (400 MHz, d₆-acetone) δ 85 ppm (distorted dd), 68 ppm (broad), 52 ppm (distorted dd), and 50 ppm (broad).

4.17 References

1. Lanemen, S. A.; Fronczek, F. R.; Stanley, G. G. Synthesis of a Binucleating Tetratertiary Phosphine Ligand System and the Structural Characterization of both Meso and Racemic Diastereomers of Ni₂Cl₄(eLTTP). *Inorg. Chem.* **1989**, *28*, 1872-1878.
2. Monteil, A. R. *Investigation into the Dirhodium-Catalyzed Hydroformylation of 1-Alkenes and Preparation of a Novel Tetrphosphine Ligand*. Ph.D. Dissertation, Louisiana State University, Baton Rouge, **2006**.
3. Kalachnikova, E. *Improved Synthesis, Separation, Transition Metal Coordination and Reaction Chemistry of a New Binucleating Tetrphosphine Ligand*. Louisiana State University, Baton Rouge, **2015**.
4. Schreiter, W. J. *Investigations into Alkene Hydration and Oxidation Catalysis*. Louisiana State University, Baton Rouge, **2013**.
5. Chari, M. A. Amberlyst-15: an efficient and reusable catalyst for multi-component synthesis of 3,4-dihydroquinoxalin-2-amine derivatives at room temperature. *Tetrahedron Lett.* **2011**, *52*, 6108-6112.
6. Vaisman, B.; Shikanov, A.; Domb, A.J. The Isolation of Ricinoleic Acid from Castor Oil by Salt-solubility-based Fractionation for the Biopharmaceutical Applications. *J. Am. Oil. Chem. Soc.* **2008**, *85*, 169-184.
7. Drago, R. S.; Cannady, J. P.; Leslie, K. A. Hydrogen-Bonding Interactions Involving Metal-Bound Dioxxygen. *J. Am. Chem. Soc.* **1980**, *102*, 6014-6019.
8. Askham, F. R.; Stanley, G. G.; Marques, E. C. A New Type of Transition-Metal Dimer Based on a Hexaphosphine Ligand System: Co₂(CO)₄(eHTP)²⁺ (eHTP = (Et₂PCH₂CH₂)₂PCH₂P(CH₂CH₂PEt₂)₂). *J. Am. Chem. Soc.* **1985**, *107*, 7423-7431.
9. Winkhaus, G.; Wilkinson, G. Some Diolefin Carbonyl Complexes. *Royal Society of Chemistry.* **1961**, *120*, 602-605.
10. Lanemen, S. A.; Fronczek, F. R.; Stanley, G. G. A Ligand-Imposed Cradle Geometry for a Dicobalt Tetracarbonyl Tetratertiary Phosphine Complex. *Inorg. Chem.* **1989**, *28*, 1206-1207.
11. Holt, D. G. L.; Larkworthy, L. F.; Povey, D. C.; Smith, G. W.; Leigh, G. F. Facile Synthesis of Complexes of Vanadium(II) and the Crystal and Molecular Structures of Hexaquaavanadium(II) Trifluoromethylsulphonate. *Inorg. Chim. Acta.* **1990**, *169*, 201-205.

Chapter 5: Conclusion/Future Studies

5.1 Oxidative Cleavage of Alkenes

The dinickel complexes, tetraphosphine ligands, cobalt complex $[\text{Co}(\text{H}_2\text{O})_6][\text{BF}_4]_2$, and a few other phosphine ligands (dppm, PPH_3 and $\text{P}(\text{C}_{18}\text{H}_{33})$) all showed reactivity for the oxidative cleavage of oleic acid. However, attempts to make the reaction catalytic were unsuccessful. We initially believed that this reaction could be made catalytic based on Dr. Stanley's proposed mechanisms, with the second mechanism (Figure 5.1) being the most plausible for this reaction based on the bulky unsaturated fatty acid. This mechanism involves the direct interaction of the alkene with the peroxide bridged ligand rather than alkene coordination to the metal. Since the fatty acids are 18-carbon chains, they would be less likely to coordinate to the metal center directly.

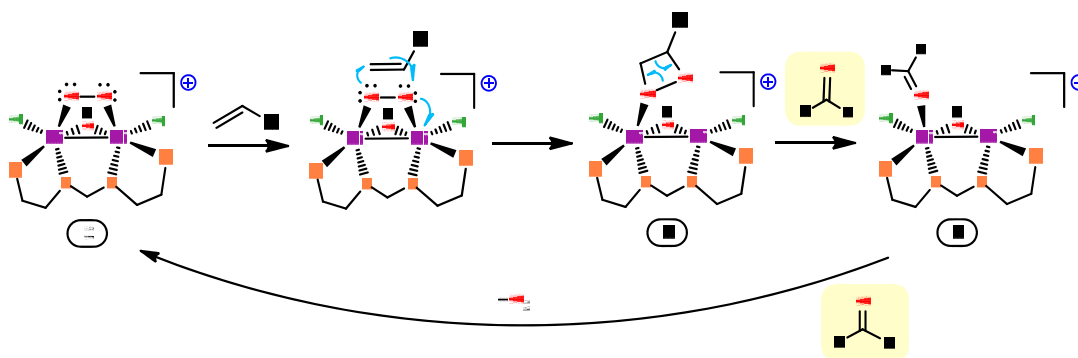


Figure 5.1 Dr. Stanley's second proposed mechanism for the oxidative cleavage of alkenes

We believe, however, this reactivity is more complex than that. It is most likely not a straight radical based reactivity either. Dr. Schreiter used inhibitors to test for radical character in the oxidative cleavage reactions. His studies indicated that in certain cases the reactions were inhibited;¹ this finding points to some radical behavior, but typically radical reactions produce a variety of oxidation products such as aldehydes, ketones, carboxylic acids, esters and ethers (Chapter 1). This reaction, on the other hand, appears to only produce aldehydes, albeit in extremely low yields (Chapter 2).

Additionally, the proposed Ni-based mechanisms were disproven with the discovery of the oxidative cleavage using only the tetrphosphine ligands. Dr. Kalachnikova demonstrated through ^{31}P NMR studies that the old tetrphosphine ligand was not as sensitive to air as we thought. After 8 days of exposure to air, the ^{31}P signals due to *meso*-et,ph-P4 were still around 68% by integration.² With these results in mind, she also demonstrated that the oxidative cleavage of alkenes occurs with only the tetrphosphine ligand and H_2O /polar organic solvent mixture in air. No pure O_2 or metal complexes were needed for the aldehydes to be produced in low yields.

Due to the range of species tested and active for oxidative cleavage, including the monometallic cobalt complex $[\text{Co}(\text{H}_2\text{O})_6][\text{BF}_4]_2$, it would be very difficult and tedious to track down how this reaction proceeds. With such a small amount of product being produced as well, there is really no benefit in putting more time into studying this reaction. It can be said that due to cobalt's affinity for oxygen, it is not entirely surprising that the reaction works far better with Drago's monometallic catalyst. Cobalt adducts that oxidize alkenes are well known and well documented in the literature (Chapter 1).

5.2 ^{31}P NMR Studies of the Dinickel Complexes' Reactivity with H_2O

Dr. Schreiter studied the reactivity of the old P4 dinickel complex, *meso*- $\text{Ni}_2\text{Cl}_4(\text{et,ph-P4})$, with H_2O in a fair bit of detail. His studies showed the complex to fall apart and form other complexes, including the double ligand species, *meso*- $[\text{Ni}_2(\mu\text{-Cl})(\text{et,ph-P4})_2]^{3+}$, upon the addition of H_2O .¹ We have also began studying the old P4 *rac* dinickel complex and the new P4-Ph dinickel complex, *meso*- $\text{Ni}_2\text{Cl}_4(\text{et,ph-P4-Ph})$. In Dr. Schreiter's preliminary studies with the old P4 *rac* dinickel complex, he believed it also formed a similar double ligand species as with the *meso* dinickel complex.¹ However, we disagree with his proposal and believe it is more likely that the formation of the bridged-hydroxide dinickel complex, *rac*- $[\text{Ni}_2(\mu\text{-OH})\text{Cl}_2(\text{et,ph-P4})]^{1+}$ is

occurring in these reactions based on ^{31}P NMR data and DFT calculations. The ^{31}P NMR data reveals a symmetrical pattern for this species, shown below in Figure 5.2. This pattern is similar to what was predicted for this complex during DFT studies.

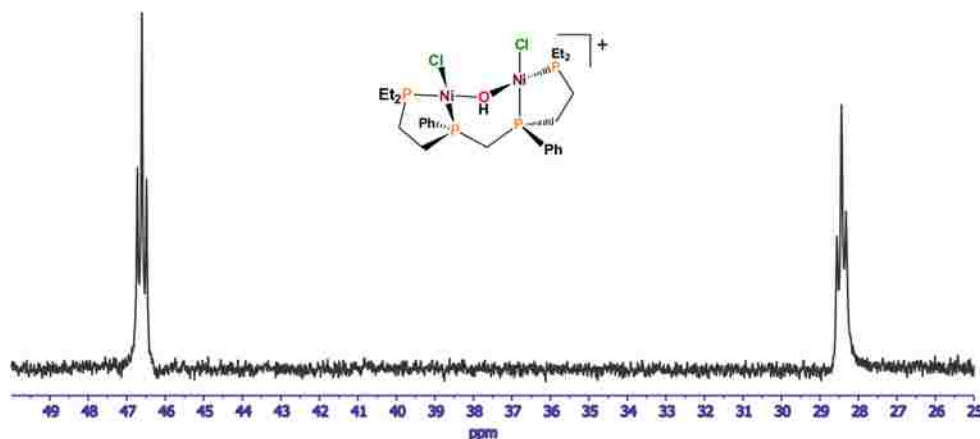


Figure 5.2 Partial ^{31}P NMR Spectrum of the reaction of *rac*- $\text{Ni}_2\text{Cl}_4(\text{et,ph-P4})$ with D_2O immediately after addition (spectrum zoomed in to show pseudo-triplets)

Dr. Alex Monteil isolated and characterized a similar bridged-hydroxide dinickel complex with the new P4-Ph ligand, *meso*- $[\text{Ni}_2(\mu\text{-OH})\text{Cl}_2(\text{et,ph-P4-Ph})]^{1+}$ (Figure 5.3).³ We believe, based on our preliminary ^{31}P NMR studies with the new P4-Ph *meso* dinickel complex that this species is the most dominant and stable complex formed during its reaction with H_2O as well. LC-MS (ESI) data run by Dr. Kalachnikova from an oxidative cleavage reaction with the new P4-Ph dinickel complexes also support this proposal (Chapter 2).

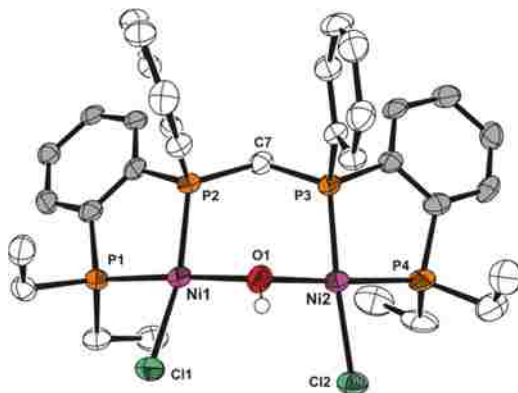


Figure 5.3 ORTEP plot for *meso*- $[\text{Ni}_2(\mu\text{-OH})\text{Cl}_2(\text{et,ph-P4-Ph})]^{1+}$

Further studies, including COSY NMR, are currently underway to prove our proposal of this complex. Also, the new P4-Ph *rac* dinickel complex has not been studied due to its higher sensitivity to H₂O, even with 10% H₂O, the complex precipitates out of solution. We are currently working on investigating this complex's reactivity with only 5% H₂O in hopes to collect spectra and determine if the bridged-hydroxide complex is also forming.

5.3 Synthetic Strides Towards a Bimetallic Cobalt-Carbonyl Catalyst

The pursuit of a bimetallic cobalt system for hydroformylation and aldehyde-water shift catalysis has been a challenging on-going three-year project. Numerous synthetic strategies were explored changing multiple variables in attempt to yield successful results. There were some small victories, but the majority of the results were failed reactions that taught the lessons of what did not work for this system.

Cobalt is not a very reactive metal; it does not form particularly strong metal-ligand bonds, which can be expected for a first row transition metal. Most of the reduction attempts using the multitude of reducing agents either resulted in partial decomposition of the starting material (1:1 H₂/CO autoclave reduction) or some over-reduction of the complex to Co⁰ and even cobalt metal (super hydride). In a few of the H₂/CO autoclave reduction experiments, some black material formed during the reactions was believed to also be some cobalt metal.

When this project first began, we attempted the reduction of the dicobalt tetrachloride complexes with both the old P4 and new P4-Ph tetraphosphine ligands with a 1:1 H₂/CO mixture (syngas). However, it did not occur to Dr. Stanley or myself that 50% H₂ may be too much for the formation of a dicobalt-carbonyl complex. Not only are the dicobalt tetrachloride complexes unstable under high pressures, even at 40 psig, the presence of 50% H₂ turned out to be very problematic for the system. We believed the H₂ would aid in the reduction from Co (II) to Co (I),

but a better method would have been to use much less H₂ and excess CO to achieve the desired transformation. This combination may have worked for the hexaphosphine ligand system published by our group in 1985⁴, but that system needed less carbonyl ligands. In our case, the four P groups of our tetraphosphine ligands (vs the six P groups of the hexaphosphine ligand) give the metal center more electrons to coordinate more CO ligands (or H₂ ligands). In future reactions, we will study an H₂/CO reduction with a ratio of 6:1 CO/H₂ in hopes of yielding a “clean” dicobalt-carbonyl complex, perhaps the dicationic penta- or hexacarbonyl dicobalt complex we predicted during our studies, *meso*- or *rac*-[Co₂(CO)₅₋₆(*et*,*ph*-P₄) or (*et*,*ph*-P₄-Ph)]²⁺.

Several solvents and solvent combinations were also used over the three-year span to either crystallize a bimetallic cobalt complex or separate the multiple species formed during the H₂/CO autoclave reductions. The only crystals analyzed from these mixtures were the *rac*-[CoCl₂(*et*,*ph*-P₄-Ph)]¹⁺ complex, shown below in Figure 5.4, and the byproduct, trimethylammonium chloride (HNEt₃Cl). Attempts to separate the mixtures of species using DCM usually gave a blue colored material and a green colored material. EPR studies indicated that both of these complexes both had cobalt metal centers in the +2 oxidation state. FT-IR data showed the same two terminal CO bands at 1937 and 1995 cm⁻¹, and no ³¹P NMR signals were detected for either solid.

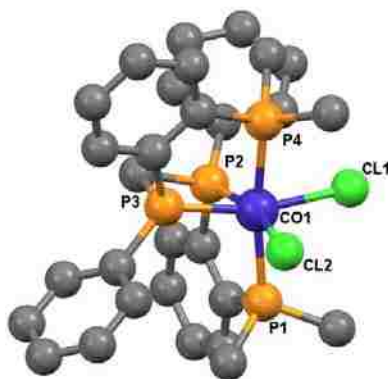


Figure 5.4 Ball-and-stick model for *rac*-[CoCl₂(*et*,*ph*-P₄-Ph)]¹⁺. Hydrogen atoms and methyl groups on the external P atoms have been omitted for clarity

The removal of byproducts formed during the reduction experiments was another huge problem to tackle with this project. Though the Zn reduction appeared to give the best experimental results, the removal of the ZnCl₂ byproduct proved to be a major issue. Different solvents were used for the reduction in an attempt to combat this problem, but since the dicobalt tetrachloride complexes are only soluble in a few polar organic solvents (acetone, DCM, CH₃CN, and DMF, for the most part), we were severely limited by the different solvent systems we could use. Additionally, attempted removal of ZnCl₂ using these solvents in combination with non-polar solvents such as hexanes was unsuccessful. In most cases, both the ZnCl₂ and the desired complex, [Co(CO)₅₋₆(et,ph-P4)]²⁺, would partially precipitate out of the mixture.

Experiments with Co₂(CO)₈ proved to be just as problematic. A direct substitution or ligand exchange experiments should have ideally been the quickest and most facile route to yield a neutral cobalt (0) species. This neutral species could have been oxidized to yield a cationic complex, similar to the dirhodium cationic system shown to be an excellent hydroformylation catalyst. However, Co₂(CO)₈ is very unstable and degrades over the course of a few weeks, even when stored in cold temperatures unexposed to air or moisture. It is my belief that the instability of Co₂(CO)₈ is the major reason why any experiments using it are highly irreproducible. FT-IR studies, shown in Figures 3.33-3.35, clearly indicate that a mixture of cobalt carbonyl complexes was being formed, and in some cases, the starting material was still present after the reaction appeared to be complete.

Hydroformylation attempts with the dicobalt tetrachloride complex and a dicobalt complex isolated from the Zn reduction experiments were performed, but no aldehyde was produced in either case. We believe the mixture of complexes present, some of which may be completely inactive for hydroformylation, shuts down the catalysis. Also because we could never crystallize

the material, we were not sure if halogen ligands, particularly chlorides, were still coordinated to the metal centers after the reduction attempts.

The exploration of a non-halide containing starting material appears to be the best route for the synthesis of this complex. Previous synthetic routes showed the halides were not as easily removed as we originally believed and direct experiments to remove them were unsuccessful. The two simple complexes, $[\text{Co}(\text{H}_2\text{O})_6][\text{BF}_4]_2$ and $[\text{Co}(\text{CH}_3\text{CN})_6][\text{BF}_4]_2$, are relatively inexpensive to synthesize and the methods are well documented in the literature.⁵ Work began with the hexaaqua species because the synthetic route was simpler than the acetonitrile version. Thus far, the two attempts using H_2/CO and Zn to reduce the complexes formed from the combination of the hexaaqua species with the tetraphosphine ligands, $[\text{Co}_2(\text{H}_2\text{O})_x(\text{et,ph-P4})][\text{BF}_4]_4$, have been unsuccessful. It is my belief, however, that use of another mild reducing agent, with an easily isolable by product, would be the most suitable choice for the reduction of this complex. These studies are currently underway in the Stanley group.

5.4 References

1. Schreiter, W. J. *Investigations into Alkene Hydration and Oxidation Catalysis*. Ph.D. Dissertation, Louisiana State University, Baton Rouge, May **2013**.
2. Kalachnikova, E. *Improved Synthesis, Separation, Transition Metal Coordination and Reaction Chemistry of a New Binucleating Tetraphosphine Ligand*. Ph.D. Dissertation, Louisiana State University, Baton Rouge, May **2015**.
3. Monteil, A. R. *Investigation into the Dirhodium-Catalyzed Hydroformylation of 1-Alkenes and Preparation of a Novel Tetraphosphine Ligand*. Ph.D. Dissertation, Louisiana State University, Baton Rouge, December **2006**.
4. Askham, F. R.; Stanley, G. G.; Marques, E. C. A New Type of Transition-Metal Dimer Based on a Hexaphosphine Ligand System: $\text{Co}_2(\text{CO})_4(\text{eHTP})^{2+}$ (eHTP = $(\text{Et}_2\text{PCH}_2\text{CH}_2)_2\text{PCH}_2\text{P}(\text{CH}_2\text{CH}_2\text{PEt}_2)_2$). *J. Am. Chem. Soc.* **1985**, *107*, 7423-7431.
5. Holt, D. G. L.; Larkworthy, L. F.; Povey, D. C.; Smith, G. W.; Leigh, G. F. Facile Synthesis of Complexes of Vanadium(II) and the Crystal and Molecular Structures of Hexaaquavanadium(II) Trifluoromethylsulphonate. *Inorg. Chim. Acta.* **1990**, *169*, 201-205.

Appendix: Additional ^1H and ^{31}P NMR Data

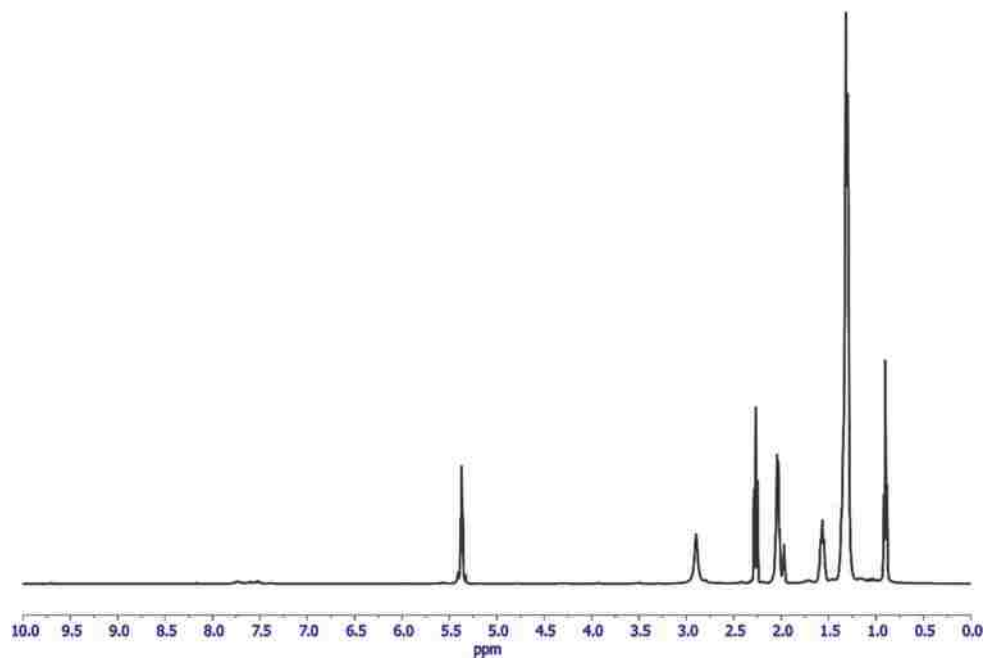


Figure A.1 ^1H NMR spectrum of oxidative cleavage of oleic acid with *meso*-et,ph-P4 in 10% $\text{D}_2\text{O}/\text{d}_3\text{-CH}_3\text{CN}$

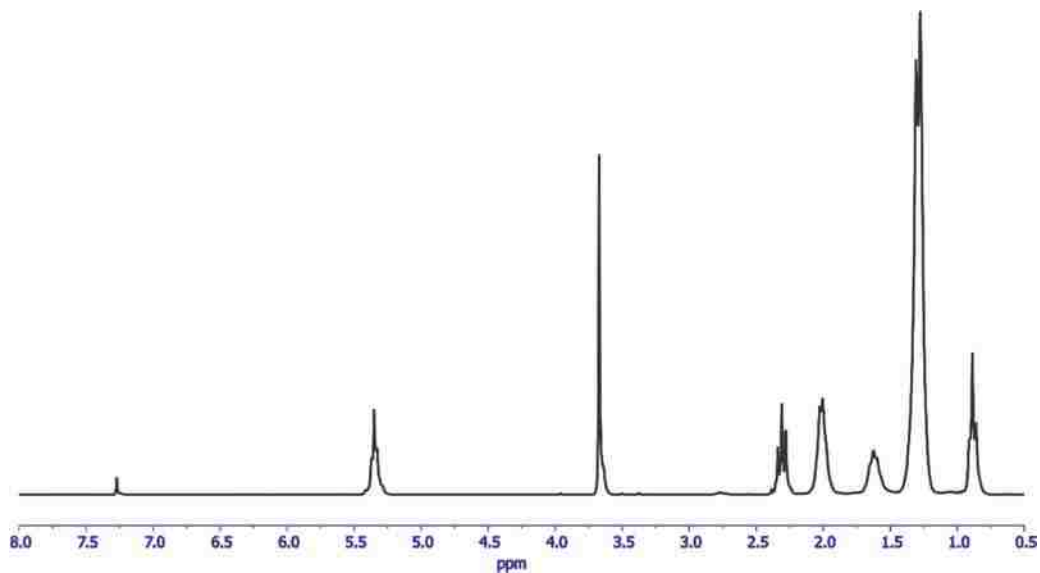


Figure A.2 ^1H NMR spectrum of oleic acid methyl ester (after esterification)

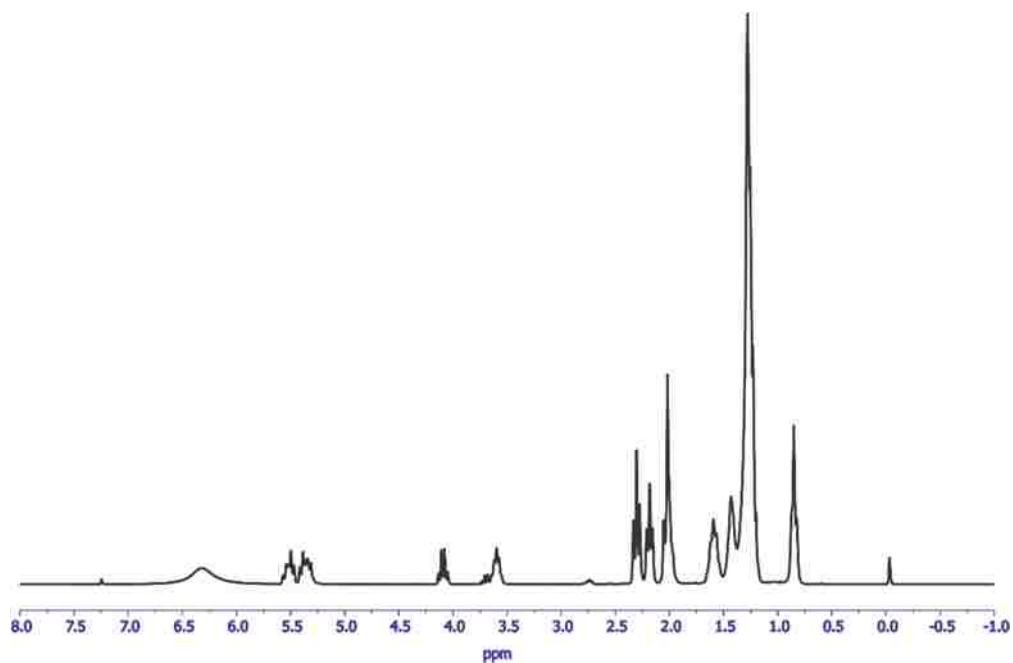


Figure A.3 ^1H NMR spectrum of ricinoleic acid (after saponification of castor oil)

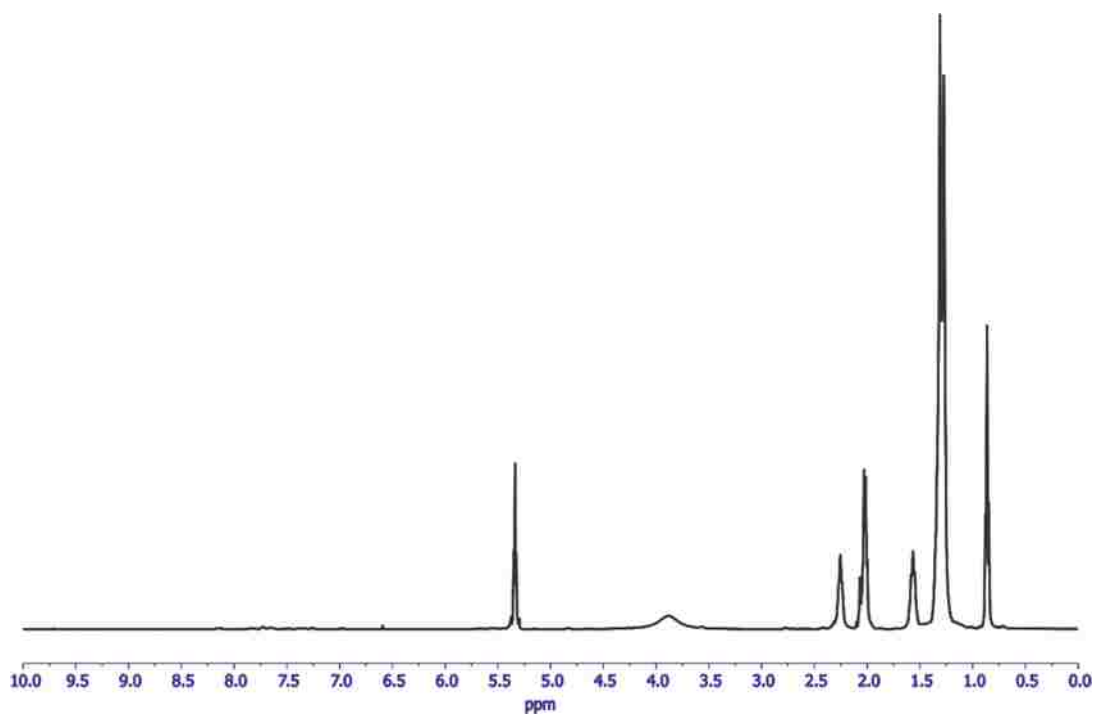


Figure A.4 ^1H NMR spectrum of oxidative cleavage of oleic acid for quantification experiment

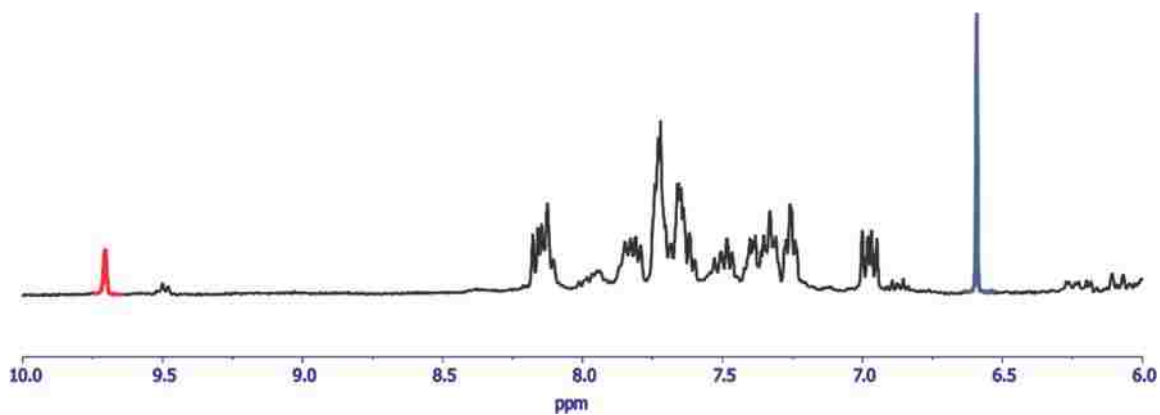


Figure A.5 ^1H NMR spectrum of oxidative cleavage of oleic acid for quantification experiment. Spectrum expanded to show internal standard signal at 6.6 ppm (blue peak) and aldehyde signal at 9.7 ppm (red peak)

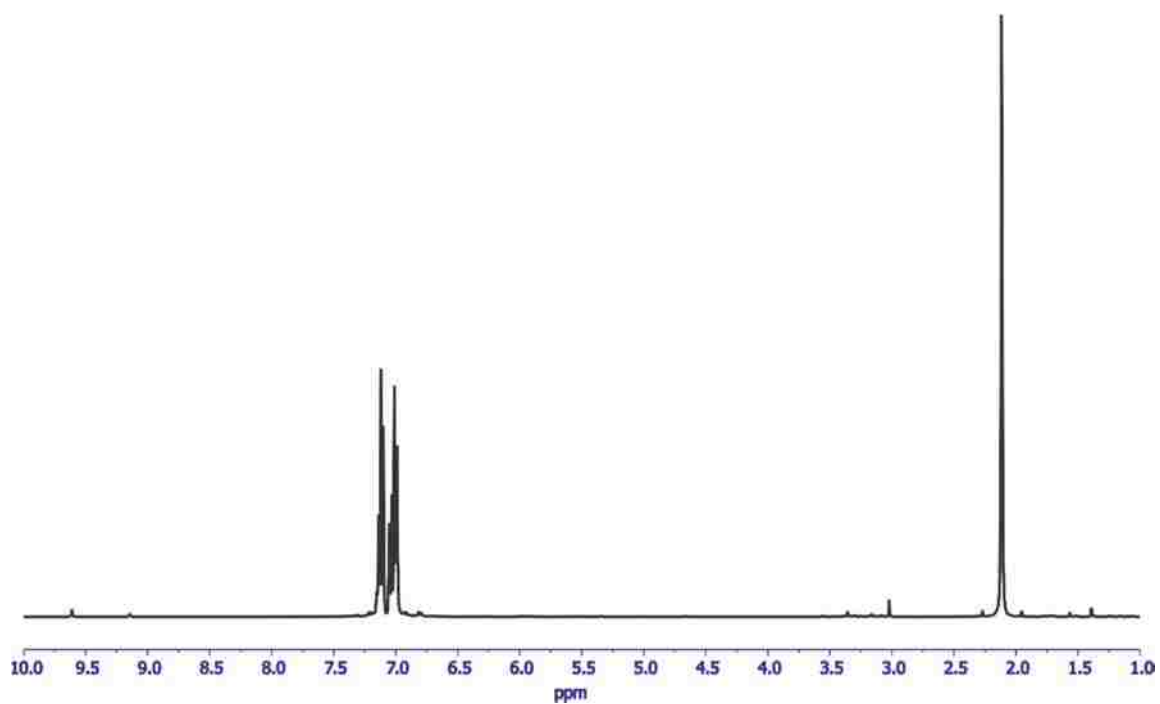


Figure A.6 ^1H NMR spectrum of reaction mixture after oxidative cleavage of isoeugenol using Drago's catalyst

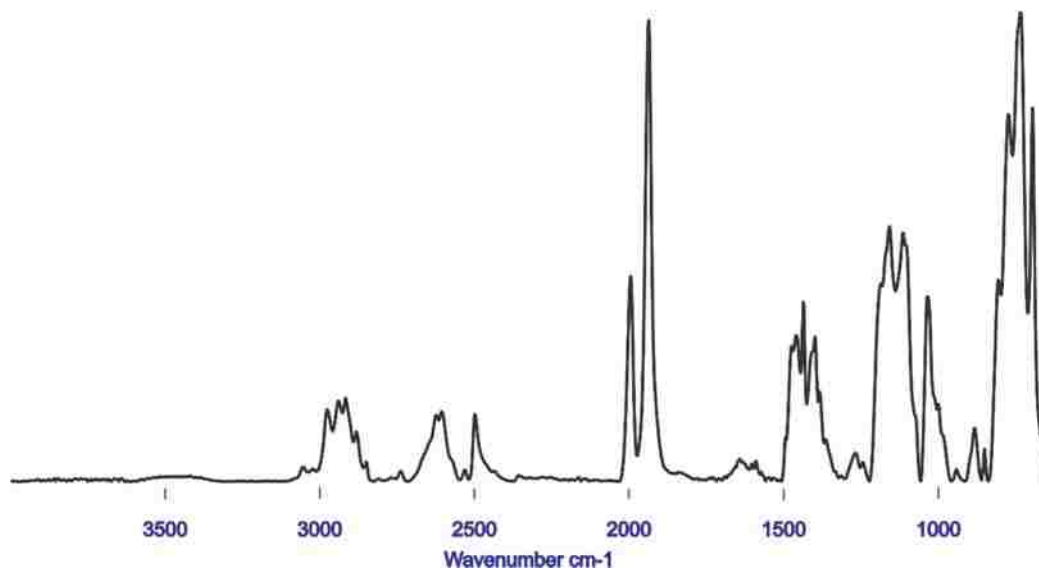


Figure A.7 FT-IR spectrum of autoclave reduction of *meso*-Co₂Cl₄(et,ph-P₄) in DCM at 50 psig H₂/CO and 60°C

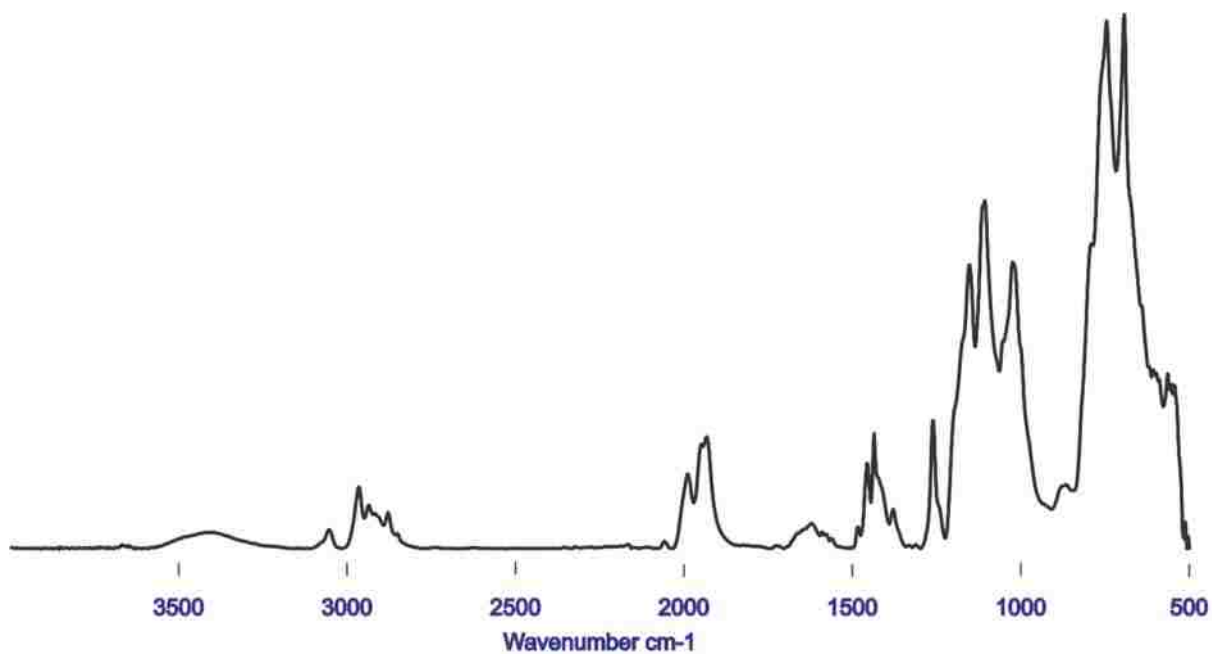


Figure A.8 FT-IR spectrum of NaBH₄ reduction of *rac*-Co₂Cl₄(et,ph-P₄-Ph) at room temperature for 2 hours in a mixture of C₆H₆/EtOH

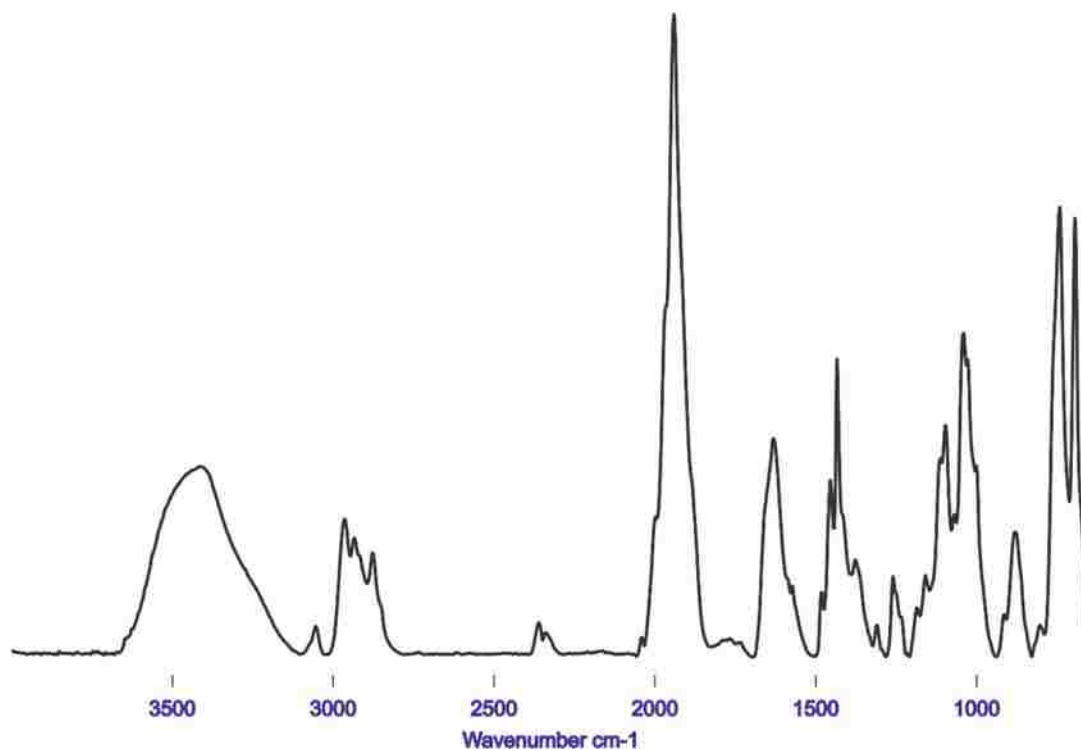


Figure A.9 FT-IR spectrum of super hydride reduction of *meso*-Co₂Cl₄(*et,ph*-P₄-Ph) under CO atmosphere at room temperature for 2 hours in THF

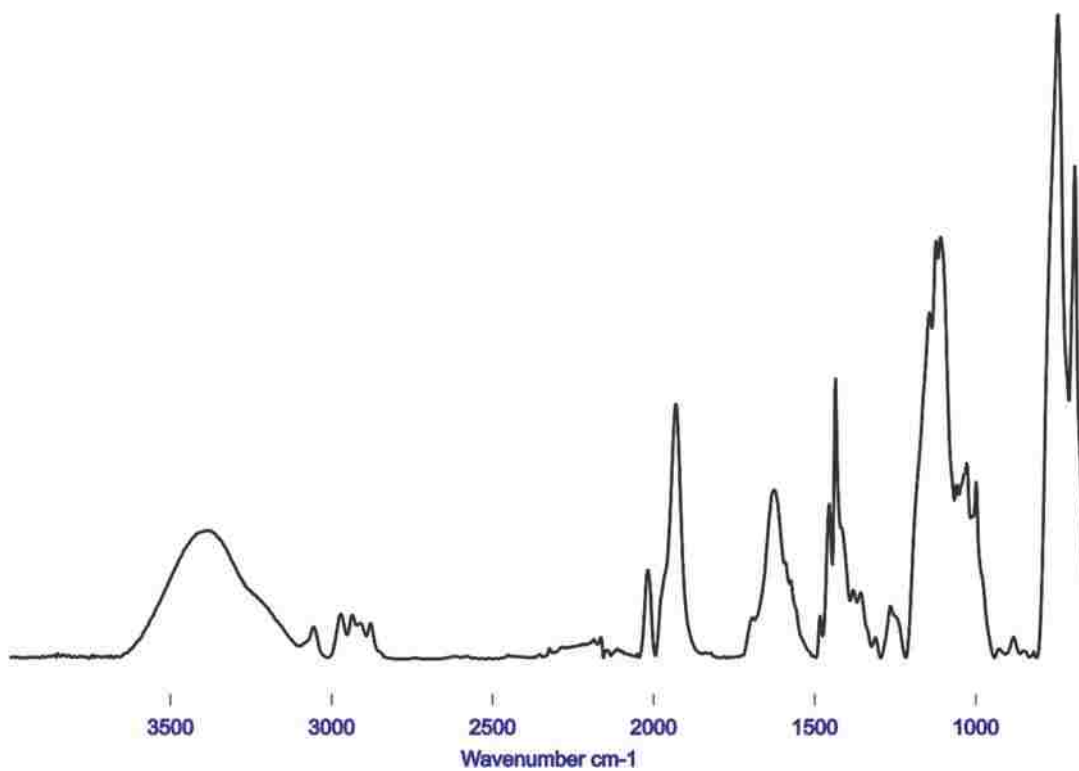


Figure A.10 FT-IR spectrum of Mg reduction of *meso*-Co₂Cl₄(*et,ph*-P₄-Ph) in acetone under CO

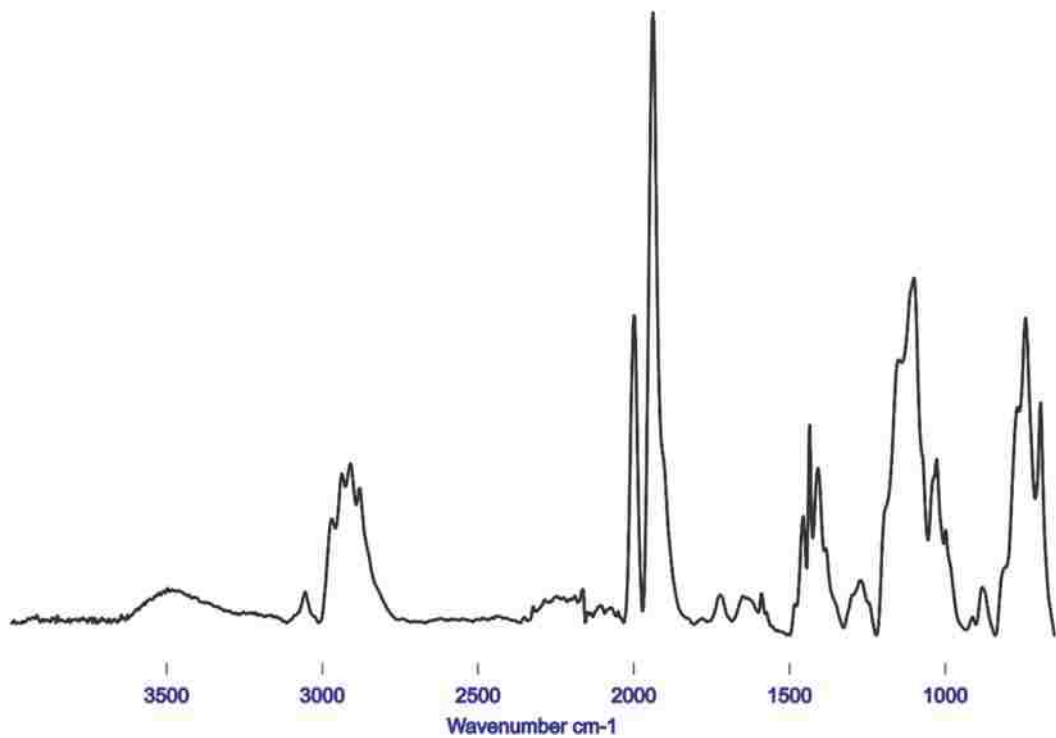


Figure A.11 FT-IR spectrum of Zn reduction of *rac*-Co₂Cl₄(*et*,*ph*-P₄) in CH₃CN at room temperature under CO atmosphere overnight

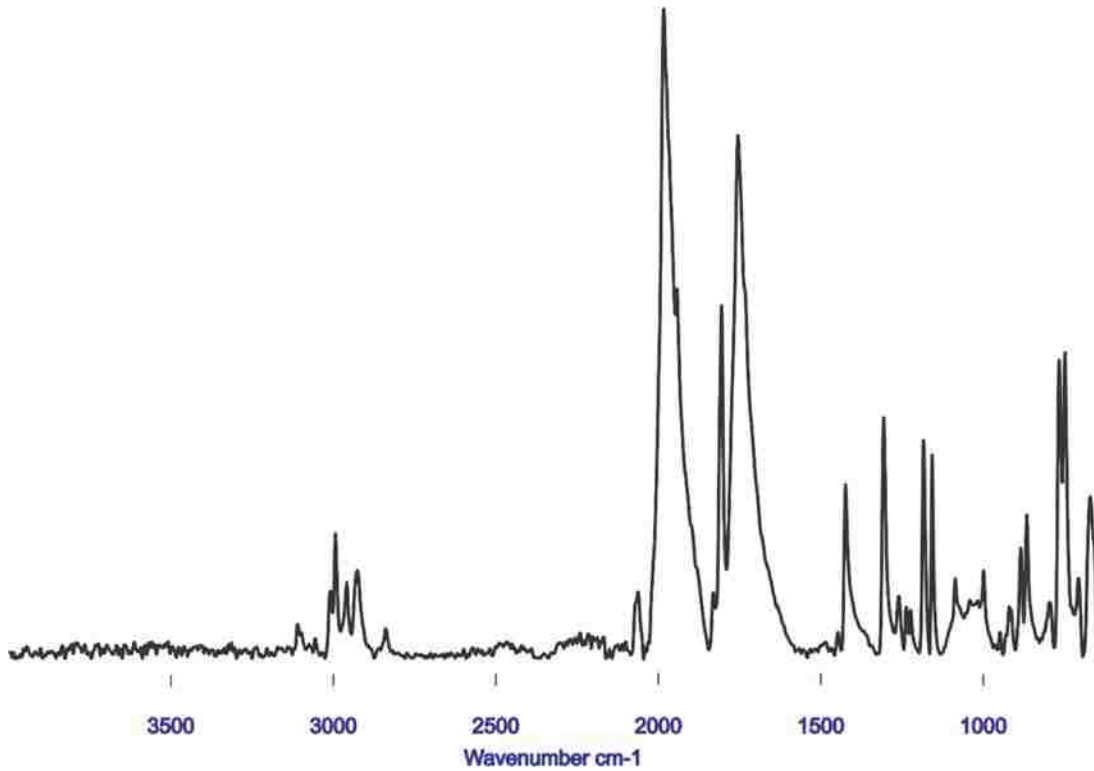


Figure A.12 FT-IR spectrum of Co₂(CO)₄(*nbd*)₂ (synthetic attempt)

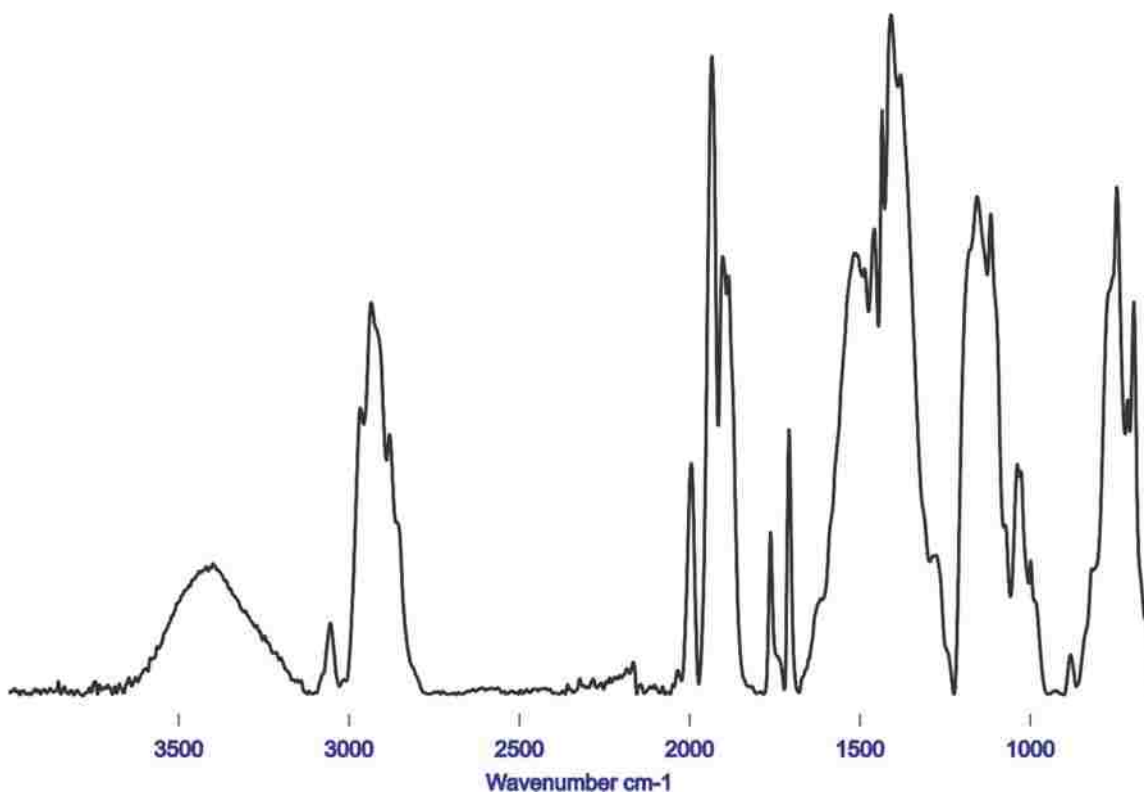


Figure A.13 FT-IR spectrum of the reaction of $\text{Co}_2(\text{CO})_4(\text{nbd})_2$ and *meso*-et,ph-P4 in hexane

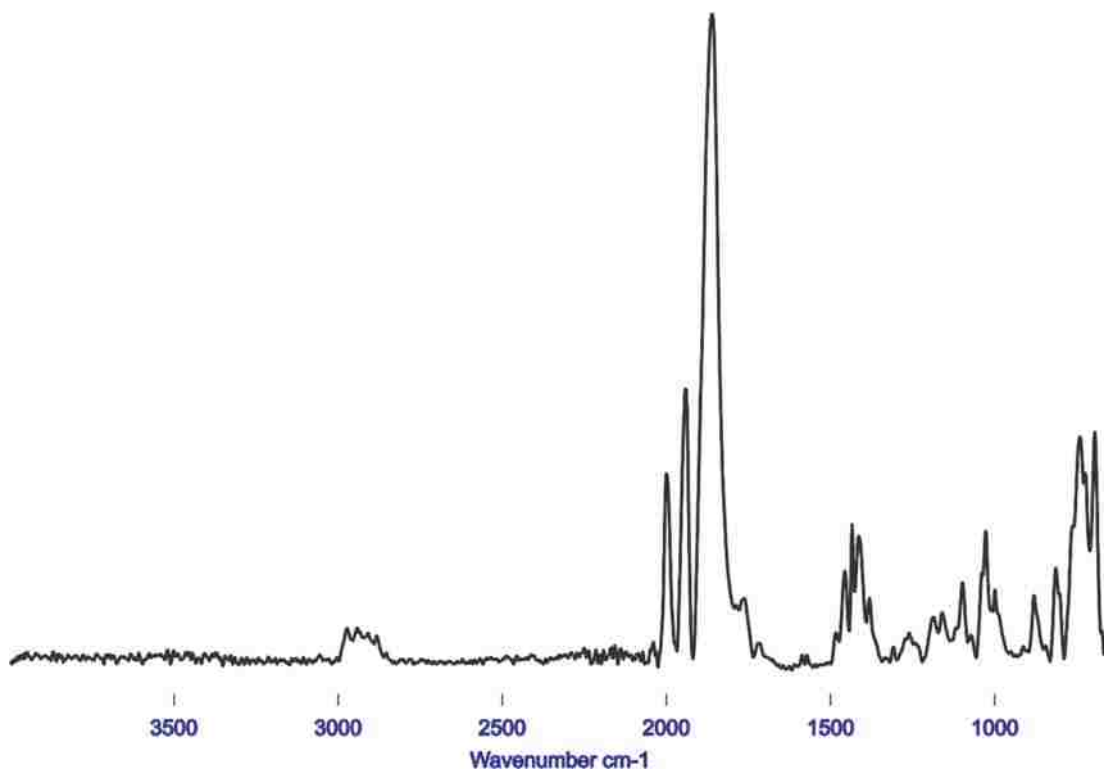


Figure A.14 FT-IR spectrum of reaction of $\text{Co}_2(\text{CO})_8$ and *meso*-et,ph-P4 in THF

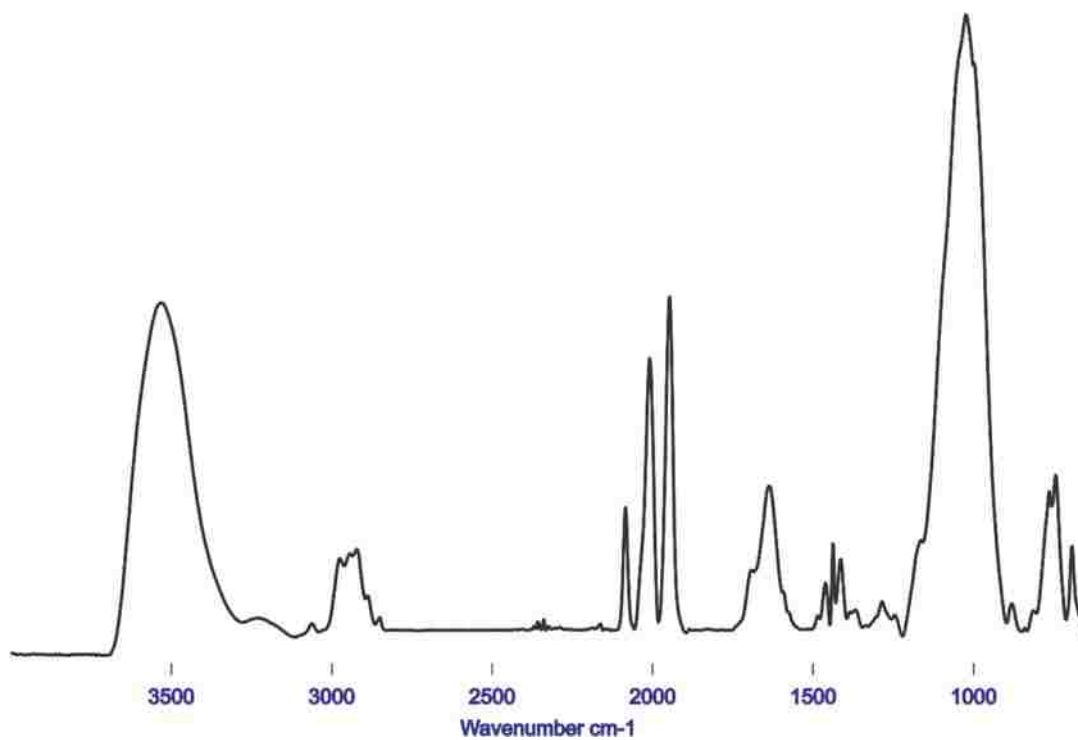


Figure A.15 FT-IR spectrum of attempted Zn reduction of $rac\text{-}[\text{Co}_2(\text{H}_2\text{O})_x(\text{et,ph-P}_4)][\text{BF}_4]_4$ under CO atmosphere

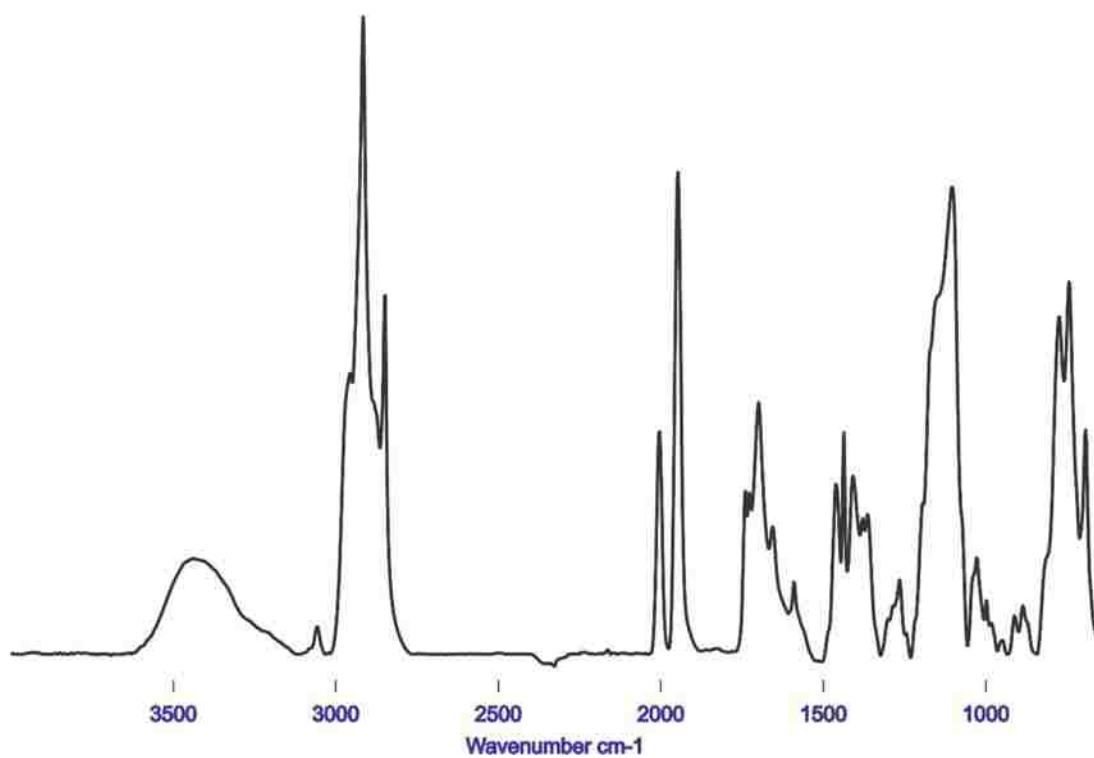


Figure A.16 FT-IR spectrum of isolated material from hydroformylation of 1-hexene using a dicobalt complex

VITA

Ciera Vonn Duronslet was born in 1988 in St. James, LA to Mrs. Nicholle Duronslet Bridgewater and Mr. Milton Bartholomew, Jr. She earned her Bachelor's of science degree in Chemistry from Nicholls State University in May 2010. In Fall 2010, she joined the graduate program in chemistry at Louisiana State University. Ciera plans to graduate with the Doctor of Philosophy degree in chemistry in December 2016.